



# **Università degli Studi di Messina**

*Dipartimento di Scienze Chimiche, Biologiche,  
Farmaceutiche, ed Ambientali*

*Dottorato di Ricerca in “Scienze Chimiche”*

*Doctor of Philosophy in “Chemical Sciences”*

## **Supercritical fluid extraction and chromatography coupled with mass spectrometry for the analysis of biological and food samples**

---

**Tutor**

Prof. Francesco Cacciola

**PhD Thesis of**

Fabio Salafia

**Coordinator**

Prof.ssa Paola Dugo

XXXIII Ciclo 2017-2020

<b>Scope of the research work</b>	1
<b>1 Supercritical fluid</b>	2
<b>1.1 Properties of supercritical fluids</b>	2
<b>1.2 Supercritical carbon dioxide</b>	7
<i>1.2.1 Characteristics and properties</i>	7
<i>1.2.2 Density</i>	8
<i>1.2.3 Diffusivity</i>	9
<i>1.2.4 Polarity</i>	12
<i>1.2.5 Solvating power</i>	13
<b>1.3 Modifiers</b>	16
<i>1.3.1 Main characteristics of the polar modifiers</i>	16
<i>1.3.2 Solubility of mixtures of binary fluids</i>	18
<b>References</b>	23
<b>2 Supercritical fluid extraction</b>	
<b>2.1 Introduction</b>	26
<b>2.2 Sample preparation</b>	27
<b>2.3 Extraction optimization</b>	29
<i>2.3.1 Pressure, temperature and density</i>	30
<i>2.3.2 Modifiers for extraction</i>	31
<i>2.3.3 Flow rate and extraction time</i>	34
<i>2.3.4 Extraction theory for different matrices</i>	36
<b>2.4 Extraction collection</b>	41
<i>2.4.1 Liquid phase collection</i>	41
<i>2.4.2 Solid phase collection</i>	44
<b>References</b>	46

<b>3 Supercritical fluid chromatography</b>	
<b>3.1 Evolution of the SFC</b>	48
<b>3.2 Chromatographic parameters</b>	50
<i>3.2.1 Retention parameters</i>	50
<i>3.2.2 Chromatographic resolution</i>	52
<b>3.3 Van Deemter equation in SFC</b>	58
<b>3.4 Chromatographic methods</b>	60
<b>3.5 SFC columns</b>	62
<i>3.5.1 Stationary phase</i>	62
<i>3.5.2 Particle size</i>	63
<b>3.6 SFC Detector</b>	68
<b>3.7 Mass Spectrometry</b>	70
<i>3.7.1 Ion sources</i>	70
<i>3.7.2 Analyzers</i>	73
<i>3.7.3 Detector</i>	76
<b>References</b>	78
<b>4 Limonoids</b>	
<b>4.1 General characteristics</b>	82
<b>4.2 Pharmacological activities</b>	85
<b>4.3 Analysis of limonoids</b>	87
<b>References</b>	89
<b>5 Carotenoids and apocarotenoids</b>	
<b>5.1 Characteristics of carotenoids and apocarotenoids</b>	92
<b>5.2 Protective and preventive bioactivities</b>	95

<b>5.3 Methods of analysis</b>	98
<b>References</b>	100

## **6 Supercritical fluid chromatography mass spectrometry for the characterization of limonoid aglycones in Citrus essential oils**

<b>6.1 Introduction</b>	102
<b>6.2 Experimental section</b>	103
<i>6.2.1 Samples and sample preparation</i>	103
<i>6.2.2 SFC-APCI-QqQ MS Analysis</i>	104
<i>6.2.3 Using the MS/MS system</i>	105
<i>6.2.4 SFC-QqQ MS optimization</i>	106
<i>6.2.5 Tentative identification of isobaric compounds</i>	108
<i>6.2.6 Quali/quantitative characterization</i>	112
<b>6.3 Conclusions</b>	115
<b>References</b>	116

## **7 Extraction and characterization of carotenoids and apocarotenoids from microalgae by supercritical fluid system**

<b>7.1 Introduction</b>	118
<b>7.2 Experimental section</b>	119
<i>7.2.1 Standards and samples</i>	119
<i>7.2.2 SFE-SFC-MS Instrumentation</i>	120
<i>7.2.3 Configuration of the SFE-SFC system</i>	120
<i>7.2.4 Optimization of the analytical method</i>	121
<i>7.2.5 Results of microalgae analyses</i>	123

<b>7.3 Conclusions</b>	128
<b>References</b>	129

## **8 Characterization of Native Composition of Orange *cv Pera* peel with carbon dioxide extraction and separative system**

<b>8.1 Introduction</b>	132
<b>8.2 Experimental section</b>	133
8.2.1 <i>Standard and sample</i>	133
8.2.2 <i>Optimization of the analytical method</i>	134
8.2.3 <i>Results of <i>cv. Pera</i> peel analyze</i>	135
<b>8.3 Conclusions</b>	138
<b>References</b>	139

## **9 Apocarotenoids profiling in different Capsicum species by supercritical fluid extraction and supercritical fluid chromatography**

<b>9.1 Introduction</b>	141
<b>9.2 Experimental section</b>	141
9.2.1 <i>Standard and sample</i>	141
9.2.2 <i>Optimization of the analytical method</i>	143
9.2.3 <i>Capsicum species chillies profile</i>	144
<b>9.3 Conclusions</b>	149
<b>References</b>	150

## **10 Online supercritical fluid extraction supercritical fluid chromatography method for determination of carotenoids and apocarotenoids in human blood samples**

<b>10.1 Introduction</b>	151
<b>10.2 Experimental section</b>	152
<i>10.2.1 Standards and blood samples</i>	152
<i>10.2.2 SFE-SFC-APCI-MS instrumentation</i>	153
<i>10.2.3 Optimization of the analytical method</i>	154
<i>10.2.4 SFE-SFC-MS intact blood analyses</i>	156
<b>10.3 Conclusions</b>	159
<b>References</b>	161

## **11 Analysis of human colostrum for the determination of carotenoids and apocarotenoids**

<b>11.1 Introduction</b>	164
<b>11.2 Experimental section</b>	166
<i>11.2.1 Standards and samples</i>	166
<i>11.2.2 Instrument and analytical conditions</i>	166
<i>11.2.3 Method validation</i>	168
<i>11.2.4 SFE-SFC-MS intact human colostrum analyses</i>	168
<b>11.3 Conclusions</b>	174
<b>References</b>	175

# Scope of the research work

My research work, during my Ph.D. course, was mainly focused on the development of analytical methods based on the use of supercritical carbon dioxide (CO<sub>2</sub>) for the analysis of food and biological samples.

In particular, the techniques used were: supercritical fluid chromatography coupled to mass spectrometry (SFC-MS) and supercritical fluid extraction online supercritical fluid chromatography coupled to mass spectrometry (SFE-SFC-MS).

Specifically, the use CO<sub>2</sub> under supercritical condition, has allowed the development of green analytical methods, in which the use of organic solvents, both for extraction and separation processes, is drastically reduced.

The on-line SFE-SFC-MS system, has allowed the development of advanced extractive and separative methods potentially applicable in fields clinical, health and food fraud.

Furthermore, the use of a mass spectrometer as a detector allowed to obtain detailed and precise information on the composition of the matrices analyzed for some classes of molecules with fundamental biological activities.

The on-line SFE-SFC-MS it was used for the extraction and detection of carotenoids and its oxidative-cleavage derivatives apo-carotenoids determination in food and biological samples.

Moreover, the SFC-MS system was also employed for a detailed elucidation on limonoids in cold-pressed *Citrus* essential oils.

# 1 Supercritical fluids

---

## 1.1 Properties of supercritical fluids

Supercritical fluids (SFs) were discovered already 200 years ago by Charles Cagniard de la Tour, demonstrating in 1822 for the first time the existence of a supercritical state with a series of experiments [1].

The supercritical state is explained with the phase diagram for a pure component such as carbon dioxide (Figure 1.1).

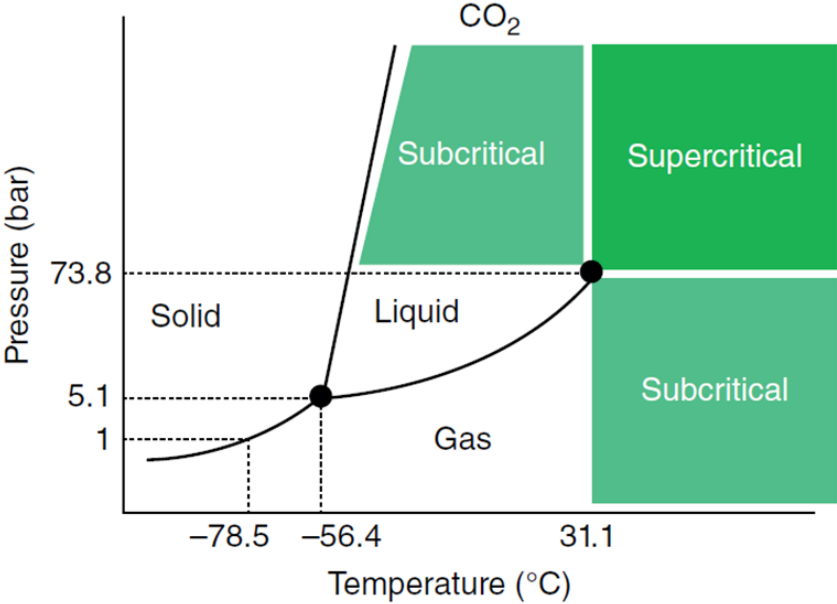
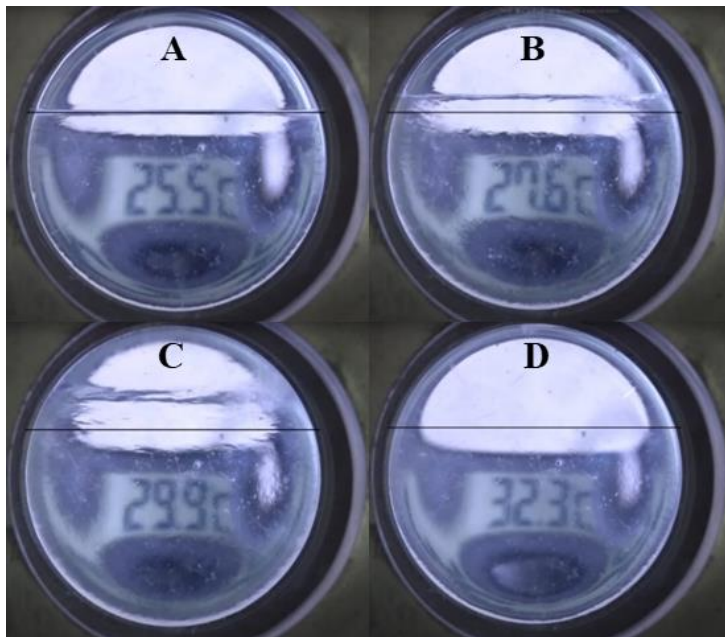


Figure 1.1 Phase diagram for pure carbon dioxide [2].

Three different states of matter (gas, liquid and solid) may be distinguished depending on temperature, and pressure, in fact they are defined and separated by precise curves.



Two phases can coexist on these boundary curves while the triple point marks the coexistence of the three commonly known phases: solid, liquid and gas. Moving on the boundary curve gas-liquid the liquid becomes less dense because of thermal expansion, and the gas becomes more dense as the pressure rises, the liquid-gas phase boundary curve ends at the critical point ( $P_C$ ), where the gas phase and liquid phase have the same density. Above the critical point, liquid and gas exist as one phase (Figure 1.2).



**Figure 1.2** In Figure A the line divides liquid and gas phase (meniscus), by increasing the temperature the meniscus gradually disappears (B and C), in D there is the complete disappearance of the meniscus because the gas and the liquid have the same density,  $\text{CO}_2$  it is in the supercritical state.

The transition from the gaseous or liquid phase to the supercritical phase does not involve a phase transition, therefore it is not a fourth phase of matter.

In Figure 1.1 are present two regions identified as subcritical phases along with the supercritical fluid region. These separations are a source of confusion [3], the supercritical region is formally separate by the subcritical regions, however the apparent boundaries are not phase transitions, only arbitrary definitions [3].

The physical properties of a supercritical fluid vary between those of a gas and those of a liquid by control of pressure and temperature. The SFs are used at densities ranging from 10 to 80% compared to the density of the liquid, using a pressure ranging from 50 to 300 atm. The diffusion coefficients of SFs are similar to those of a gas, whereas their viscosities are typically 10–100 times lower than liquids, these features provide limited pressure drop in the system and faster separation kinetics for chromatographic systems. The density and solvent power of the SFs are comparable to those of liquids, therefore they have excellent capacity of extraction and chromatographic separation; nevertheless they are more compressible than liquids, and that implies their density will severely change with pressure and temperature. The most features of the SFs lies in the fact that its properties are intermediate between those of gases and those of liquids (Table 1.1). By suitably changing the temperature or pressure (or both), it is possible to change the characteristics of the fluid to adapt them, for example, to enhance the solubility of a component of specific interest or to improve the chromatographic separation of a mixture of compounds. For these

favorable physical properties the SFs are most used in chromatography and extraction applications [4].

**Table 1.1** Properties of supercritical fluids in comparison with liquids and gases.

	Density $\rho$ (g/mL)	Diffusion $D_m$ (m <sup>2</sup> /s)	Viscosity $\eta$ (g/cm·s)
Liquid	1	$10^{-10}$ - $10^{-9}$	$10^{-2}$
Supercritical fluid	$10^{-1}$ -1	$10^{-7}$ - $10^{-6}$	$10^{-4}$ - $10^{-3}$
Gas	$10^{-3}$	$10^{-4}$	$10^{-4}$

In theory, all substances can be transitioned into their supercritical fluid state, but very few are applicable from a practical point of view, because they must have a low molecular weight, a critical temperature close to the ambient temperature ( $T_c$  10-40 °C) and a not too high critical pressure ( $P_c$  40-60 atm). In Table 1.2 the critical points of some compounds are represented, which have already been utilized as SFs [5].

Supercritical water is being used for the oxidative destruction of toxic waste for its oxidative power in the field of "green chemistry", although its critical parameters are much less convenient than those of other substances. There is a particular interest also in subcritical water because of the behavior of its polarity in these conditions.

Ammonia has similar behavior to that of water, but not often used. Many halocarbons are excellent for extracting short chain hydrocarbons but they have the disadvantage of being very expensive and of being harmful to the environment.

Nitrous oxide is excellent for extraction of polar compounds, but its high oxidizing power reduces its use with oxidizable and organic modifying analytes and can also cause violent explosions [6].

Many of the SFs studied are toxic, corrosive and polluting and some are unsuitable for the analysis of thermolabile compounds because they have high critical temperature and critical pressure.

**Table 1.2** Critical temperature and pressure of some compounds [6].

Substance	Critical Temperature $T_c$ (K)	Critical Pressure $P_c$ (bar)
Carbon dioxide	304	74
Water	647	221
Ethane	305	49
Propane	370	42
Ethene	282	50
n-Pentane	470	33
Xenon	290	58
Ammonia	406	114
Nitrous oxide	310	72
Fluoroform	299	49
Chloroform	301	39
Isopropanol	509	47
Methanol	514	79
Ethanol	517	63

## 1.2 Supercritical carbon dioxide

### *1.2.1 Characteristics and properties*

The best mobile phase for supercritical fluid chromatography is CO<sub>2</sub>. The critical point of carbon dioxide is 7.38 MPa and 31.1 °C [7], which means that the supercritical state is readily accessible and safe for analysis of bio-molecular systems, pharmaceutical compounds, and numerous of thermally labile molecules. Moreover, CO<sub>2</sub> is safe (low toxicity, non-inflammable, non-corrosive), inert, easily available at high purity and at a low price finally, it separates easily from the extracted solute because at atmospheric temperature and pressure it is a gas.

CO<sub>2</sub> is not a polar molecule but has a significant quadrupolar moment as it does not have a homogeneous distribution of the electronic density due to the presence of polarized carbon-oxygen bonds. CO<sub>2</sub> is therefore miscible with apolar organic solvents (*n*-hexane, toluene, etc.) and with polar solvents, even if limited, such as water, alcohols and acetonitrile. Due to the different polarity between the carbon atom and the two oxygen atoms CO<sub>2</sub> act both as weak Lewis base and weak Lewis acid, therefore, it creates conventional and nonconventional hydrogen-bonds [4].

CO<sub>2</sub> has interesting affinity for fluorinated compounds as metal complexes and fluoropolymers, but for polymers and hydrocarbons of high molecular weight it is not such a good solvent [6].

### 1.2.2 Density

A small change in pressure in an SF leads to a large change in density, compared to the same molecule in liquid form, moreover, the closer the temperature and pressure to the critical point the more the density is affected by the pressure. By increasing the temperature of the SF, the system pressure must necessarily be increased to obtain the same density as the fluid.

In table 1.3 are present the density values of CO<sub>2</sub> in the supercritical phase (scCO<sub>2</sub>).

**Table 1.3** Density mg/mL for scCO<sub>2</sub> as a function of pressure and temperature [8].

T (°C)	P (MPa)						
	7.4	10	20	30	40	50	60
31	0.42	0.76	0.89	0.94	0.99	1.02	1.04
40	0.23	0.62	0.83	0.91	0.96	0.99	1.02
50	0.19	0.38	0.78	0.88	0.92	0.96	0.99
60	0.17	0.29	0.72	0.83	0.89	0.93	0.97
70	0.16	0.25	0.66	0.78	0.86	0.90	0.94
80	0.15	0.22	0.59	0.74	0.82	0.88	0.92
90	0.14	0.21	0.54	0.70	0.79	0.85	0.89
100	0.13	0.19	0.48	0.66	0.76	0.82	0.87

Density values above 80 g/mL are important for extraction processes with scCO<sub>2</sub>, especially for lipids because the maximum extraction capacity for a supercritical fluid is obtained when it has a density similar to the compound to be extracted [9].

In Saitow's work an equation is described to theoretically calculate the density of SFs (equation 1.1) [10].

$$\rho = \frac{6\pi \cdot \eta \cdot \xi \cdot \lambda_C}{k_B \cdot T \cdot C_P} \quad \text{Equation 1.1}$$

The equation refers to a spherical fluid system and  $\rho$  is the density,  $\eta$  viscosity,  $\xi$  correlation length,  $\lambda_C$  the critical part of thermal conductivity,  $k_B$  Boltzmann constant,  $T$  temperature and  $C_P$  specific heat capacity at constant pressure.

The theoretical values are similar to experimental data when the density increases linearly with pressure, but when the density increases suddenly the data of the equation of state are different from the experimental values. The density prediction with equation of Saitow is more accurate for temperature and pressures values far from  $P_C$  values. However, a large number of experimental data for  $scCO_2$  have been collected over time and the density values for certain temperature and pressure conditions are very precise.

### *1.2.3 Diffusivity*

SFs have a high diffusivity and low viscosity, which allows them to have a high mass transfer.

The mass transfer is a key factor in extraction because controlling the kinetics of the process and yields, and in chromatography because affects the separation and resolution of the peaks.

SFs, like all fluids, are subject to self-diffusion (also known as Brownian motion), that is a chaotic diffusion of molecules in the absence of a chemical potential gradient, and binary diffusion (chemical diffusion) that is a no chaotic diffusion of molecules occurring due to a concentration gradient of the compound [11].

Self-diffusion coefficients can be calculated by the Stokes Einstein equation and from variants created by Wilke Chang (equation 1.2) [8].

$$D = \frac{k_B \cdot T}{C_P \cdot \pi \cdot \eta \cdot a} \quad \text{Equation 1.2}$$

The Stokes-Einstein equation correlates the translational diffusion coefficient,  $D$ , of a sphere of fluid of radius  $a$ , which moves within a solvent system with a dynamic viscosity,  $\eta$  with a temperature  $T$  and a specific heat capacity at constant pressure  $C_P$ .

The binary diffusion of a compound varies with time, for example in the extraction, and can be calculated with the equation of Fick's second law of diffusion (equation 1.3) [8].

$$\frac{\partial c}{\partial t} = D_b \cdot \Delta_c \quad \text{Equation 1.3}$$

The differential equation correlates the variation in the concentration of a component ( $\partial c$ ) with respect to time ( $\partial t$ ) with the binary diffusion ( $D_b$ ) with respect to the concentration ( $\Delta_c$ ).

In literature there are few experimental binary diffusion coefficients due to measurement difficulties.

Experimentally the supercritical  $\text{CO}_2$  was used to determine the binary diffusion coefficients of acetone, benzene, naphthalene, 1,3,5-trimethylbenzene, phenanthrene, pyrene and chrysene with the Taylor dispersion method, in which it is measured, through a capillary tube, the dispersion of a solute in a laminar flow.

Increasing the molecular weight and dimensions decreases diffusion coefficients. Molecules with heavy isotopes have shorter bonds and therefore lower molar volumes than molecules with normal isotopes, this is the cause of higher diffusion coefficients [12].

Diffusion coefficients decrease considerably with increasing density and viscosity of the SFs, while effects of temperature are minimal, for



example the diffusion coefficients of scCO<sub>2</sub> only increase with 10% when temperature increases from 30 °C to 60 °C. For liquid CO<sub>2</sub> there is an opposite effect, the diffusion coefficient is almost double in the same temperature range (figure 1.3).

With the addition of an organic solvent, the viscosity and density of the mixture increases in comparison with pure scCO<sub>2</sub> (using same conditions of temperature and pressure) and the diffusivity decreases [11].

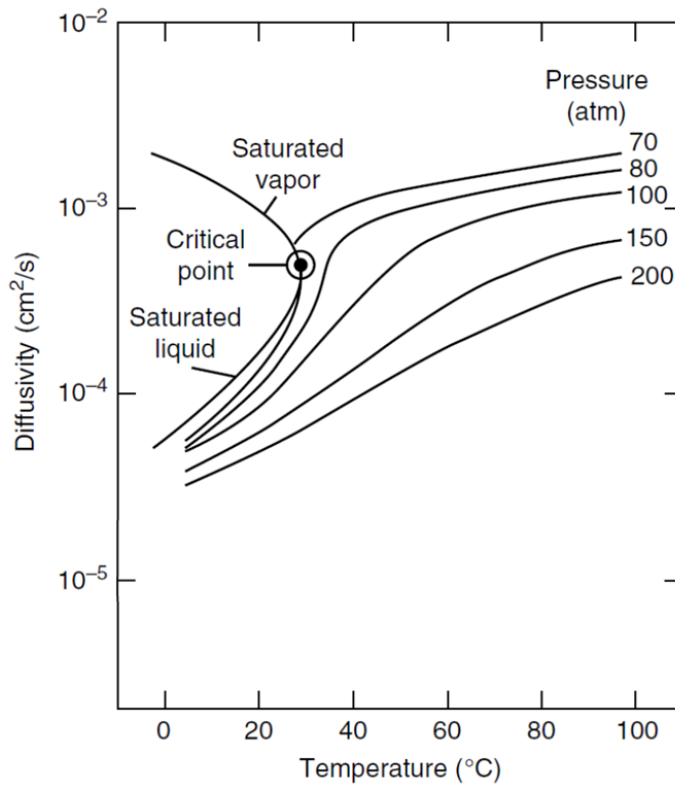


**Figure 1.3** The variation in CO<sub>2</sub> diffusivity with respect to the variation in temperature for different pressures [4].

### 1.2.4 Polarity

Polarity is a property quantifying the dipolar moment of a molecule, it is not influenced by temperature, pressure or passage in the supercritical phase.

CO<sub>2</sub> is not polar as it has an overall dipole moment equal to zero, but it exhibits a significant bond dipole moment due to the different polarity between the carbon atom and the two oxygen atoms, this creates a quadrupolar moment (Figure 1.4). This allows, as already mentioned, the formation of weak hydrogen bonds with polar molecules. This characteristic allows CO<sub>2</sub> act both as weak Lewis base and weak Lewis acid, therefore, it creates conventional and nonconventional hydrogen-bonds [4].

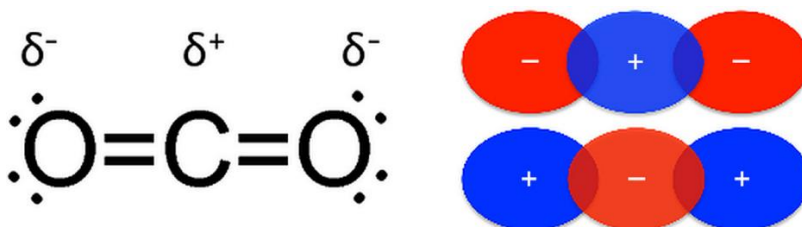


**Figure 1.4** Representation of the dipole moment and the quadrupolar moment of the CO<sub>2</sub> [8].

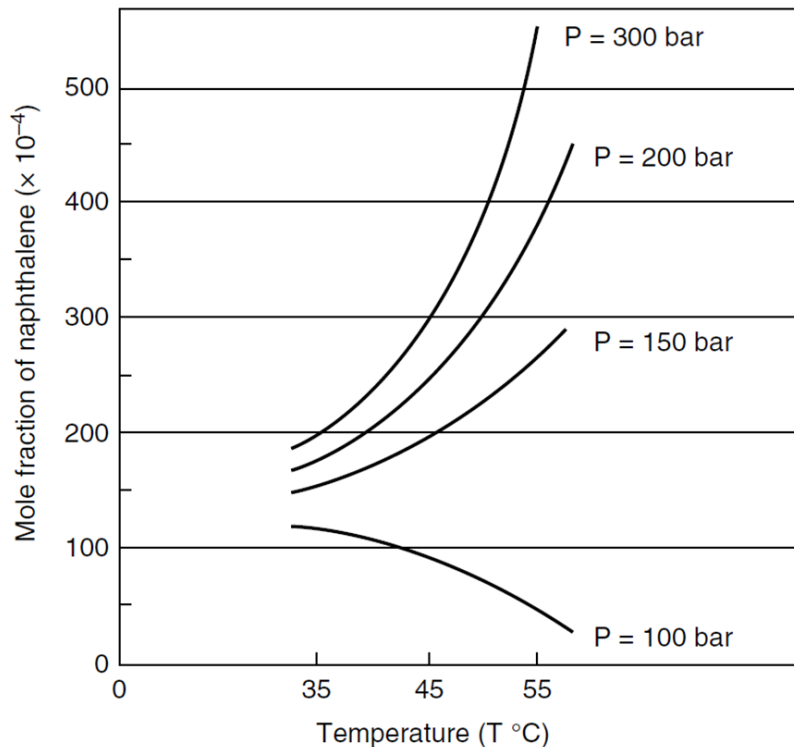
When a cosolvent is used, the intermolecular interactions cause an increase in density and a decrease in the volume of the mixture. When the pressure increases, especially near the critical point, the space between the molecules of solvent and CO<sub>2</sub> decreases, which creates a larger number of hydrogen bonds [13].

Increasing the temperature has the opposite effect, the breaking of the hydrogen bonds cause a decrease in the miscibility of the cosolvent with the scCO<sub>2</sub>.

An example of the dielectric properties of  $\text{scCO}_2$  is its higher solubility of water, methanol and ethanol in comparison to carbon monoxide in supercritical state. The explanation for this effect is the hydrogen bonding between the oxygen in  $\text{CO}_2$  and the hydrogens in the solvents [14].

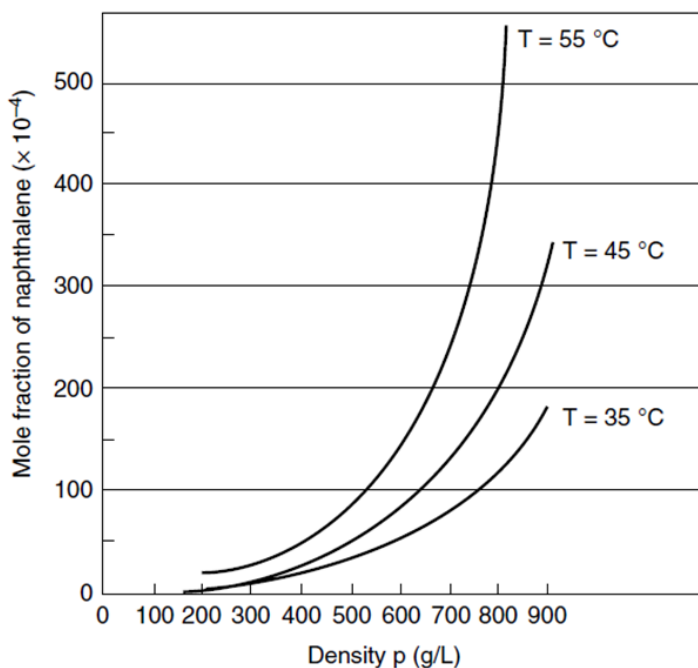
### 1.2.5 Solvating power

The solvating power of SFs are dependent on temperature and pressure. At low pressure, the solvating power decreases with rising temperature, while at high pressures it increases exponentially as shown in figure 1.5 which represents the solubility of naphthalene in  $\text{scCO}_2$ .



1.5 Solubility of naphthalene in  $\text{scCO}_2$  as a function of temperature at different pressures [4].

By correlating the solvent power with the density as the temperature changes, a graph is obtained with a different solubility-temperature relationship (Figure 1.6). By increasing the density of scCO<sub>2</sub> the solvating capacity increases exponentially for any temperature.



**1.6** Solubility of naphthalene in scCO<sub>2</sub> as a function of density at different temperatures [4].

This peculiar phenomenon occurs because density and solvating power are directly related, the increase in pressure causes an increase in density and consequences an increase in the solubility of a compound in the supercritical fluid, while an increase in temperature has the opposite effect.

At low pressure, the density decreases drastically with an increase in temperature therefore the solvating power decreases considerably. At higher pressure, changes in temperature have much less effect on

density and therefore also on the solvating power. Therefore, the solvating power is related to the density of the supercritical fluid and can be modified through temperature and pressure [4].

This characteristic of SFs is unique because the solvating capacity of liquids and gases does not change significantly, consequently, it can be used to obtain excellent extractions on a large variety of compounds [15].

The first study on solubility of compounds into CO<sub>2</sub> was developed by Giddings et al. [16] based on Hildebrand solubility parameter ( $\delta$ ) [17]. For estimate the solubility parameter of a supercritical fluid Giddings used the following relation (equation 1.4):

$$\delta = 1.25 \cdot P_C^{1/2} \cdot (\rho_f / \rho_l) \quad \text{Equation 1.4}$$

$P_C$  is the critical pressure, and  $\rho_f$  and  $\rho_l$  the reduced density of the supercritical and the liquid fluid [16]. The  $\delta$  parameter represents shows the ability for CO<sub>2</sub> to dissolve the compounds, and it is determined as the ratio of the cohesive energy  $\Delta E$  and the molar volume of the considered compound ( $\delta = \text{cal/cm}^3$ ).

Liquid CO<sub>2</sub> with a density of 1.23g/mL has a solubility value of 10.7 cal/cm<sup>3</sup>, similar to that of pyridine.

With a density of 0.9 g/mL in supercritical conditions, the solvating capacity is close to that of aromatic compounds such as benzene and toluene.

By decreasing the density of CO<sub>2</sub> to 0.6 g/mL,  $\delta$  approaches that of pentane (6.5 cal/cm<sup>3</sup>).

The theoretical values of solubility of CO<sub>2</sub> are generally higher than the experimental values, therefore the Giddings formula is an approximation of the solvent power of CO<sub>2</sub> [18].

### **1.3 Modifiers**

As already mentioned, scCO<sub>2</sub> has an excellent solvating power for non-polar compounds while it has a limited ability to solubilize polar compounds. In order to increase the elution strength of the mobile phase, small amounts of a polar solvent, called modifier or co-solvent, is usually added to scCO<sub>2</sub>.

Most common used modifiers for increase the polarity are isopropanol (IPA), methanol (MeOH), acetonitrile (ACN), and ethanol (EtOH).

Small quantities of water can also be added to the scCO<sub>2</sub> to increase the solubility of polar compounds, aliphatic hydrocarbons to decrease the polarity, toluene to insert aromaticity, [R]-2-butanol to obtain a chiral mobile phase, and tributyl phosphate to enhance extraction or separation of metal complexes.

#### *1.3.1 Main characteristics of the polar modifiers*

The modifier will change some physicochemical properties of the mobile phase such as the viscosity and dielectric constant, and can generate further interactions such as hydrogen bonding or dipole-dipole, leading to modifications in selectivity of extraction and variation of peaks retention time.

With modifier addition the critical point of the mobile phase will considerably shift because the critical temperature and the critical

pressure will increase, depending on the percentage and the nature of the modifier added to carbon dioxide, as shown in Figure 1.7 for a series of scCO<sub>2</sub> and methanol mixtures. This means that in most of the extractions and separations with SF, the state of the mobile phase should be defined as “subcritical”, rather than “supercritical”, because with a working temperature typically between 40°C and 60°C, increasing the amount of modifier in the system quickly increases the pressure and temperature values to maintain the supercritical state, if it does not inevitably occur the system switches to a subcritical state [19].

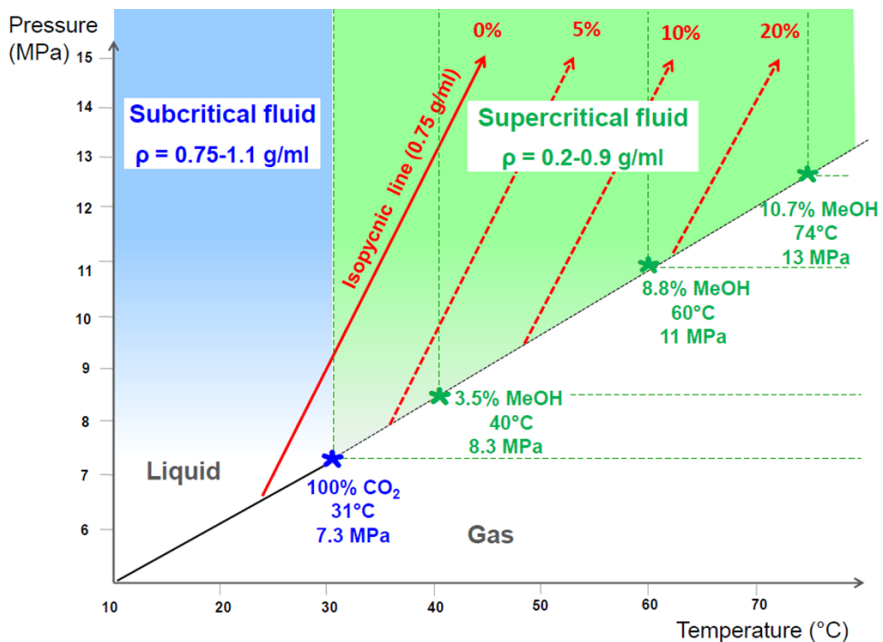


**Figure 1.7** Phase diagram for pure carbon dioxide (in blue) and carbon dioxide mixed with methanol at different proportions (in green) [18].

Conditions as pressures and temperature much below the critical point results in separation of the fluid into two phases, one scCO<sub>2</sub> and another with only modifier [20].

When this phenomenon does occur, solubility of the analytes is modified, inducing strong changes in the extraction capacity and of the fluid chromatographic retention, and a noisy baseline is observed for spectrophotometer detectors due to the liquid-gas heterogenous mixture [20]. However, Sandra et al. [21] developed an experiment in which he showed that the increase from 10 to 25% of modifier (MeOH) did not disturb the signal of the evaporative light-scattering detector (ELSD) because the analytes were solubilized in the liquid part of the mobile phase [20].

Such phase separation was never reported for so-called "subcritical" condition with a pressure value above critical pressure but with a temperature lower than the critical temperature. This subcritical condition is however, widely used in chromatography therefore is no need to change the operating temperature and pressure when developing a method in order to necessarily maintain the supercritical conditions. Keeping the back pressure above the critical pressure of the mobile phase composition, the temperature can be maintained below the critical temperature, obtaining a subcritical system.

This operational feature is very important because the high critical temperature in the mixtures of CO<sub>2</sub>-solvent would be inadequate for most for most thermolabile compounds analyzed and for chromatographic columns [20].

### *1.3.2 Solubility of mixtures of binary fluids*

Interactions between CO<sub>2</sub> and co-solvents are important for evaluating the chemical-physical properties of the fluid, they have been studied with the help of solvatochromic parameters [22].



The parameters considered are  $\pi^*$  (describing the polarity and polarizability) the  $\alpha$  acidity (includes the ability to donate hydrogen bonds with hydrogen atoms), and the  $\beta$  basicity (includes the ability to accept hydrogen bonds with oxygen or nitrogen atoms). These parameters have been calculated with spectroscopic measurements for mixtures of CO<sub>2</sub> with methanol and acetone at a temperature of 35 °C (figure 1.8) [23].

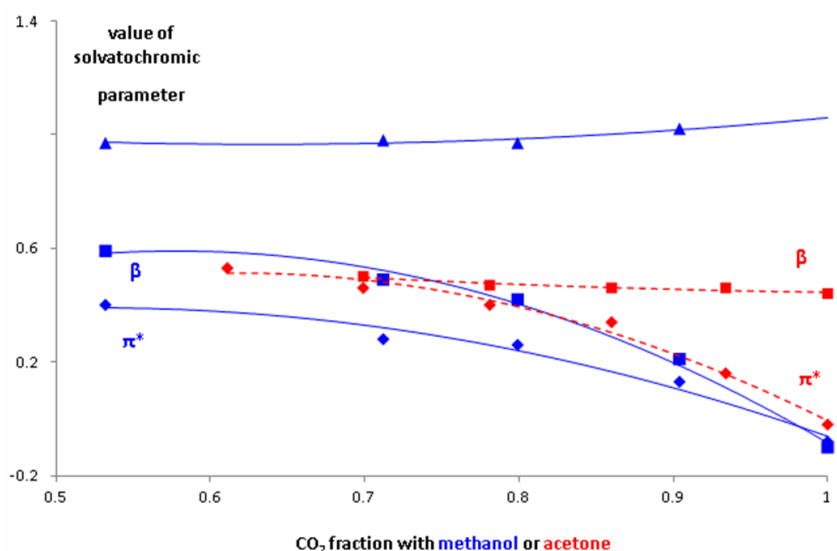


**Figure 1.8** Variation of the solvatochromic parameters with respect to the increase in the percentage of co-solvent determined by spectrophotometer [18].

The increase in the methanol fraction in the binary mixture causes an increase in  $\pi^*$  and  $\beta$  of the mixture, while  $\alpha$ , which represents acidity, remains constant.

For the CO<sub>2</sub>-acetone mixture the polarity increases ( $\pi^*$ ) while the basicity ( $\beta$ ) remains constant, for the acetone the acidity has not been calculated because it has no hydrogens which can form hydrogen bonds.

Other studies were performed at different pressures for CO<sub>2</sub>-alcohols mixtures. These articles have shown that an increase in pressure causes a decrease in polarity and basicity, this effect is thought to be due to the greater interaction of the CO<sub>2</sub> and co-solvent molecules because they are closer.

The CO<sub>2</sub>-methanol mixture was studied also from 0 to 100% co-solvent by a solvatochromic approach at 25°C, the results showed significant increase in the  $\pi^*$  polarity and polarizability parameter [18].

Deye et al. [24] studied the solvation of the binary CO<sub>2</sub>-methanol mixture by spectroscopic measurements, using Nile Red dyes with E<sub>NR</sub> scale (the E<sub>NR</sub> scale represents the intensity of the fluorescence of the Nile Red dye, the higher the polarity the lower the dye fluorescence). Figure 1.9 represents the change in E<sub>NR</sub> with the percentage of methanol in the binary mixture.

The solvent power of CO<sub>2</sub> mixed with 5% methanol is close to diethyl-ether, when 10% methanol is used it is similar to 1,4-dioxane, with 20% methanol it compares to ethyl acetate, with 40% methanol it has the solvent power of methylene chloride [18].

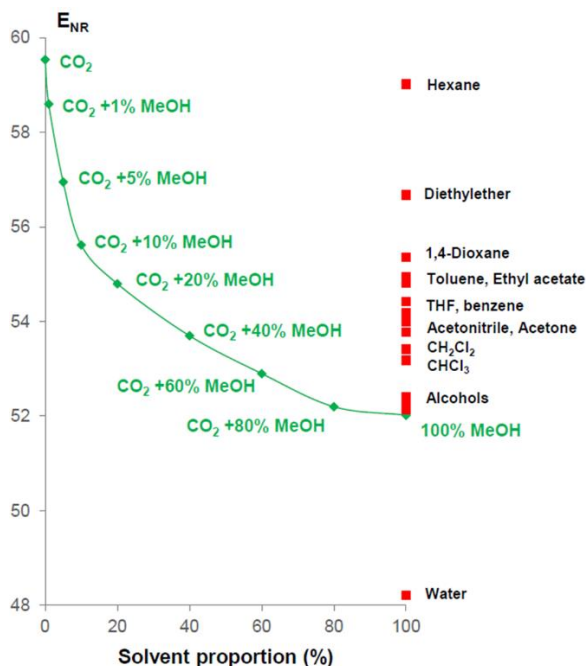


**Figure 1.9** Variation of  $E_{NR}$  compared to the percentage of methanol in the mixture of CO<sub>2</sub>-methanol and solvents with similar  $E_{NR}$  for comparison [18].

Small additions of methanol cause a sharp decrease in the  $E_{NR}$  and therefore large increases in the strength of the solvent. The authors of the study speculated that the dye used is surrounded by a solvation sphere of methanol, called "cluster", which is not equal to composition of the binary mixture. Therefore, the similarities of the solvating powers described above may not be correct as the polarity of the binary mixture is overestimated.

Within a cluster, the concentration of the modifier is higher, creating micro-zones with much greater polarity than the composition of the fluid. Furthermore, in conditions of pressure and temperature close to the critical point, the clustering is more widespread because there is a greater compressibility of the fluid.

Therefore, small amounts of a polar modifier can significantly increase the solubility of a polar solute, but they will not affect the solubility of non-polar analytes.

Furthermore, the greater the difference in polarity between the co-solvent and the pure scCO<sub>2</sub>, the greater the change in polarity when the modifier is added, but at the same time the lower the quantity of co-solvent that can be mixed with the scCO<sub>2</sub> [4].

## References

- [1] B. Berche, M. Henkel, R. Kenna. Critical phenomena: 150 years since Cagniard de la Tour. *Rev. Bras. Ens. Fis.*, 2009, 31 2602.
- [2] L. Laboureur, M. Ollero, D. Touboul. Lipidomics by supercritical fluid chromatography. *International Journal of Molecular Sciences*, 2015, 16, 13868.
- [3] T. L. Chester. Unified chromatography from the mobile phase perspective. *ACS Symposium Series*, 1999, 748, 6.
- [4] L. M. Miller, J. D. Pinkston, L. T. Taylor. *Modern Supercritical Fluid Chromatography: Carbon Dioxide Containing Mobile Phases*. Publisher John Wiley & Sons Inc, 2019.
- [5] S. Moret, G. Purcaro, L. S. Conte. *Il campione per l'analisi chimica*. Publisher Springer-Verlag Mailand, 2014.
- [6] A. A. Clifford, J. R. Williams. *Introduction to Supercritical Fluids and Their Applications*. Publisher Humana Press, 2000.
- [7] "Phase change data for Carbon dioxide". National Institute of Standards and Technology. Retrieved, 2008, 01, 21.
- [8] F. Pena-Pereira, M. Tobiszewski. *The Application of Green Solvents in Separation Processes Chapter 7*. Publisher Elsevier, 2017.
- [9] J. M. del Valle, J. C. de la Fuente. Supercritical CO<sub>2</sub> extraction of oilseeds: review of kinetic and equilibrium models. *Critical Reviews in Food Science and Nutrition*, 2007, 46, 131.
- [10] K. Saitow, D. Kajiya, K. Nishikawa. Dynamics of Density Fluctuation of Supercritical Fluid Mapped on Phase Diagram. *Journal of the American Chemical Society*, 2004, 126, 422.
- [11] A. D. McNaught, A. Wilkinson. *Compendium of chemical terminology The Gold Book, Second Edition*. IUPAC, 1997.
- [12] G. Jancso. *Radiochemistry and nuclear chemistry V I Isotope effects, isotope separation and isotope fractionation*. Publishers EOLSS Co. Ltd, Oxford, 2009.

- [13] D.S. Bulgarevich, T. Sako, T. Sugeta, K. Otake, Y. Takebayashi, C. Kamizawa, M. Uesugi, M. Kato. Microscopic solvent structure of subcritical and supercritical methanol from ultraviolet/visible absorption and fluorescence spectroscopies, *Journal of Chemical Physics*, 1999, 111, 4239.
- [14] P. Raveendran, Y. Ikushima, S.L. Wallen. Polar attributes of supercritical carbon dioxide. *Accounts of Chemical Research*, 2005 37, 478.
- [15] L.T. Taylor. *Supercritical Fluid Extraction*. Wiley Analytical Science Chapter 2, 1996.
- [16] J.C. Giddings, M.N. Myers, J.W. King. Dense Gas Chromatography at Pressures to 2000 Atmospheres. *Journal of Chromatographic Science* 1969, 7, 276.
- [17] J.H. Hildebrand, R.L. Scott. *The solubility of non-electrolytes*. Dover, 3rd ed., 1964.
- [18] E. Lesellier, C. West. The many faces of packed column supercritical fluid chromatography-A critical review. *Journal of Chromatography A* 2015, 1382, 2.
- [19] J. D. Pinkston, D. T. Stanton, D. Wen. Elution and preliminary structure-retention modeling of polar and ionic substances in supercritical fluid chromatography using volatile ammonium salts as mobile phase additives, 2004, 115.
- [20] *Supercritical fluids chromatography* 1<sup>st</sup> Edition, Elsevier, 2017.
- [21] G. Vanhoenacker, P. Sandra, F. David, A. Pereira, C. Brunelli. A simple instrumental approach for "Supercritical" fluid chromatography in drug discovery and its consequences on coupling with mass spectrometric and light scattering detection. *LCGC North America*, 2011, 29, 1006.
- [22] R. W. Taft, M. J. Kamlet. The solvatochromic comparison method. 2. The alpha-scale of solvent hydrogen-bond donor (HBD) acidities *Journal of the American Chemical Society*, 1976 98, 2886.
- [23] V.T. Wyatt, D. Bush, J. Lu, J.P. Hallett, C.L. Liotta, C.A. Eckert, Determination of solvatochromic solvent parameters for the characterization of gas-expanded liquids. *The Journal of Supercritical Fluids*, 2005, 36, 16.

[24] J.F. Deye, T.A. Berger, A.G. Anderson. Nile Red as a solvatochromic dye for measuring solvent strength in normal liquids and mixtures of normal liquids with supercritical and near critical fluids. *Analytical Chemistry*, 1990, 62, 615.

## 2 Supercritical fluid extraction

---

### 2.1 Introduction

Supercritical CO<sub>2</sub> is advantageous to use as a solvent for extractive processes compared to classic organic solvents because, as already mentioned in chapter 1, it has a low toxicity, is non-flammable and non-corrosive is also easily available with high purity and low price and it separates easily from the extracted solute because at temperature and atmospheric pressure is a gas.

In addition, the supercritical fluids have intermediate properties between those of a liquid and those of a gas; in particular, they have density like that of a liquid and viscosity like that of a gas.

Therefore, supercritical fluids have a solvent capacity similar to that of traditional solvents but the diffusion of the analyte (mass transfer) from the matrix to the supercritical fluid will be faster.

All this can mean lower solvent consumption and, consequently, lower costs compared to traditional liquid-liquid extractions or through Soxhlet (considering also the costs related to the disposal of solvents).

Choosing the correct supercritical fluid, temperature, pressure, and sample collection method is important in order to perform a highly selective extraction of the analyte of interest

The extracts obtained will contain more analytes than those obtained with organic solvents, and them require partial or even no purification after the extraction.



Other advantages offered by this technique are the possibility of automation and its applicability in varied sectors (polymers, food, pharmaceutical, environmental). SFE is a valid alternative to traditional extractions, as it limits the consumption of organic solvents, reduces analysis times and can be easily automated [1].

## **2.2 Sample preparation**

A matrix, to be extracted correctly with an SFE system, must be a solid powder with a high surface area and good extraction permeability.

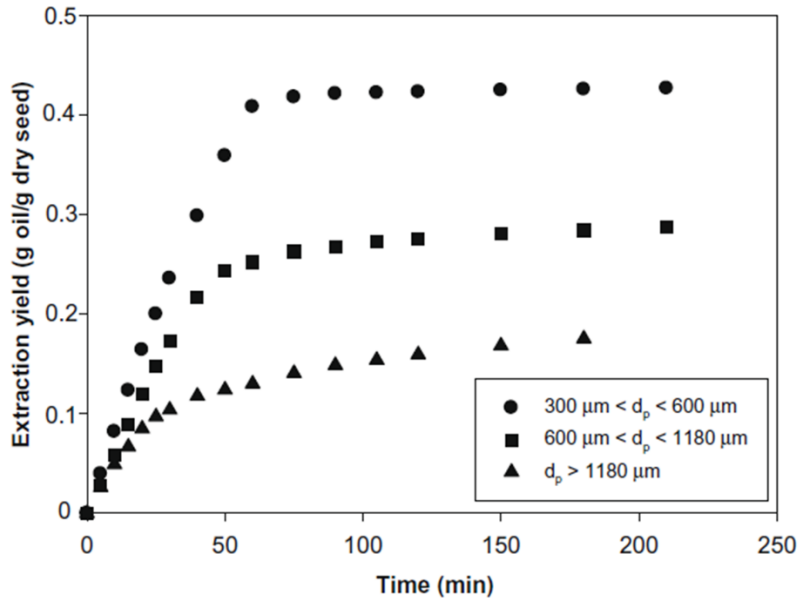
The smaller the particles, the greater the surface of the matrix in contact with the supercritical fluid and the shorter the path that the analyte must travel to diffuse into the fluid.

However, particles that are too small cause a reabsorption effect of the analytes on the surface of the particles and the formation of "preferential paths" in the packed system of the matrix. These problems can be solved by increasing the flow and extraction temperature [2].

Döker et. al [3] experimentally demonstrated these phenomena with the extraction yields of ground sesame seed oil, with particles having a diameter of 1180  $\mu\text{m}$ , 600-1180  $\mu\text{m}$  and 300-600  $\mu\text{m}$  with temperature at 50 °C, pressure 350 bar and flow 1.81 g CO<sub>2</sub>/min (Figure 2.1).

Extractions with 1180  $\mu\text{m}$  particles have lower yields than smaller particles, regardless of time.

Interesting is the exponential increase in yield with the increase in the extraction time of small particles, this effect is determined by the supercritical fluid to penetrate more easily inside the matrix.



**2.1** Extraction yield of sesame oil over time with different grain sizes of ground sesame (1180  $\mu\text{m}$ , 600-1180  $\mu\text{m}$  and 300-600  $\mu\text{m}$ ) [2].

To obtain a good extraction is necessary to completely fill the container in which the sample is inserted and remove dead volumes that decrease the extraction efficiency and yield.

A powder is used to fill the extraction container and "dilute" the solid sample with which it is mixed.

The powder increases the contact surface of the matrix with the supercritical fluid and fills the empty spaces inside the container to facilitate its extraction.

These powders must be composed of inert materials that do not interact with the analytes of the matrix to be extracted, this characteristic is very important because it could greatly influence the yield of the extract.

The liquid matrices, generally, are not analyzed as such but absorbed on a solid porous support or a powder.

Matrices with a high percentage of water must be dried or freeze-dried before extraction. While samples containing a small amount of water are mixed with an adsorbent powder containing alumina or magnesium sulfate.

For samples containing negligible amounts of water it is preferable not to use a desiccant adsorbent powder but only a sample dispersion system.

These differences in the treatment of the matrix are due to two opposite phenomena that can occur in the extraction process. Water, in small percentages, acts as a modifier of scCO<sub>2</sub> improving the extraction of molecules with polar groups, without significantly changing the extraction of non-polar molecules.

If the sample has an excessive amount of water, the supercritical fluid does not solubilize it and two phases are formed in the extraction vessel. Excess water solubilizes the more polar compounds and creates a barrier between scCO<sub>2</sub> and non-polar compounds [2]

### **2.3 Extraction optimization**

To optimize an extraction process, it is necessary to consider some variables such as: pressure, temperature and density of the supercritical fluid but also flow rate, type and quantity of the modifier. Some parameters are optimized according to pre-established ranges (pressure 150-500 atm, temperature 35-150 °C, flow 1-3mL/min), while the most used modifiers are methanol, ethanol and acetonitrile [3].

### 2.3.1 Pressure, temperature and density

Extraction of an analyte with a supercritical fluid depends on three pressure parameters: miscibility pressure (the solute begins to diffuse into the supercritical fluid), pressure of maximum solubility (in which the maximum solubility of the analyte is obtained) and pressure fractionation (pressure interval between the two previous parameters and which allows to obtain a very selective extraction).

Figure 2.2 represents the extraction yield versus flow for carotenoids and tocopherols in tomato waste at two pressure values (380 bar and 460 bar), with a constant temperature of 60 °C [5].

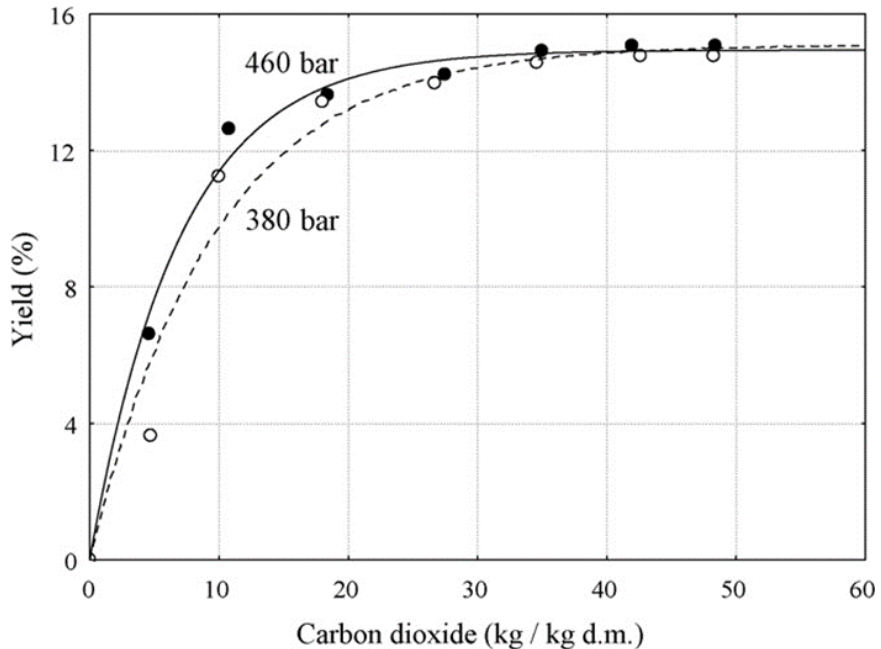


**Fig. 2.2** Extraction yield of tocopherols and carotenoids from tomato waste at different pressures, 380 bar and 460 bar [5].

The increase of the pressure causes an increase of the supercritical fluid's density, therefore improves its solvent power and therefore increases the extraction yield for all the compounds present in the

matrix, however this phenomenon causes a lower extraction selectivity. Generally, for selective extractions a pressure value is used that is within the fractionation pressure range to obtain greater selectivity, while for non-selective extraction processes the pressure value of maximum solubility is preferred. Exceeding this value, no extractive advantage is obtained for the analyte considered [5].

The increase in temperature doesn't always determine an increase in extractive yields, as for pressure, because it depends on the nature of the analyte and the density of the fluid.

The increase of the temperature causes a decrease of the density of the supercritical fluid and therefore a decrease of its solvent power but also a greater mobility of the molecules that tend to transfer from the matrix to the supercritical fluid more easily, especially the volatile molecules, because their mobility increases [2].

If the pressure is too low, or the temperature too high, the solvent power of the fluid will be very low, it will behave more like a gas than a liquid and the extraction yield will be low. Consequently, the main parameter to be optimized is the pressure, to which the density of the fluid is connected, while the temperature is a secondary parameter due to its difficulty of optimization.

### *2.3.2 Modifiers for extraction*

Extraction with scCO<sub>2</sub> is limited to non-polar compounds due to the specific characteristics of carbon dioxide, described in the previous chapter.

Solvents and additives are used to apply this technique also for the extraction of medium polar compounds. They interact with the polar

groups of the molecules present in the matrix, facilitating their diffusion in the supercritical fluid.

The most used compounds for this purpose are organic solvents like methanol ethanol and acetonitrile, and are called modifier.

They can be inserted directly into the extraction cell, before the extraction process or added during the extraction process, using the pumps. This method is the most used because it allows to keep the fluid conditions constant and to have a greater reproducibility of the process. Using polarity modifiers causes an increase in the  $T_C$  and critical pressure  $P_C$  of the fluid. The increase in critical parameters depends on the nature of the modifier and on the quantity, the greater is polarity and quantity, the greater the  $P_C$  and  $T_C$ .

Generally, to maintain the supercritical conditions of the fluid, the modifier must not exceed 8-10% of total flow, higher percentages cause a subcritical phase of the fluid, with percentages higher than 80% we speak of compressed fluids [6].

The modifier used is determined by its ability to solubilize the compound (or class of compounds) but also by its ability to swell the solid matrix to facilitate the penetration of  $scCO_2$  to extract the analyte. Some compounds can be extracted using small percentages of water as the sole co-solvent or together with organic solvents. Water improves the extraction process, but it causes a significant increase in  $T_C$  and  $P_C$ , so the system needs very high pressures and temperatures to keep the system as a single fluid and avoid phase separations.

Some extraction processes are conducted with the use of vegetable oils, this process is used to improve the extraction of very expensive compounds or for food consumption.

**Table 2.1** Yield of lycopene ( $\mu\text{g/g}$ ) extracted from tomato peel with pure  $\text{scCO}_2$  and with three co-solvents (5%) at different temperatures and pressures [7].

Pressure	Temperature	25 MPa			30 MPa			35 MPa		
		45 °C	60 °C	75 °C	45 °C	60 °C	75 °C	45 °C	60 °C	75 °C
Modifier	%									
-	0	11.0 $\pm$ 1.6	13.1 $\pm$ 1.0	14.2 $\pm$ 1.1	12.2 $\pm$ 1.1	14.0 $\pm$ 1.1	19.5 $\pm$ 2.1	14.7 $\pm$ 1.2	15.2 $\pm$ 1.1	25.5 $\pm$ 1.8
Ethanol	5	34.7 $\pm$ 2.0	38.8 $\pm$ 2.1	42.6 $\pm$ 1.7	35.9 $\pm$ 1.4	37.0 $\pm$ 1.7	43.1 $\pm$ 1.3	37.7 $\pm$ 2.2	40.2 $\pm$ 2.4	45.3 $\pm$ 2.1
Water	5	31.8 $\pm$ 1.2	38.5 $\pm$ 1.9	41.3 $\pm$ 2.2	34.2 $\pm$ 1.1	39.3 $\pm$ 2.1	43.5 $\pm$ 1.1	35.2 $\pm$ 1.8	40.5 $\pm$ 2.0	42.6 $\pm$ 1.4
Oil	5	33.0 $\pm$ 1.5	47.3 $\pm$ 2.3	52.2 $\pm$ 2.1	36.3 $\pm$ 1.3	48.2 $\pm$ 1.9	55.4 $\pm$ 2.3	35.2 $\pm$ 2.1	53.3 $\pm$ 1.9	60.9 $\pm$ 2.3

Table 2.1 shows the extraction yields of lycopene in tomato peel with pure scCO<sub>2</sub> and with three modifiers at different temperatures and pressures with a flow of 1 mL/min and an extraction time of 60 minutes. The tests made by Shi et al., for all temperatures and pressures, show an order of yield: olive oil > methanol > water > pure scCO<sub>2</sub>. Furthermore, with 35MPa and 75 °C the yield with oil (co-solvent) is 2.4 times greater than yield without modifier [6]. In addition to modifiers, also co-additives can be added to scCO<sub>2</sub>, they interfere in the interaction between the analyte to be extracted and the matrix, facilitating the desorption of the analyte. To further improve extractions, they also used reactive co-additives that interact either with the matrix, eliminating the sites of interaction with the analyte, or with the molecule to be extracted, creating a chemical species more soluble in scCO<sub>2</sub> [8].

### *2.3.3 Flow rate and extraction time*

The flow rate is a parameter that depends on four factors: matrix-solute interactions, analyte solubility, mass transfer and longitudinal dispersion.

If the solute does not interact with the matrix, the diffusion of the analyte in the supercritical fluid mainly depends on its degree of solubility. High flows cause an increase in yield, as in the case of the extraction of vegetable oils (Onur Döker et al.), because facilitates the mass transfer of the analyte from the matrix to the fluid, avoiding its saturation.

If the solute interacts with the matrix, the most important parameter to consider is the equilibrium of phase. The increase in flow doesn't cause



an increase in yield because the analyte doesn't transfer quickly but remains bound to the matrix.

This phenomenon is characterized by two parameters, the external and the internal mass coefficient. The first represents the transfer of the analyte from the surface of the matrix (in direct contact with the scCO<sub>2</sub>) to the fluid, is a fast process, while the second represents the transfer of the analyte from the innermost part of the matrix to the fluid, is a slow process.

Using too low flows of scCO<sub>2</sub> causes longitudinal dispersion of the analyte with a consequent decrease in yield.

Small extraction containers and narrow connecting pipes are widely used to avoid this dispersion phenomenon, although these characteristics depend on the size of the system used.

The extraction time depends on the optimization of the previously described parameters (pressure, temperature, quantity and type of modifier and flow rate), on the nature of the matrix (hardness, ease of penetration of fluids, type of material) and from the pre-treatment that was done (drying, freeze-drying, level of grinding, treatment with filling and dehydrating powders) [9].

The extraction is generally carried out in two phases, static and dynamic, with sometimes different times and flows (Figure 2.3).

In the static phase the supercritical fluid and the matrix are in contact in the sealed vessel, in the dynamic phase the supercritical fluid flows through the sample.

In the static extraction phase, the supercritical fluid penetrates inside the matrix, swelling it and causing an initial desorption process of the analyte. In this phase it is not necessary to use high flows while a

minimum time is required to impregnate the matrix and induce the initial desorption of the analyte.

In the dynamic step, the fluid flows continuously through the matrix, this allows the easy migration of the analyte towards the fluid because an equilibrium of the phase is not created. In the dynamic phase use of a correct flow rate is important, the optimal extraction time is obtained when the yield doesn't change by increasing the extraction time [8].

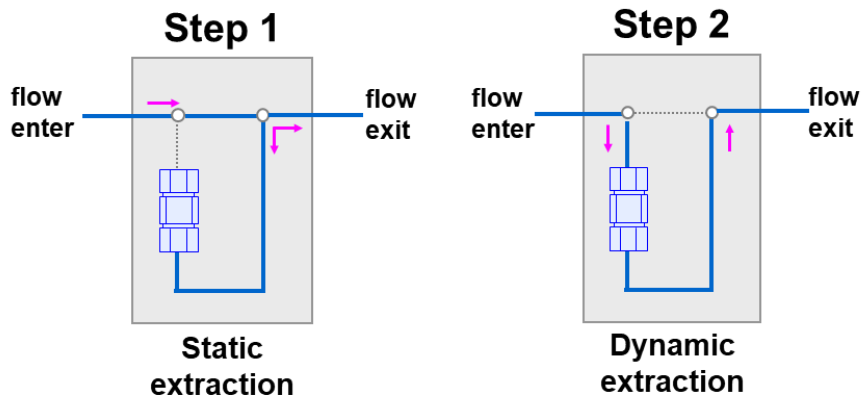


**Fig. 2.3** Schematic representation of the extraction steps. Step 1 static extraction (the fluid in contact with the matrix do not change), step 2 dynamic extraction (the fluid in contact with the matrix changes).

#### 2.3.4 Extraction theory for different matrices

Plant and animal samples, and biological fluids require different pre-treatments (grinding, freeze-drying, drying, dehydration with powders) and specific optimization of the extraction process.

Theoretical models have been developed, obtained with experimental evidence, which facilitate the optimization of extraction processes and scale-up projects.

The most used models are “broken and intact cell” (BIC) and “shrinking nucleus” (SC).

In the BIC model (Figure 2.4) the particle of material to be extracted is divided into two parts. The outermost contains cells that are broken due to pre-treatment processes, the extraction fluid penetrates easily, and the solute is extracted quickly because the mass transfer rate is high. The innermost part of the particle consists of intact cells, the fluid penetrates with difficulty and the mass transfer is slow.

The extraction process with the BIC model is characterized by three stages.

- Constant extraction rate: the solute diffuses from the broken cells towards the fluid, with a constant speed which depends on the external diffusion coefficient of the particle ( $x_b$ ). The analyte quickly saturates the fluid, therefore, the particles in the initial part of the extraction vessel have lost the solute contained in the broken cells but not that in the intact cells, while the particles at the end of the extraction vessel have not completely lost the analyte contained in broken cells.
- Decrease in the extraction rate: the analyte, in broken cells, is completely extracted while the analyte in intact cells migrates outwards, this process occurs slowly and depends on the internal diffusion coefficient of the particle ( $x_i$ ). The extraction rate rapidly decreases to a constant value.
- Minimum extraction rate: the analyte inside the intact cells migrates totally outside the particle and spreads in the supercritical fluid, this process is very slow. The extraction rate gradually decreases to zero.

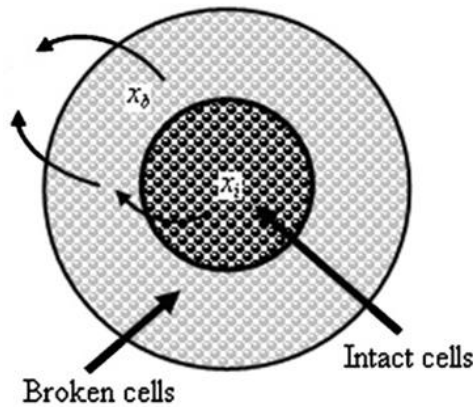


**Fig. 2.4** Representation of the BIC model of a particle. The analyte transfers from broken cells to the fluid with external diffusion coefficient  $x_b$  and from intact cells to broken cells with internal diffusion coefficient  $x_i$  [9].

The SC model (Figure 2.5) divides the particle into three parts: a film of fluid surrounding the particle, the outer part of the particle (called the shell characterized by channels and pores caused by the sample pre-treatment processes) and the inner part of the particle (called nucleus). The supercritical fluid surrounds the particle creating a film and penetrating the shell through channels and pores. In this phase there is an intra-particle diffusion of the analyte that spreads from the cells to the film and subsequently to the outermost fluid. The speed of this process is characterized by different diffusion coefficients. At the same time the analyte moves from the intact nucleus towards the shell of the particle with the consequent reduction in the dimensions of the intact nucleus. The transfer of the analyte, from the particle to the fluid, is increasingly slow due to the decrease in the size of the core and the increase in the size of the shell. The extraction rate gradually decreases and strongly depends on the particle size [9].

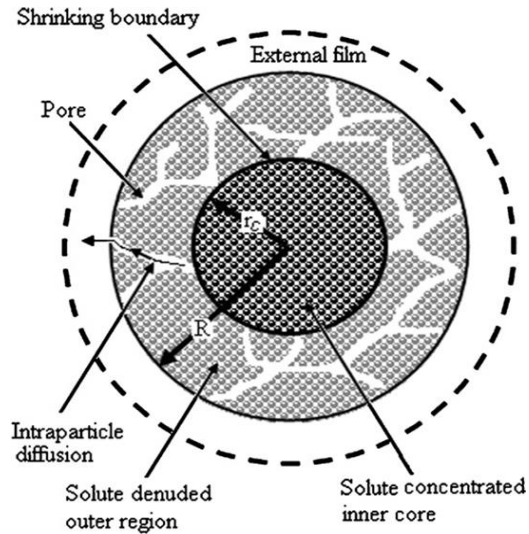


**Fig. 2.5** Representation of the SC model of a particle. The analyte diffuses from the shell to the film of fluid surrounding the particle and from the intact nucleus to the shell and the boundary of the intact nucleus narrows [9].

The BIC model theorizes extractions with higher yields and shorter times than the SC model (with the same experimental parameters). Both are used for the theoretical calculation of the extraction yield, often with the use of variants. Onur Doker et al. (Figure 2.6) compared the experimental data of the extraction of sesame oil from seeds with the theoretical data obtained from the two models. The theoretical SC model represent with good approximation the experimental data [4].

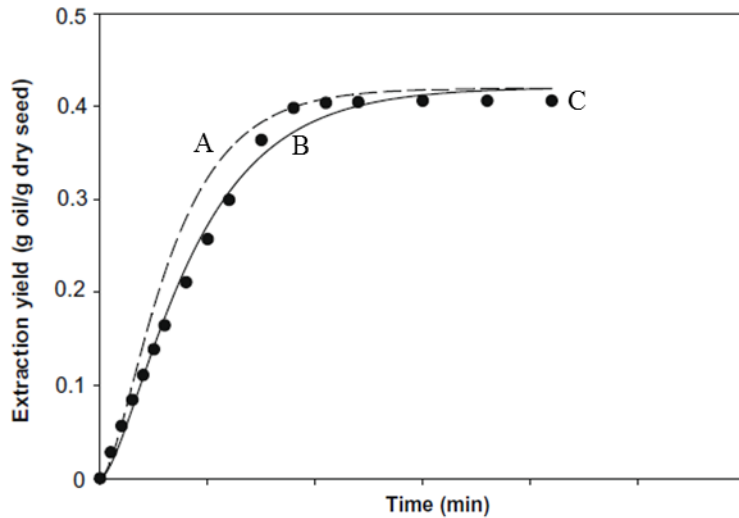


**Fig. 2.6** A represents the curve of the BIC model, B represents the curve of the SC model, C represents the curve obtained with the experimental data [4].

Pascale Subra et al. (Figure 2.7) obtained experimental data for the extraction of  $\beta$ -carotene from carrots very similar to the theoretical data of the BIC model [9].

The use of a model (with modifications or not) depends mainly on the matrix used and its pre-treatment.

Often, it is difficult to understand the most suitable method to use, but they are important for explaining the phenomena related to the extraction processes and improving the scale-up [9].

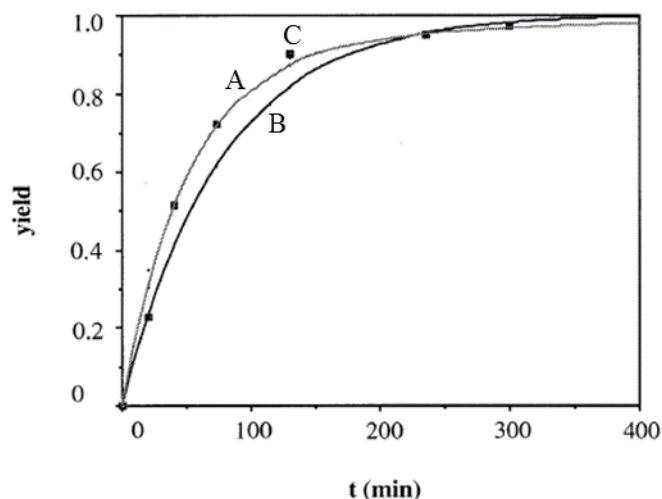


**Fig. 2.7** A represents the curve of the BIC model, B represents the curve of the SC model, C represents the curve obtained with the experimental data [9].

## 2.4 Extraction collection

The compound extracted with the SFE process is collected using a liquid phase system, the tube leaving the SFE system is immersed in a vial containing a liquid or solid phase system, that trap the extract.

### 2.4.1 Liquid phase collection

The liquid phase trapping system is the most used because it is very convenient, versatile and allows to trap even large quantities of analyte. This process depends above all on the nature and quantity of organic solvent used, because it must solubilize the extracted analyte.

An experiment done by Turner et. al. [11] describes the importance of the solvent for the yields of Vitamin A (Retinol) and Vitamin E ( $\alpha$ -Tocopherol) with SFE using milk powder. Table 2.2 show that recoveries are better with the 1:1 v/v mixture of diisopropyl ether and

ethanol (DIPE-EtOH), compared to using pure isopropanol (IPA), methanol (MeOH) or acetone.

The greater collection capacity of this mixture of solvents is most likely due to its ability to solubilize larger quantities of microparticles and microaggregates that contain the analytes considered.

**Tab. 2.2** Recovery of Vitamin A and Vitamin E from milk powder.

<b>Collection solvent</b>	<b>Vitamin A recovery (%)</b>	<b>Vitamin E recovery (%)</b>
<b>DIPE-EtOH</b>	102	85
<b>IPA</b>	108	68
<b>MeOH</b>	97	55
<b>Acetone</b>	89	42

For an optimal collection of the extract, the parameters to be considered are the flow rate, the temperature of the outlet tube of the SFE system and the temperature of the solvent.

High flow rates cause low yields due to high transport of the analyte by the gaseous CO<sub>2</sub>, uncontrolled temperatures of the collector tube cause its freezing and blockage of the extract, the low temperatures of the organic collection solvent allow the loss of volatile analytes, while high temperatures are used for non-volatile compounds, considering their thermolability [11].

The exit tube is often depressurized so that the CO<sub>2</sub> passes into the gas phase at the end of the tube, in this way the analyte is completely released into the solvent. In this system, the flow rate of the SFE must be low to obtain an optimal pressure drop and good yields because CO<sub>2</sub> tends to transport the analyte even in the gaseous phase.



The depressurization necessitates a heating system to avoid freezing and blocking of the tube. In this system, the SFE flow rate must be low to obtain an optimal pressure drop and good yields because CO<sub>2</sub> tends to transport the analyte even in the gaseous phase [12].

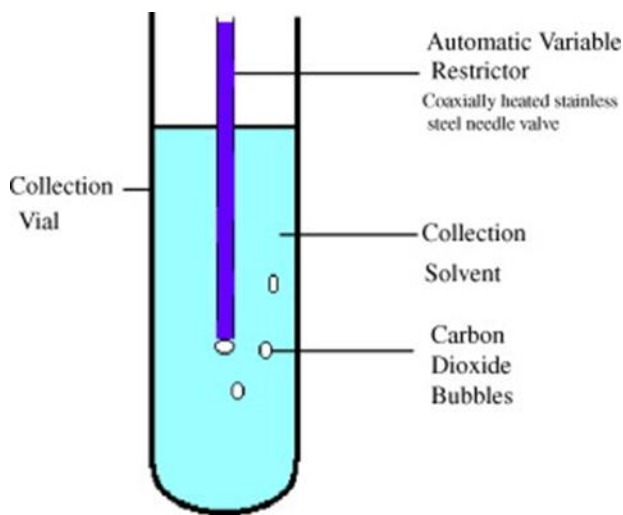


**Fig. 2.8** Representation of the process of entrapment of the extract in an organic solvent [12].

The size of the CO<sub>2</sub> bubbles are small using a restrictor at the exit from the extraction system, this represents a higher transfer rate of the analytes from the gas phase (CO<sub>2</sub>) to the liquid phase (organic solvent). Viscous solvents and very long vials are used to increase the contact time between these two phases.

These devices were used by Bøward et. al for the extraction of polycyclic aromatic hydrocarbons, improving the yield from 48% to 75% while maintaining constant flow parameters, temperature and type of collection solvent [13].

Systems that pressurize the collection container are used to increase the yields of highly volatile analytes, alternatively a low temperature condenser connected to the collection system is used [14].

#### *2.4.2 Solid phase collection*

The solid phase trapping system is composed of an adsorbing porous solid material (octadecylsilane, diol, silica, florisil or alumina) and an inert support (steel, glass or fused silica), the analyte trapped on the porous solid is eluted using a specific solvent [8].

The adsorbent solid can be composed of different materials. In this case it traps the analyte very effectively (increasing the final yield) and allows a solvent to selectively elute the analyte from the extracted mixture, increasing selectivity.

The fundamental parameter, for solid phase collection, is the maximum adsorption capacity, that is the maximum quantity of analyte that the collection system can adsorb. This value, for real samples, is always lower than the values obtained with the use of a standard due to the co-extracted compounds that overload the system.

To eliminate this problem, generally, a solvent is used to extract the compounds trapped in the adsorbent solid which can be reused again, creating an “intermittent extraction”.

For this process it is important to use an organic solvent that has good solubility and selectivity for the analyte of interest or for the co-extracted compounds [15].

The use of large volumes of polar modifiers or solvents in the extraction process causes little entrapment of the analyte in the porous solid support. Necessarily, the temperature of the collection system is

maintained above the boiling point of the modifier, so low boiling modifiers are used.

Solid phase collection techniques allow better recoveries than liquid phase collection for non-volatile components [16].

While volatile compounds can be collected, with the solid phase system, using cryogenic cooling. The CO<sub>2</sub> is depressurized at the outlet from the SFE and is channeled towards the adsorbent material keeping the temperatures of the harvesting system very low. This allows the deposition of the volatile analytes on the adsorbent support separating them from the non-volatile co-extracts [17].

## References

- [1] F. Pena-Pereira, M. Tobiszewski. The Application of Green Solvents in Separation Processes Chapter 7. Publisher Elsevier, 2017.
- [2] S. M. Pourmortazavi, S. S. Hajimirsadeghi. Supercritical fluid extraction in plant essential and volatile oil analysis. *Journal of Chromatography A* 2007, 1163, 1.
- [3] A. A. Clifford, J. R. Williams. Introduction to Supercritical Fluids and Their Applications. Publisher Humana Press, 2000.
- [4] O. Döker, U. Salgin, N. Yildiz, M. Aydogmus, A Çalimli. Extraction of sesame seed oil using supercritical CO<sub>2</sub> and mathematical modeling. *Journal of Food Engineering* 2010, 97, 360.
- [5] E. Vági, B. Simàndi, K. P. Vàsarhelyiné, H. Daood, A. Kéry, F. Doleschall, B. Nagy. Supercritical carbon dioxide extraction of carotenoids, tocopherols and sitosterols from industrial tomato by-products. *The Journal of Supercritical Fluids* 2007, 40, 218.
- [6] E. Lesellier, C. West. The many faces of packed column supercritical fluid chromatography – A critical review. *Journal of Chromatography A* 2015, 1382, 2.
- [7] J. Shi, C. Yi, S. J. Xue, Y Jiang, Y. Mac, D. Li. Effects of modifiers on the profile of lycopene extracted from tomato skins by supercritical CO<sub>2</sub>. *Journal of Food Engineering* 2009, 93, 431.
- [8] S. Moret, G. Purcaro, L. S. Conte. Il campione per l'analisi chimica. Publisher Springer-Verlag Mailand, 2014.
- [9] Z. Huang, X. Shib, W. Jiang. Theoretical models for supercritical fluid extraction. *Journal of Chromatography A* 2012, 1250, 2.
- [10] P. Subra, S. Castellani, P. Jestin, A. Aoufi. Extraction of  $\beta$ -carotene with supercritical fluids: Experiments and modelling. *The Journal of Supercritical Fluids* 1998, 12, 261.
- [11] C. Turner J. W. King, L. Mathiasson. Supercritical fluid extraction and chromatography for fat-soluble vitamin analysis. *Journal of Chromatography A* 1998, 12, 261.

- [12] S. M. Pourmortazavi, S. S. Hajimirsadeghi. Supercritical fluid extraction in plant essential and volatile oil analysis. *Journal of Chromatography A* 2007, 1163, 2.
- [13] S. Bøwadt, F. Pelusio, L. Montanarella, B. R. Larsen. Trapping techniques in supercritical fluid extraction. *Journal Trace and Microprobe Techniques* 1993, 11, 117.
- [14] M. Oszagyán, B. Simándi, J. Sawinsky, Á. Kéry, E. Lemberkovics, J. Fekete. Supercritical Fluid Extraction of Volatile Compounds from Lavandin and Thyme. *Flavour and Fragrance Journal* 1996, 11, 157.
- [15] A. Meyer, W. Kleiböhmer. Supercritical fluid extraction of polycyclic aromatic hydrocarbons from a marine sediment and analyte collection via liquid-solid trapping. *Journal of Chromatography A* 1993, 657, 327.
- [16] R. M. Smith. Supercritical fluids in separation science – the dreams, the reality and the future. *Journal of Chromatography A* 1999, 856, 83.
- [17] J. Vejrosta, A. Ansorgová, J. Planeta, D. G. Breen, K. D. Bartle Anthony A. Clifford. Solute trapping in off-line supercritical fluid extraction using controlled modifier condensation. *Journal of Chromatography A* 1994, 683, 407.

## 3 Supercritical fluid chromatography

---

### 3.1 Evolution of the SFC

The SFC technique was used, for the first time, in 1962 by Klesper et al. [1] to separate a mixture of porphyrins using two gases (dichlorodifluoromethane and monochlorodifluoromethane) as the mobile phase and polyethylene glycol as the stationary phase. The mobile phases solubilized the porphyrins when temperatures and pressures were higher than the  $T_C$  and  $P_C$  of the corresponding gases.

Subsequently Sie et al. [2, 4] used carbon dioxide as a supercritical fluid for the analysis of different classes of molecules. They published, between 1966 and 1967, works describing the tools created to keep  $CO_2$  in supercritical conditions.

In the late '60s, the first commercial systems for stabilizing the supercritical conditions of a fluid was developed and Giddings et al. [5] defined supercritical fluid chromatography as the meeting point between gas chromatography and liquid chromatography.

In the '70s, supercritical fluid instruments were optimized and studies were made to develop preparative SFC systems.

There was a lot of research on the development of new columns in the '80s this led to the wide commercialization of SFC tools. Novotny et al. [6] demonstrated that open capillary columns, made of fused silica, were better than packed columns for SFC systems because the pressure drop was lower and this resulted in a higher separation efficiency. The problem with these columns was that the density of the supercritical

fluid could only be changed with a change in flow and not with pressure. In the '90s this type of columns were less used due to this limitation.

Sugiyama et al. [7], in 1985, developed an on-line SFE-SFC system using packed columns in order to extract and separate the caffeine from ground coffee. The identification of the extracted and separated compounds was done with a UV photodiode system (PDA), it immediately became the main detector for packed column SFC systems.

In the '80s, Saito et al. [8] developed an electronic system to stabilize the back pressure that allowed efficient separation without contaminations. This type of back pressure regulator has become the standard device in packed column SFC systems.

The first organic solvents were used to modify the polarity of supercritical CO<sub>2</sub> following the commercialization of the back pressure systems. The percentage of modifier used was increased with the improvement of the pumps, and in 1991, Cui and Olesik [10] obtained and described the subcritical phase of supercritical fluids. The variation in pressure and temperature of this fluid phase was not related to the variation in density and therefore to the variation in the extraction capacity and permeability of the fluid. This is caused by the temperatures and pressure used because they are lower than the P<sub>C</sub> and T<sub>C</sub> values.

In the '90s, studies focused on the use of packed columns, they became the main columns used for SFC systems, and on enantio-separations with the development of chiral stationary phases.

From the 2000s onwards, the SFC technique has been improved with numerous technological innovations (improved detectors) and greater performance of the mechanical parts (pumps, back pressure system, columns, etc.) [10].

Today SFC systems are used for the analysis of numerous sample such as food, biological matrices, and applications in various ommic sciences including lipidomics, metabolomics and proteomics.

## **3.2 Chromatographic parameters**

The purpose of chromatography is to separate the individual components of a mixture from each other. The parameters considered in the chromatographic process are many, in this paragraph the most important will be described.

### *3.2.1 Retention parameters*

The retention time ( $t_R$ ) is the time needed for a solute to elute from one end of the column to the other and then be detected by the detector.

Dead time ( $t_0$ ) is the retention time of a solute that is not retained by the stationary phase and therefore flows at the same speed as the mobile phase.

The retention volume ( $V_R$ ) is the volume of mobile phase required to elute the solute from one end of the column to the other.

It is defined with the equation 3.1:

$$V_R = t_R \cdot F \quad \text{Equation 3.1}$$



$t_R$  is the retention time of the compound and  $F$  is the flow rate of the mobile phase.

The ratio between the amount of compound present in the stationary phase and that present in the mobile phase is called the distribution coefficient ( $K_D$ ) and calculated with equation 3.2:

$$K_D = \frac{C_S}{C_M} \quad \text{Equation 3.2}$$

$C_S$  and  $C_M$  are the analyte concentrations, respectively, in the stationary and mobile phases.

The most important parameter to describe the solute migration speed in the column is the retention factor ( $k'$ ), which expresses the retention time ( $t_R$ ) of a solute as a function of the dead time ( $t_0$ ), (equation 3.3):

$$k' = \frac{t_R - t_0}{t_0} \quad \text{Equation 3.3}$$

$k'$  can also be calculated using the distribution coefficient (equation 3.4):

$$k' = \frac{t_R - t_0}{t_0} = K_D \cdot \frac{V_S}{V_M} = \frac{n_S}{n_M} = \frac{V_R}{V_0} - 1 \quad \text{Equation 3.4}$$

where  $t_0$  is the dead time,  $t_R$  is the retention time of the compound,  $V_S$  and  $V_M$  are the volumes of the stationary phase and in the mobile phase,  $n_S$  and  $n_M$  are the moles of compound distributed in the two phases, while  $V_R$   $V_0$  are, respectively, the retention volume and the dead volume.

The flow rate  $F$  represents the quantity of fluid in milliliters that flows from the column in one minute, it is calculated equation 3.5 by knowing

the internal diameter of the column through which the mobile phase flows:

$$F = \frac{1}{4} \cdot \pi \cdot d_c^2 \cdot \varepsilon_u \cdot u \quad \text{Equation 3.5}$$

The average linear velocity ( $u$ ) is the amount of column in centimeters that is covered in one second by the flow, it is calculated (equation 3.6) by knowing the length of the column ( $L$ ) and the retention time of an unretained compound ( $t_0$ ) [11]:

$$u = \frac{L}{t_0} \quad \text{Equation 3.6}$$

### 3.2.2 Chromatographic resolution

The resolution ( $R_s$ ) is the parameter that represents the chromatographic separation between two compounds that elute consecutively, therefore, it can be considered the index of the capacity of the separative process.  $R_s$  can be calculated experimentally (equation 3.7) using the retention parameters of the two peaks:

$$R_s = \frac{t_{R2} - t_{R1}}{0.5 \cdot (w_2 + w_1)} \quad \text{Equation 3.7}$$

$w_1$  and  $w_2$  are the peak widths of the two compounds measured at the base. The degree of separation between two chromatographic peaks increases as  $R_s$  increases, which can therefore be considered an index of the effectiveness of the separative process.

Resolution can be theoretically calculated by considering numerous parameters grouped into three factors: capacity factor (described above), selectivity factor and efficiency factor.

The **selectivity factor** ( $\alpha$ ) is the quantitative measure of the separation between two solutes, therefore it represents the ability of a "chromatographic system" to differentiate two substances. A chromatographic column is very selective for two solutes when their differential migration is high, i.e. the retention times of the two solutes are different.

The selectivity factor is influenced by three factors: composition of the mobile phase, composition of the stationary phase and temperature.

The selectivity factor  $\alpha$  is defined by the equation 3.8:

$$\alpha = \frac{k_2'}{k_1'} = \frac{t_{R2} - t_0}{t_{R1} - t_0} \quad \text{Equation 3.8}$$

$k_1$  and  $k_2$  are the retention factors, while  $t_{R1}$  and  $t_{R2}$  are the retention times of the two compounds.

To modify the selectivity factor one can act: modifying the mobile phase, varying the pH of the mobile phase, modifying the stationary phase and changing the temperature.

The **efficiency factor** is a parameter linked to the column, it determines the shape and widening of the chromatographic peaks, therefore represents the efficiency of the column. To understand the efficiency factor in detail, it is necessary to introduce two fundamental concepts, the equivalent height of a theoretical plate (HETP or H) and the number of theoretical plates of a column (N).

The column is considered as divided in a number of theoretical plates, each characterized by the partition equilibrium between different phases (stationary phase and mobile phase) of the different compounds. The separation process efficiency is proportional to the N, therefore, to

the column length, or can be considered inversely proportional to the H.

The efficiency of a column is represented by N, and it is calculated (equation 3.9) knowing the length of the column (L) and H:

$$N = \frac{L}{H} \quad \text{Equation 3.9}$$

H is calculated using the Van Deemter Equation (equation 3.10) [11]:

$$H = A + \frac{B}{u} + C \cdot u \quad \text{Equation 3.10}$$

According to this formulation, H corresponds to the sum of three terms:

- **Eddy diffusion (A or H<sub>e</sub>)**

A reflects the contribution of the multi-path dispersion along the column, due to possible irregularities in the packing or to the presence of particles with different sizes so that multiple diffusion channels are formed; such term is also known as Eddy diffusion and can be calculated with equation 3.11.

$$A = 2 \cdot d_p \cdot \lambda \quad \text{Equation 3.11}$$

$\lambda$ : constant linked to the regularity of the packing of the column

$d_p$ : stationary phase particle diameter

A is directly proportional to the diameter of the stationary phase particles and is independent of the average linear flow velocity of the mobile phase [12].

- **Longitudinal diffusion (B)**

B is created based on the concentration gradient of the solute, determining the Gaussian shape of each chromatographic peak, can be expressed as equation 3.12.

$$B = 2 \cdot \gamma \cdot \frac{D_m}{u} \quad \text{Equation 3.12}$$

$$D_m = \frac{k \cdot T}{6 \cdot \pi \cdot \eta \cdot r} \quad \text{Equation 3.13}$$

$D_m$ : diffusion coefficient of the solute in the mobile phase (equation 3.13). For supercritical fluids  $D_m$  can be calculated from the Wilke Chang equation (equation 1.2).

$u$ : mean linear velocity of flow of the mobile phase

B depends on the distribution of the particles of the stationary phase, it is directly proportional to the  $D_m$  of the solute in the mobile phase and it is inversely proportional to the average linear flow velocity of the mobile phase (higher velocity, shorter time available for the longitudinal diffusion) [12,13].

- **Mass transfer (C or  $H_m+H_s$ )**

C is the so-called resistance to mass transfer, taking into account the transfer to both mobile ( $H_m$ ) (equation 3.14) and stationary phase ( $H_s$ ) (equation 3.15):

$$H_m = \Omega \cdot d_p^2 \cdot \frac{u}{D_m} \quad \text{Equation 3.14}$$

$\Omega$ : factor dependent on column diameter

$d_p$ : stationary phase particle diameter

$D_m$ : diffusion coefficient of the solute in the mobile phase

$u$ : mean linear velocity of flow of the mobile phase

$H_m$  depends on the column diameter. It is directly proportional to the square of the particle diameter and to the flow velocity of the mobile phase, while it is inversely proportional to the  $D_m$  of the solute in the mobile phase.

$$H_S = Q \cdot U \cdot d_{liq}^2 \cdot \frac{u}{D_S} \quad \text{Equation 3.15}$$

$Q$ : factor dependent on the type and shape of the particles of the stationary phase.

$U$ : constant relative to the speed of migration of the solute from the stationary phase to the mobile phase (solute / stationary phase interaction)

$d_{liq}$ : thickness of the liquid coating deposited on the solid support

$D_S$ : diffusion coefficient of the solute in the stationary phase

$u$ : mean linear velocity of flow of the mobile phase

The  $H_S$  depends on the diameter and shape of the stationary phase particles and on the speed of migration (desorption) of the solute from the stationary phase to the mobile phase. It is directly proportional to the average linear flow velocity of the mobile phase, while it is inversely proportional to the  $D_m$  of the solute in the stationary phase.

$C$  is therefore expressed by equation 3.16 [12,13]:

$$C = H_m + H_S \quad \text{Equation 3.16}$$

**Van Deemter's equation** 3.9 is obtained from the contributions of various physical and kinetic phenomena and can be rewritten as equation 3.17:

$$H = H_e + H_d + H_m + H_s = A + \frac{B}{u} + C \cdot u \quad \text{Equation 3.17}$$

In equation 3.17, a high value of mean linear flow velocity ( $u$ ) causes a decrease in longitudinal diffusion (B) but an increase the mass transfer (C). Conversely, a low value of  $u$  determines an increase in B and a decrease in parameter C.

Hence, due to the presence of two opposite contributions for  $u$ , it is necessary to determine the optimal flow for which both terms B and C are minimal which corresponds to the minimum of the curve representing H with respect to the linear velocity  $u$  in Figure 3.1 [12].

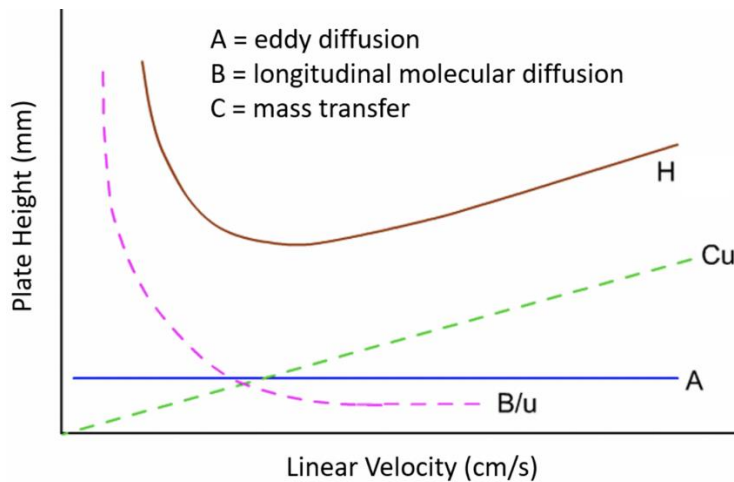


**Figure 3.1** Graphic representation Van Deemter Plot.

The resolution can be theoretically calculated (equation 3.18) knowing the three contributions that determine it (capacity factor, selectivity factor and efficiency factor).

$$R = \frac{1}{4} \sqrt{N} \cdot \frac{\alpha-1}{\alpha} \cdot \frac{k'_B}{k'_B+1} = \quad \text{Equation 3.18}$$

To obtain an excellent resolution between two chromatographic peaks it is necessary:

- A minimum broadening of the band expressed by N
- Different retention times of the solutes, therefore a good separation through the parameter  $\alpha$
- An adequate migration rate within the column expressed as  $k'_B$

### 3.3 Van Deemter equation in SFC

The parameter B, which represents the longitudinal diffusion, is of little importance in LC because the diffuse coefficients in liquids are low, so the contribution of  $B/u$ , in the van Deemter equation, is minimal (Figure 3.2 A). Parameter B is very important in GC due to the high values of diffusion coefficients in gases which are a few orders of magnitude greater than the values of liquids. This results in a significant contribution of  $B/u$  in the van Deemter equation (Figure 3.2 B).

In practice, these theoretical assessments result in greater peak in GC than in LC due to variations in mobile phase and flow rate, and a significantly higher optimal  $u$  value for GC systems than LC systems (Figure 3.2) [11].



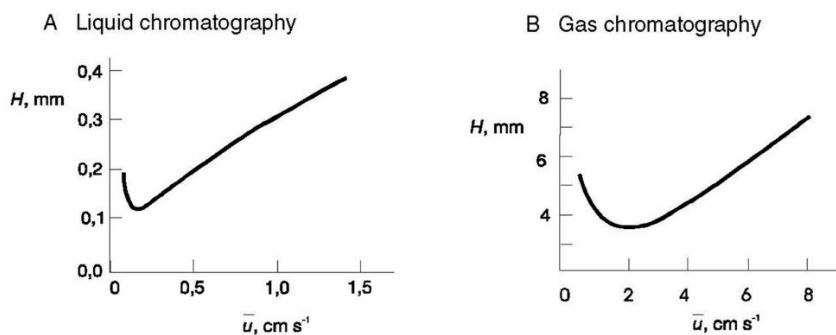


**Figure 3.2** Van Deemter Plot for liquid chromatography (A) and gas chromatography (B) [11].

Supercritical fluids have intermediate characteristics between those of a liquid and a gas, so longitudinal diffusion in SFC techniques is a more relevant parameter than in LC systems (Figure 3.3). This phenomenon determines an optimal value of  $u$  for SFC greater than LC and a bandwidth less sensitive to variations in mobile phase and flow rate compared to GC.

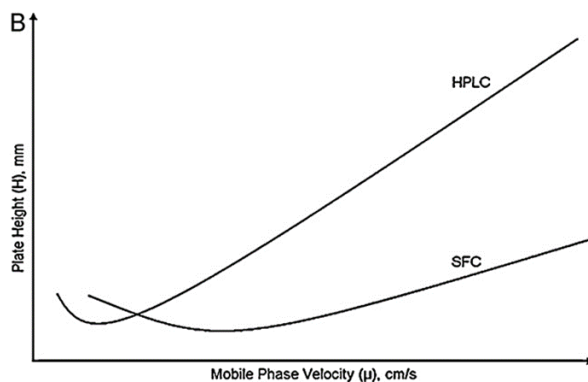


**Figure 3.3** Comparison of the Van Deemter curves for HPLC and SFC [14].

The Van Deemter plot for SFC is less "steep" than in LC (Figure 3.3), this is caused by a lower mass transfer C with the increase of  $u$  in SFC

systems due to the greater diffusivity of the analyte in the supercritical fluid, similar to the GC Van Deemter plot.

Experimentally, for SFC, the efficiency decreases (increase in the height of the theoretical plates) slowly as the flow rate increases [14].

### **3.4 Chromatographic methods**

Chromatography is a physical method of separation, consisting of two phases, mobile and stationary phase.

Liquid chromatography (LC), gas chromatography (GC) and supercritical fluid chromatography (SFC) are based on the same principles, the mobile phase (liquid, gas or supercritical) moves through the stationary phase (solid or liquid) carrying the compounds to be separated.

The compounds separate through the interactions that are created between them and the two phases or for their different sizes. The compounds that interact more with the mobile phase elute faster, while the compounds that interact more with the stationary phase elute more slowly, this phenomenon determines the separation of the analytes.

The interactions between the analytes and the two phases can be of various types: electrostatic, dipole-dipole, Van Der Waals forces and ion, therefore there are different types of chromatography, based on the different mechanism of separation of the solutes.

- In adsorption chromatography the solutes are separated according to their ability to be adsorbed on the stationary phase.
- In partition chromatography the stationary phase is a thin liquid film that covers a solid support; the separation is caused by the different

distribution of solutes between the stationary phase and the mobile phase.

- Ion exchange chromatography is formed by solid supports functionalized with anionic (eg,  $-\text{COO}^-$ ,  $-\text{SO}_3^-$ ) or cationic (eg,  $-\text{NH}_3^+$ ,  $-\text{N}(\text{CH}_3)_3^+$ ) groups defined as "strong" and "weak", that create electrostatic interactions with the analyt.

- Exclusion chromatography (or gel-permeation chromatography) it is a separative method that does not rely on the interaction of the stationary or mobile phase with solutes, but on the difference in their size. Small molecules penetrate all the pores and channels of the stationary phase and have longer elution times than large molecules that follow a more linear and less tortuous path.

The most commonly used chromatography is bound phase chromatography (BPC), in which the inert silica support is functionalized with more or less polar organic groups

In liquid chromatography, BPC is divided into reverse phase chromatography (RP-LC), the most used, and normal phase chromatography (NP-LC).

The interactions that are created between the stationary phase and the analytes allow the separation of molecules of different nature, polar and non-polar, organic and inorganic, this technique is very versatile and therefore widely used.

The RP-LC technique is characterized by polar mobile phases (water, methanol, acetonitrile, etc.) and non-polar stationary phases consisting of modified silica, i.e. silica covalently linked to non-polar carbon chains ( $\text{C}_8$ ,  $\text{C}_{18}$ ,  $\text{C}_{30}$ ).

The NP-LC technique is characterized by non-polar mobile phases (hexane, isopropanol, etc.) and polar stationary phases formed by silica gel functionalized with polar groups (OH, NH<sub>2</sub>, CN).

Also, in SFC the most used chromatographic method is BPC, in which the stationary phase used can be functionalized with both polar and non-polar groups. SFC systems can use a wide range of stationary phases because the characteristics of scCO<sub>2</sub> and the possibility of using a wide variety of modifiers, but in any case with low percentages of water, allows the employment of both non-polar and polar stationary bonded phases with the same mobile phase [15,16]

### **3.5 SFC columns**

#### *3.5.1 Stationary phase*

SFC can replace RP-LC, NP-LC, and hydrophilic interaction chromatography (HILIC), provided that the compounds of interest are soluble in the CO<sub>2</sub>. All HPLC stationary phases are also suitable to use in SFC, from octadecyl silica (ODS) bonded silica to pure silica. However, some of them showed some problems, the most evident being the poor selectivity and the low separative efficiency SFC compared to the HPLC counterpart; moreover, the poor compactness of the peaks obtained for the separation of acidic or basic analytes required the use of additives in the in the organic modifiers [15].

More recently, new stationary phases especially designed for SFC have been developed, in the attempt to overcome such issues [17]. The silica-based polymer-encapsulated has been probably the first type of stationary phase to find larger use in SFC, consisting of fully porous

silica particles coated with a polysiloxane layer functionalized with polar groups or alkyl substituents. Such columns are not more in use nowadays, mainly because of problem associated to the free residual silanol activity, which was hampering the separation of more polar compounds. A few novel SFC-specific stationary phases have been recently introduced to minimize such inconvenience, which include bonding and ligands designed and optimized for use with CO<sub>2</sub>. One of the most popular is a chemically bonded phase with a 2-ethylpyridine substituent, affording few undesirable interactions with polar groups of the compounds due to total or partial protonation of the pyridine, reducing the interactions with the silanol groups, this effect is obtained only if the modifier is acidified [18]. The use of such a phase decreases or eliminates the need for additives, and it is well suited to the analysis of a wide range of basic, as well as neutral and acidic compounds. The same mechanism of unwanted interaction (hydrogen bonding or steric protection) can be encountered with silica-based support having amino, amide, urea and sulfonamide groups [17].

### *3.5.2 Particle size*

Over the past decade, the creation of higher performing systems and the development of pumps that can create higher and more stable pressures laid the foundation for the development of columns with ever smaller particle sizes. This aspect is fundamental to increase the chromatographic efficiency and decrease the analysis times, maintaining an optimal flow.

It has been calculated that using a column 25 cm long packed with 5 μm particles an inlet pressure about 25 bar is necessary for the

chromatographic analysis, while decreasing at 1  $\mu\text{m}$  the particles diameter the required pressure is of 2000 bar [19,20]. Consequently, a significant improvement of all instrumentation was essential for LC systems.

The name of the new instrumentations was ultra-high-pressure or ultra-high-performance chromatography (UPLC or UHPLC) [21].

The columns used for this type of technique are defined sub-2, because they are filled with particles whose diameter is less than 2  $\mu\text{m}$ .

These columns have also been applied in SFC by creating ultra-high-pressure supercritical fluid chromatography (UHPSFC) systems, obtaining remarkable and much better results than UHPLC systems.

Comparing the graphs of Van Deemter for classical systems (HPLC and SFC) that use columns with particle diameter of 5  $\mu\text{m}$  and ultra-systems (UHPLC and UHPSFC) that use columns with particle diameter of 1.7  $\mu\text{m}$  (Figure 3.4), it is interesting to note the almost total flattening of the curve in the region of the linear velocity greater than the optimal value for the UHPSFC, which means that the sub-2 columns can be used at high flow rates without any loss of efficiency in systems efficiency in systems using  $\text{scCO}_2$ .

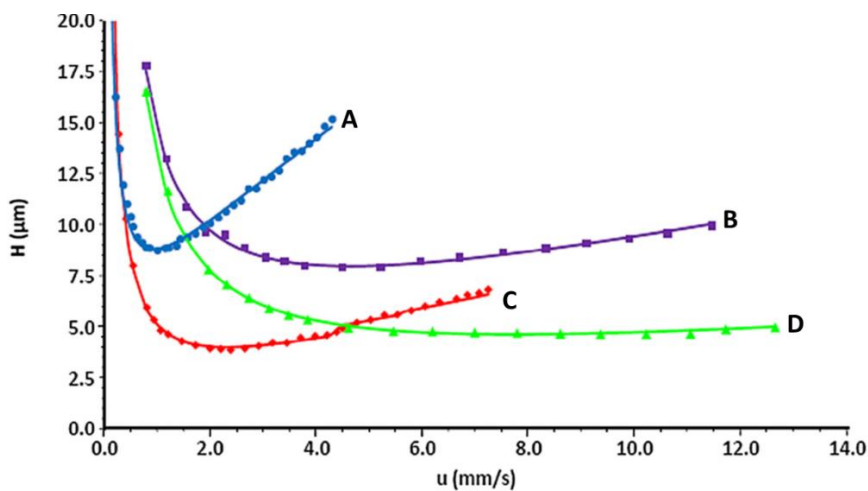


**Figure 3.4** Comparison Van Deemter plots for HPLC (A) and SFC (B) with 5  $\mu\text{m}$  particle size column and UHPLC (C) and UHPSFC (D) with 1.7  $\mu\text{m}$  particle size column.

Figure 3.5 shows the Van Deemter plots behavior of multiple column packings, including sub-2, monolithic, and cast core. Monolithic columns was approximately introduced in the same years of sub-2 particles and consists of one single piece of porous material such as organic polymers or silica, characterized by the presence of mesopores that allow by a very limited flow resistance compared to a particle-packed column [22].

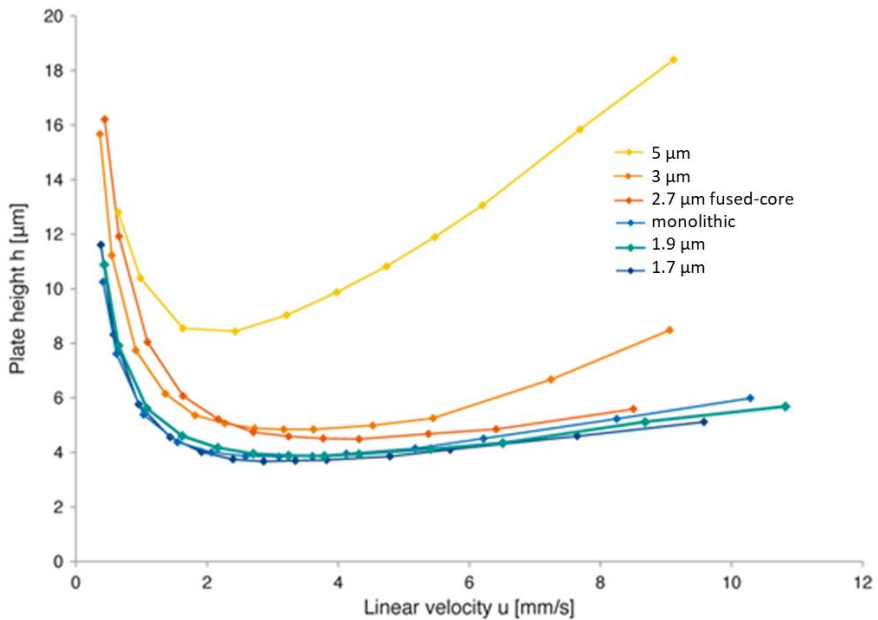


**Figure 3.5** Van Deemter Plot with different columns and particle sizes.

The presence of such mesopores (Figure 3.6 A) made these columns low efficient for small molecules, while they are still widely employed for macromolecules analysis, such as proteins. In the case of gradient analysis, the re-equilibration time is also reduced, thus further decreasing the total analysis time and maximizing the throughput especially if a large number of samples have to be analyzed.

The main drawback of monolithic technology is the limitation of the length of the column and therefore the number of theoretical plates that compose it.

Columns with lengths greater than 15 cm are difficult to create and are often not as efficient as they should be [23,24].



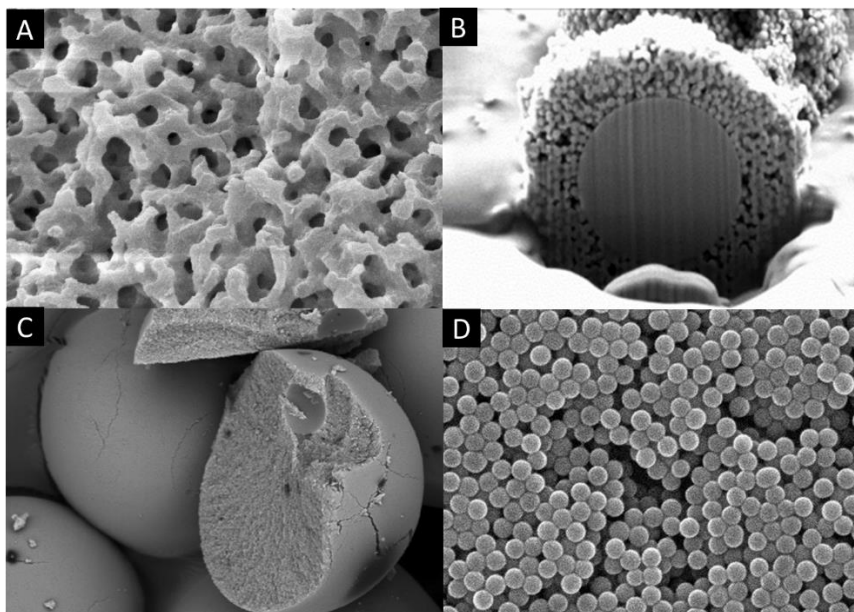


**Figure 3.6** Images, with the Scanning Electron Microscope (SEM), of a portion of a monolithic column (A), of a fused-core particle (B) and of a porous particle (C) and the particle packing of fused-core and porous (D).

Fused-core particles (Figure 3.6 B) were introduced on the market in 2006 and are also known as partially porous or core-shell particles to pinpoint the presence of a solid core in which the analytes cannot diffuse, different from common particles which are totally porous.

A typical fused-core particle is shown in Figure 3.7, it has a solid core of silica with a diameter of  $1.7\ \mu\text{m}$  surrounded by a  $0.5\ \mu\text{m}$  thick porous shell that represents the only possibility diffusion of total particle diameter.

For fused-core particles, the transfer rate of the analytes, from the stationary phase to the mobile phase, is significantly greater than that of classic particles (Figure 3.6 C) of identical size because the analytes do not diffuse deep inside the particle [25].

This peculiarity allows them a lower mass transfer in stationary phase (Hs) and therefore a low C value in the Van Deemter equation.

These characteristics determine that the columns with fused-core particles allow more compact peaks than the classic porous columns and lower pressures than those generated by sub-2 columns [26].

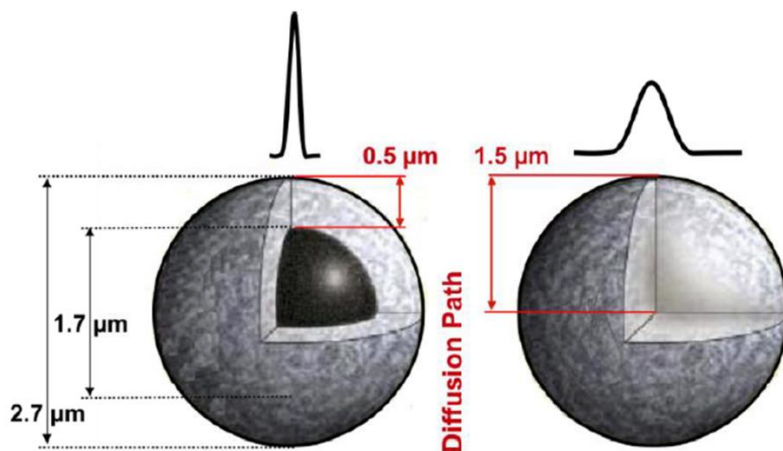


**Figure 3.7** Fused core technology (on the left) and comparison with totally porous particles (on the right).

### 3.6 SFC Detector

With SFC systems it is possible to couple both GC and LC type detectors. In particular, in an SFC configuration, similar to a GC system, where only pure CO<sub>2</sub> is used as the mobile phase, it is possible to couple: flame ionization detector (FID), infrared detector (IR), electron capture detection (ECD), electronic ionization mass spectrometer (EI-MS), chemiluminescence and various other detection. With an SFC configuration similar to LC system, in the presence of a modifier, are used: evaporative Light Scattering Detectors (ELSD),

ultraviolet/visible detector (UV/VIS), charged aerosol detection (CAD), acoustic flame detection (AFD), mass spectrometer with soft ionization (MS) and circular dichroism (CD) for chiral compounds.

The detectors most used in SFC systems are UV (non-destructive system) and MS (destructive system) which give different information, precisely for this reason, both are often coupled to the SFC systems.

Among UV detectors it is possible to distinguish between those selecting only one wavelength to pass the sample, usually corresponding to the analyte maximum absorption (UV detectors), and those in which a total scan of UV or UV/VIS wavelength is performed through in order to obtain a typical UV or UV/VIS spectrum (photo diode array, PDA).

In this case useful information on the chemical nature of the analytes can be achieved, but an unequivocal identification is almost impossible. Furthermore, if co-elutions are present quantitative determination cannot be carried out and non-absorbing compounds cannot be detected [27]. On the other hand, MS is a universal detector, in many cases specific enough to support the positive identification of a compound, providing structural information and in some cases the molecular weight. In general, an MS instrument consists of three fundamental components, namely the ion source, to produce ions from the sample, the mass analyzer, to separate them on the basis of the mass-to-charge ratio ( $m/z$ ) and the detector [28].

## 3.7 Mass Spectrometry

### 3.7.1 Ion sources

The ionization process occurring into the ion source can be classified in hard and soft.

The hard sources impart a lot of energy to the molecules that are excited, their relaxation involves the breaking of the bonds and the formation of fragment ions with mass-charge ratios lower than the molecular ion, this phenomenon allows the operator to determine the structure of the original molecule.

Soft sources cause little fragmentation, consequently the resulting mass spectrum often consists of the molecular ion or protonated or deprotonate molecular ion, providing only the molecular weight information.

The first MS application was based on a hard ionization process, still now extremely widespread and known as electron ionization (EI) (figure 3.8), in which a high energy electron beam was directed toward the gas phase molecules, under high vacuum conditions [29]. Since its discovery, it appeared clear that such technique was very suitable for volatile and thermally stable compounds, but excluded the investigation of large molecules. Furthermore because of a low compatibility of the liquid phase with the vacuum region of an MS, the hyphenation with GC was more straightforward compared to the hyphenation with LC, that required the removal of the mobile phase before the analyte entered the MS, thus compromising the analytical performances [30].

This technique was however used as an SFC detector without the use of organic modifiers or in any case with an extremely limited use to maintain the high vacuum present in the mass system [31].

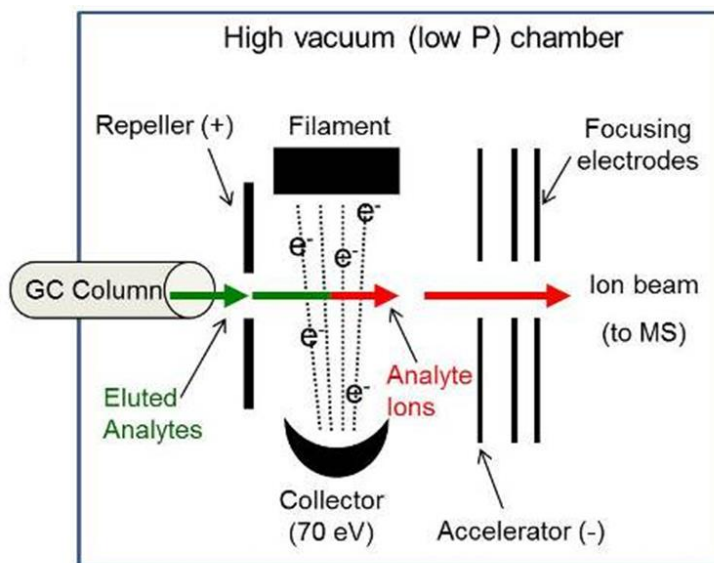


**Figure 3.8** Graphic representation of an electron impact source.

The breakthrough arrived more than 50 years ago, with the introduction of more versatile ionization techniques, allowing the generation of ions over a wide range of molecular weights. Significant examples are the plasma desorption ionization method (MALDI) [32], and the fast atom bombardment (FAB) technique [33] where the bombardment occurs in the first case by means of a high-energy laser and in the second by xenon or argon atoms, all soft techniques that work in vacuum conditions. Such techniques were quickly replaced by systems: atmospheric pressure chemical ionization (APCI) (figure 3.9 A), atmospheric pressure photoionization (APPI) (figure 3.9 B), and electrospray ionization (ESI) (figure 3.9 C), in order to handle the high amount of liquid phase involved [34,35].

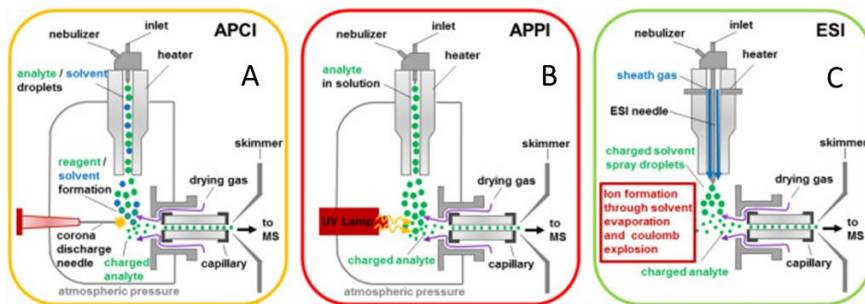


**Figure 3.9** Atmospheric pressure techniques, APCI (A), APPI (B) and ESI (C).

The source used for polar compounds is ESI; in it the sample is nebulized and ionized with the formation of a Taylor cone and subsequently of drops containing ions with positive and negative charges that detach from the capillary.

The solvent evaporates the droplets and increases the surface charge density to a critical level. Subsequently an explosion of the drop is created and the ions are expelled.

For medium polarity compounds ranging in a molecular weight from 100 to 2000 Da, APCI is preferred to ESI. While ESI is a liquid phase ionization, APCI occurs in gas phase conditions, after the nebulization (promoted by N<sub>2</sub>) and the vaporization of the solvent at a temperature of 350-550 °C; the resulting vapor is ionized using a corona discharge (source of electrons) and the mobile phase acts as a reagent gas to ionize the sample.

Finally, atmospheric pressure photo ionization (APPI) is applicable to many solutes amenable with APCI, but can give a better response for highly apolar solutes. Substantially, APPI is like an APCI source where the corona discharge has been replaced with a Kr lamp, which generates

electromagnetic radiations able to excite and ionize the mobile phase, an additive or the analytes themselves [35].

APCI, APPI and ESI are the most widely used ionization systems for SFC-MS systems. Generally, this type of interfaces is easily interchangeable on the same mass module, which is very important in SFC systems that can analyze molecules with a very wide range of polarity.

### 3.7.2 Analyzers

The analyzer can be considered the heart of the MS, since features like analysis speed, mass range, resolution, mass accuracy, dynamic range and sensitivity depend on it. The main mass analyzers are quadrupole (Q), ion-trap (IT) and time-of-flight (ToF), beside a pool of hybrid instruments such as Q-ToF, IT-ToF and QqQ (triple quadrupole).

In general, Q systems are the most used for their low cost, versatile and ease of use. They are filters analyzers where only the ions with a specific  $m/z$  value reach the detector, depending on the electric fields applied. Figure 3.10 shows the scheme of these analyzers in order to better understand their functioning.

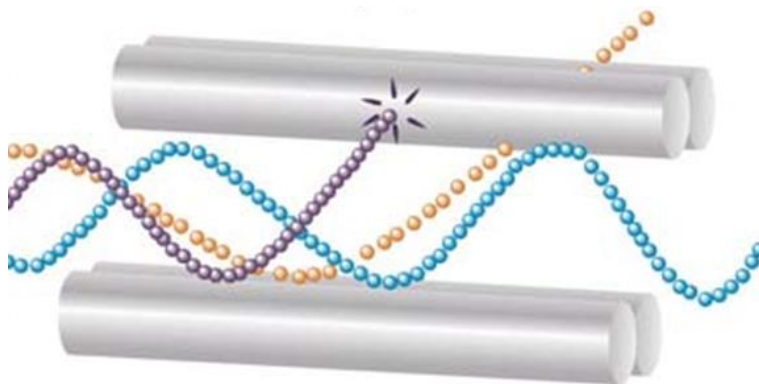


**Figure 3.10** Scheme of Q (on the left) and IT (on the right) analyzers.

In detail, Q is made up of 4 metal bars through which a combination of current (direct and alternating) and radio frequency passes, therefore, the ions acquired a different kinetic energy in function of their mass [36].

Ions with too high or too low energy will oscillate incorrectly and impact on metal bars or go out of the way. Only specific ions will have the correct oscillation to cross the four metal bars.

Because of the geometry of such analyzers that favorites a poor ion transmission, the Q systems show minor sensitivity than IT and ToF.

Nevertheless, Q technology-based instruments are preferred for quantitative applications because of the larger dynamic range (up to 6 magnitude order), normally not achieved by ToF because of a tendency to detector saturation.

Generally, MS systems can be used in full scan mode, obtaining chromatograms of the total ion current (TIC) or in the selected ion monitoring (SIM) mode where only ions with a given  $m/z$  values reach the detector. SIM system is useful for the development of selective and sensitive quantitative assays, due to the reduction of the baseline noise, i.e. signal-to-noise ratio (S/N). Furthermore, the integration of the SIM peaks is specific because it excludes any signal coming from substances totally or partially coeluted with the one considered; this possibility cannot be obtained with a UV detector.

However, the quantification, or even the detection of a target trace component, in SIM mode, can be difficult in the presence of high background ions with the same  $m/z$  values. On this case, a major selectivity is achieved by tandem techniques [37].



The analyzes QqQ (Figure 3.11) systems are the most used because they are a good compromise between costs and instrumented ability (excellent selectivity and sensitivity).

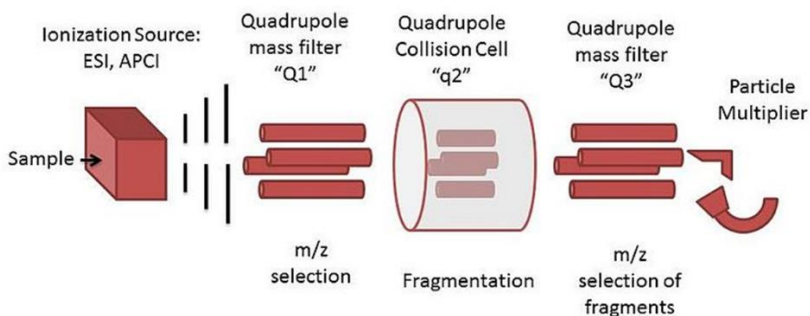


**Figure 3.11** Scheme of QqQ analyzer.

The analyzers Q1 and Q3 act as real quadrupoles by filtering the ions. The q2 is not a true quadrupole but acts as a collision cell, the ions from Q1 are blocked with a radiofrequency and fragment by a high energy gas (generally argon) through a collision induced dissociation (CID). After the fragmentation, the ions are sent to Q3 for a new discrimination.

With this system it is possible to obtain a lot of information useful for identifying and quantifying the separated compounds through chromatographic systems.

The product ion scan mode (Figure 3.12 A) allows to determine all the product ions (or daughter) obtained from the fragmentation of a specific precursor ion (or parent), while the precursor ion scan (Figure 3.12 B) allows to identify all the precursor ions, which through their fragmentation, have a specific product ion in common.

Maximum selectivity and sensitivity are achieved with the selected reaction monitoring (SRM) or multiple reaction monitoring (MRM)

modes (Figure 3.12 D) by selecting a specific precursor ion (with Q1) and a specific product ion (with q2). Normally, the fragmentation characterized by the major S/N is chosen as quantifier (Q) transition for quantitative analysis, while a second (or even more) fragmentation is selected as qualifier (q) transition, necessary to uniquely identify the analyte detected. In addition, the ratio between the intensity of the two transitions (Q/q) is typical of the given component and has to remain stable along the linearity range. If more components characterized by a similar fragmentation behavior need to be monitored, the neutral loss scan mode (NL) scan mode (Figure 3.12 C) can be adopted by monitoring the loss of a neutral molecule (water or carbon dioxide) during the fragmentation, only transitions characterized by specific difference between precursor and product ion will result in a peak in the chromatogram [38, 39].

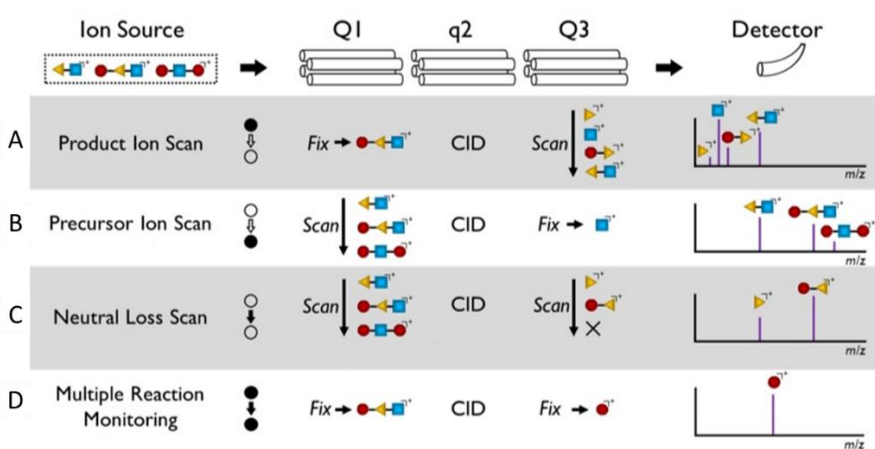


**Figure 3.12** Operation modes in QqQ.

### 3.7.3 Detector

The ions, which have been separated according to their  $m/z$  in the mass analyzer, arrive at the detector where they are converted into an

electrical signal, proportional to their abundance. There are various types of detectors that are employed in mass spectrometry, including the Faraday cup and the electron multiplier (EM).

The first is a metal conductive cup designed to catch charged particles in vacuum with suppressor electrode and then producing current, which can be measured and used to determine the number of ions striking the cup.

The second detector mentioned is operates according to the principle called secondary electron emission. When a charged ion strikes on detector surface it provokes secondary electrons that are released from atoms in the surface layer. The number of secondary electrons produced depends on the type of incident primary particle, its energy and characteristic of the incident surface. The electron multipliers may be of either the discrete dynode or the continuous dynode type (channeltron, microchannel plate or microsphere plate) [36].

## References

- [1] K. Klesper, A. H. Corwin, D. A. Turner. High pressure gas chromatography above critical temperatures, *Journal Organic Chemistry* 1962, 27, 700.
- [2] S. T. Sie, W. Va Beersum, G. W. A. Rjinders. High pressure gas chromatography and chromatography with supercritical fluids. I. The effect of pressure on partition coefficients in gas-liquid chromatography with carbon dioxide as a carrier gas. *Separation Science* 1966, 1, 459.
- [3] S. T. Sie, W. Va Beersum, G. W. A. Rjinders. High pressure gas chromatography and chromatography with supercritical fluids. II. Permeability and efficiency of packed columns with high-pressure gases as mobile fluids under conditions of incipient turbulence. *Separation Science* 1967, 2, 699.
- [4] S. T. Sie, W. Va Beersum, G. W. A. Rjinders. High pressure gas chromatography and chromatography with supercritical fluids. III. Fluid-liquid chromatography. *Separation Science*, 1967, 2, 729.
- [5] C. G. Giddings, M. N. Myers, J. W. King. Dense gas chromatography at pressures to 2000 atmospheres, *Journal Chromatography Science*. 1969, 7, 276.
- [6] M. Novotny, W. Bertsch, A. Zlatkis. Temperature and pressure effects in supercritical-fluid chromatography, *Journal Chromatography*. 1971, 61, 17.
- [7] K. Sugiyama, M. Saito, T. Hondo, M. Senda. New double stage separation analysis method: directly coupled laboratory-scale supercritical fluid extraction/supercritical fluid chromatography, monitored with a multiwavelength ultraviolet detector, *Journal Chromatography*, 1985, 332, 107.
- [8] M. Saito, Y. Yamauchi, H. Kashiwazaki, M. Sugawara. New pressure regulating system for constant mass flow supercritical-fluid chromatography and physico-chemical analysis of mass-flow reduction in pressure programming by analogous circuit model, *Chromatographia*, 1988, 25, 801.
- [9] Y. Cui, S. V. Olesik. High-performance liquid chromatography using mobile phases with enhanced fluidity. *Analytical Chemistry*, 1991, 63, 1812.
- [10] M. Saito. History of supercritical fluid chromatography: Instrumental development. *Journal of Bioscience and Bioengineering*, 2013, 115, 590.

- [11] J. F. Holler, S. R. Crouch. *Fondamenti di chimica analitica di Skoog e West*. Publisher Edisess 2015.
- [12] F. Gritti, G. Guiochon. The van Deemter equation: Assumptions, limits, and adjustment to modern high performance liquid chromatography. *Journal of Chromatography A* 2013, 1302, 1.
- [13] J.H. Knox, H.P. Scott. B and C terms in the Van Deemter equation for liquid chromatography. *Journal of Chromatography A*, 1983, 282, 297.
- [14] K. De Klerck, D. Mangelings, Y. V. Heyden. Supercritical fluid chromatography for the enantioseparation of pharmaceuticals. *Journal of Pharmaceutical and Biomedical Analysis*, 2012, 69, 77.
- [15] C. West, E. Lesellier. A unified classification of stationary phases for packed column supercritical fluid chromatography. *Journal of Chromatography A*, 2008, 1191, 21.
- [16] L. Miller, M. Potter. Preparative chromatographic resolution of racemates using HPLC and SFC in a pharmaceutical discovery environment. *Journal of Chromatography B*, 2008, 875, 230.
- [17] C. G. da Silva , C. H. Collins, E. Lesellier, C. West. Characterization of stationary phases based on polysiloxanes thermally immobilized onto silica and metalized silica using supercritical fluid chromatography with the solvation parameter model. *Journal of Chromatography A*, 2013, 1315, 176.
- [18] C. Brunelli, Y. Zhao, M. Brown, P. Sandra. Pharmaceutical analysis by supercritical fluid chromatography: Optimization of the mobile phase composition on a 2-ethylpyridine column. *Journal of Separation Science*, 2008 31, 1299.
- [19] T. Cajka, O. Fiehn. Comprehensive analysis of lipids in biological systems by liquid chromatography-mass spectrometry. *TrAC Trends in Analytical Chemistry*, 2014, 61, 192.
- [20] M.. Holčápek, R. Jirásko, M. Lísa. Recent developments in liquid chromatography–mass spectrometry and related techniques. *Journal of Chromatography A*, 2012, 1259, 3.
- [21] R. t'Kindt, E. D. Telenga, L. Jorge, A. J. M. Van Oosterhout, P. Sandra, N. H. T. Ten Hacken, K. Sandra. Profiling over 1500 lipids in induced lung

sputum and the implications in studying lung diseases. *Analytical Chemistry*, 2015, 87, 4957.

[22] K. Sandra, A. dos Santos Pereira, G. Vanhoenacker, F. David, P. Sandra. Comprehensive blood plasma lipidomics by liquid chromatography/quadrupole time-of-flight mass spectrometry. *Journal of Chromatography A*, 2010, 1217, 4087.

[23] C. Byrdwell, D. Borchman. Liquid chromatography/mass-spectrometric characterization of sphingomyelin and dihydrosphingomyelin of human lens membranes. *Ophthalmic research*, 1997, 29, 191.

[24] W. C. Byrdwell. Atmospheric pressure chemical ionization mass spectrometry for analysis of lipids. Springer, 2001, 36, 327.

[25] J. J. Salisbury. Fused-core particles: a practical alternative to sub-2 micron particles. *Journal of Chromatographic Science*, 2008, 46, 883.

[26] R. W. Brice, X. Zhang, L. A. Colón. Wiley Online Library Fused-core, sub-2  $\mu\text{m}$  packings, and monolithic HPLC columns: a comparative evaluation. *Journal of Separation Science*, 2009, 32, 2723.

[27] A. A. Clifford, J. R. Williams. *Introduction to Supercritical Fluids and Their Applications*. Publisher Humana Press, 2000.

[28] *Supercritical fluids chromatography 1<sup>st</sup> Edition*, Elsevier, 2017.

[29] R. J. A. Goodwin. Sample preparation for mass spectrometry imaging: small mistakes can lead to big consequences. *Journal of Proteomics*, 2012, 75, 4893.

[30] D. G. I. Kingston. Mass spectrometry of organic compounds-VI: Electron-impact spectra of flavonoid compounds. *Tetrahedron*, 1971, 27, 2691.

[31] B. E. Richter, D. J. Bornhop, J. T. Swanson, J. G. Wangsgaard, M. R. Andersen. Gas Chromatographic Detectors in SFC. *Journal of Chromatographic Science*, 1989, 27, 303.

[32] P. Roepstorff. Plasma desorption mass spectrometry of peptides and proteins. *Accounts of Chemical Research*, 1989 22, 421.

[33] J. A. Sunner, R. Kulatunga, P. Kebarle. *Analytical Chemistry*. Fast atom bombardment mass spectrometry and gas-phase basicities. *Analytical Chemistry* 1986, 58, 1312.

- [34] I. Marchi, S. Rudaz, J. L. Veuthey. Atmospheric pressure photoionization for coupling liquid-chromatography to mass spectrometry: a review. *Talanta*, 2009, 78, 1.
- [35] M. K. Parr, B. Wüst, J. Teubel, J. F. Joseph. Splitless hyphenation of SFC with MS by APCI, APPI, and ESI exemplified by steroids as model compounds. *Journal of Chromatography B*, 2018, 1091, 67.
- [36] G. L. Glish, R. W. Vachet. The basics of mass spectrometry in the twenty-first. *Nature reviews drug discovery*, 2003, 2, 140.
- [37] M. Holčapek, R. Jirásko, M. Lísa. Recent developments in liquid chromatography-mass spectrometry and related techniques. *Journal of Chromatography A*, 2012, 1259, 3.
- [38] P. Donato, F. Cacciola, P. Q. Tranchida, P. Dugo, L. Mondello. Mass spectrometry detection in comprehensive liquid chromatography: Basic concepts, instrumental aspects, applications and trends. *Mass Spectrometry Reviews*, 2012, 31, 523.
- [39] E. de Hoffmann. Tandem mass spectrometry: A primer. *Journal of Mass Spectrometry*, 1996, 31, 129.

# 4 Limonoids

---

## 4.1 General characteristics

Limonoids are oxygenated triterpenoids (triterpenes that have undergone intense oxidative degradation) with a common 4,4,8-trimethyl-17-furyl steroid skeleton (Figure 4.1). Oxidative degradation at the C-17 side chain results in loss of four carbon atoms and formation of bi-substituted furan, further oxidations and skeletal rearrangements in one or more of the four rings (A, B, C and D) gives rise to different groups of limonoids (Figure 4.1).

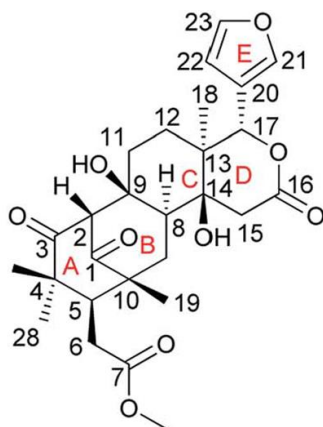


**Figure 4.1** Basic structure of limonoids [1].

Limonoids are natural compounds present in the plants of the *Rutaceae* family (belonging to the *Citrus* genus mostly originating in China) and of the *Meliaceae* (family composed largely of trees or shrubs but also of some herbaceous plants) [2].



To date, more than 3000 limonoids are known (for example *Azadirachta indica* contains more than 100 limonoids and their derivatives in its various plant parts) but those present in significant quantities are very few.

Major citrus species accumulate limonin, nomilin, deacetylnomilin, obacunone, ichang and calamin (Figure 4.2). *Citrus ichangensis* mainly accumulate ichang and ichangensin while *Citrus japonica tobbesi* (Chinese mandarin) and related species mainly accumulate limonoids such as calamine retrocalamine and cyclocalamin [2].

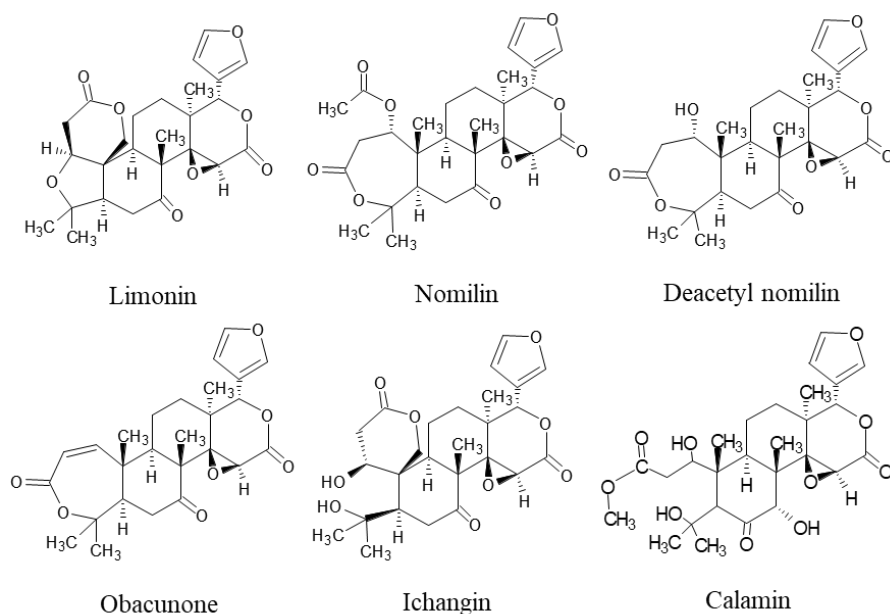


**Figure 4.2** Main limonoids in Citrus species and their respective molecular weights.

Limonin (aglycone limonoid more abundant in citrus fruits) (Figure 4.2) is the first limonoid identified, it was isolated from the Navel orange (*Citrus sinensis*) in 1938, while in 1949 it was identified as one of the components that determine the bitter taste of citrus juices.

The molecular structure of limonin was determined in the 1960s by X-ray diffractometry [3].

Limonoids occur in nature both in the non-carboxylated aglyconic form (neutral form) and in the carboxylated glucosidic form (acid form) (Figure 4.3), the former are responsible for the bitter taste of citrus fruits, they are apolar and mainly present in the parts of the fruit in which there is a lower quantity of water such as seeds and peels, the glucosidic limonoids are tasteless and are soluble in water, therefore present mainly in juice and pulps.

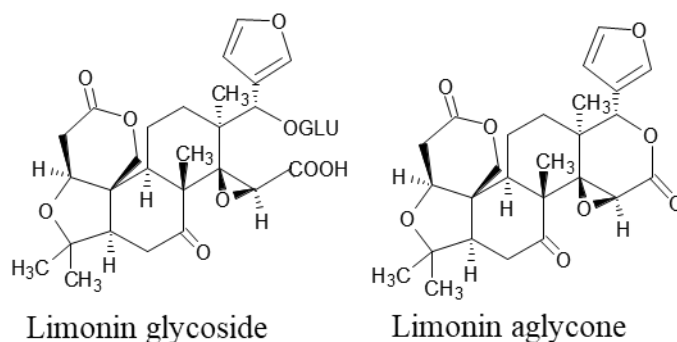


**Figure 4.3** Comparison between aglycon and glucoside limonin.

Glucosides accumulate in the pulp of ripe fruits, mainly limonin glucoside, while both aglycones and glucosides (mainly limonin and nomilin glucoside) are found in the seeds and tissues.

The glucosides stored in the fruit pulp are very stable, so the fresh tissue and freshly squeezed juice do not taste bitter. However, the tissues and seeds were crushed during fruit processing, so bitter aglycones and glucosidases (hydrolytic enzymes) are released. Enzymes hydrolyze glucosidic limonoids into aglycones, increasing the bitter taste of the juice [4].

Limonoid aglycones are endogenously converted into limonoid glucosides during fruit maturation [5].

## **4.2 Pharmacological activities**

The limonoids have various functions in the plant, such as that of removing parasites, in fact, they are abundant in young leaves and fruits. Furthermore, they showed numerous biological activities including: cytotoxicity, antioxidant, anti-inflammatory, antiviral, neuroprotective, antimicrobial, antiprotozoal, antimalarial [1].

Experimental evidence has shown that numerous limonoids have chemopreventive properties as they inhibit, *in vitro*, the growth of human breast cancer cells and block neuroblastoma cells [2].

Limonin is the compound with the best antitumor activity, in fact the limonin-17- $\beta$ -D-glucopyranoside form, *in vitro*, has some cytotoxicity to human colon cancer cells. The antitumor effect is due to the activation of the endogenous apoptotic pathway due to the release of cytochrome C, therefore, limonin can induce endogenous apoptosis via the mitochondria in cancer cells [7]. This phenomenon can be increased with limonin glucoside and curcumin, as these compounds have a synergistic effect with limonin [8].

In mice, with diets involving a consistent consumption of limonin (200 mg/kg), inhibition of cancer cell proliferation and promotion of mitochondrial apoptosis was observed [9].

Limonin also has an anti-hepatocarcinoma effect as it inhibited the growth of hepatocellular carcinoma cells (SMMC-7721) and can induce

apoptosis of hepatoma HepG2 cells by blocking the lipoproteins LRP5, LRP6 [10].

In vivo experiments have shown that it speeds up the reduction of generalized liver cancer, using specific drugs, induced by aflatoxin-b1. While in mice limonin, in a quantity of 50 mg/kg, favors the recovery of the organism after treatments for the hepatothocarcinoma induced by N-nitroethylenediamine, as it suppresses the lipid peroxidation that generates free radicals mediated by oxidative stress [11].

The limonoids obacunone, limonin, nomilin (aglycones and glycosides) inhibit, in vivo, chemically induced carcinogenesis in a number of human cancer cell lines, with significant cytotoxicity against lung, colon, oral and skin cancer [12,13].

Limonin can regulate inflammation induced by CD4<sup>+</sup>T cells, inhibiting proliferation, and it is also involved, as an inhibitor, in the inflammatory process activated by protein kinases in smooth muscle [14].

In rats with chronic airway inflammation, limonin can inhibit mucin production by activating the expression of the TAS2R gene in the lung [15].

While different aglycone limonoids can relieve chronic inflammation of the intestinal mucosa and acute inflammation of the respiratory tract. The limonoids aglycones, especially limonin, have a bacterial and fungicidal effect. Specifically, the bactericidal effect depends on the type of bacterium considered: *Bacillus subtilis* > *Staphylococcus aureus* > *Escherichia coli* > *Aspergillus Niger* > *Shigella* > *Salmonella*. Furthermore, in vitro bacteriostasis experiments have shown that limonin has an effective antibacterial action against *Xanthomonas spp.* [16].

The ways in which limonoids act on bacteria are different, for example, they can effectively inhibit intercellular communication, cell membranes formation and the type three secretion system (TTSS) of *Escherichia coli* [17].

Finally, several classes of natural products, including limonoids, have been studied for the treatment of malaria. Four naturally occurring limonoids, including limonin and obacunone, have been isolated and tested for their potential antimalarial activity against *Plasmodium falciparum*.

Many of the isolated limonoids hindered the development of the parasite, in fact, an experiment that measured the formation of new ring parasites (*Plasmodium falciparum*) after 48 hours of incubation, treated with limonin and obacunone, showed a development far below average without using these limonoids [18,19].

### **4.3 Analysis of limonoids**

Many analytical methods have been developed to identify aglycone limonoids and thus monitor bitterness in citrus juices.

The most common methods for the quantitative analysis of limonoids use HPLC systems with UV detectors. The RP-LC chromatographic method is the most used with a C18 bound silica column, acetonitrile/water and acidified acetonitrile mobile phases and maximum UV absorbance of 207 nm [20].

Normal phase HPLC-UV methods have been developed using binary and tertiary eluent mixtures, using silica HPLC columns [21,22].

The advent of coupled HPLC-MS and HPLC-MS/MS techniques has allowed the development of new methods for the analysis of aglycone and glucoside limonoids. These techniques, much more sensitive and selective than the previous ones, have made it possible to identify numerous new secondary limonoids present in citrus fruits and their commercial products and to quantify those already discovered in a more accurate manner.

Precision in quantifying limonoids by LC-MS requires the incorporation of internal standards or rigorous matrix effect studies if external standards are used due to the remarkable sensitivity of the technique [23].

The analysis of limonoids with HPLC-UV systems requires the use of standards for chromatographic comparison as the UV detector does not allow further discrimination between the compounds considered.

HPLC-APCI / MS and HPLC-APCI / MS / MS systems have been used to create fragmentation models of pure limonoids that can be used as an identification tool for unknown limonoid aglycones in citrus extracts [24].

## References

- [1] Y. Zhang, H. Xu. Recent progress in the chemistry and biology of limonoids. Royal Society of Chemistry, 2017, 7, 35191.
- [2] M. A. Berhow, S. Hasegawa, G. D. Manners. Citrus Limonoids. American Chemical Society, 2020.
- [3] S. Arnott, A. W. Davie, J. M. Robertson, G. A. Sim, D. G. Watson. The structure of limonin. Springer, 1960, 16, 49.
- [4] G. D. Manners, R. A. Jacob, T. K. Schoch, S. Hasegawa. Bioavailability of Citrus Limonoids in Humans. Journal. Agriculture. Food Chemistry, 2003, 14, 4156.
- [5] Z Herman, C. H. Fong, S. Hasegawa. Biosynthesis of limonoid glucosides in navel orange. Phytochemistry, 1991, 30, 1487.
- [6] N. Guthri, K. Morley, Shin Hasegawa, Gary D. Manner, and T. Vandenberg. Inhibition of Human Breast Cancer Cells by Citrus Limonoids
- [7] K. N. Chidamb Murthy, G. K. Jayaprakasha, V. Kumar, K. S. Rathore, B. S. Patil. Citrus limonin and its glucoside inhibit colon adenocarcinoma cell proliferation through apoptosis. Journal. Agriculture. Food Chemistry, 2011, 59, 2314.
- [8] K. N. Chidambara Murthy, G. K. Jayaprakasha, B.S. Patil. Citrus limonoids and curcumin additively inhibit human colon cancer cells. Food Funct, 2013, 4, 803.
- [9] J. Vanamala, T. Leonardi, B. S. Patil, S. S. Taddeo, M. E. Murphy, L. M. Pike, R. S. Chapkin, J. R. Lupton, N. D. Turner. Suppression of colon carcinogenesis by bioactive compounds in grapefruit. Carcinogenesis, 2006, 27, 1257.
- [10] K. Langeswaran, S. Gowthamkumar, S. Vijayaprakash, R. Revathy, M.P. Balasubramanian: Influence of limonin on Wnt signalling molecule in HepG2 cell lines. Journal of Natural Science, Biology and Medicine, 2013, 4, 126.
- [11] J. Yao, J. Liu, W. Zhao. By blocking hexokinase-2 phosphorylation, limonin suppresses tumor glycolysis and induces cell apoptosis in hepatocellular carcinoma. Onco Targets and Therapy 2018, 11, 3793.
- [12] S. Shimizu, S. Miyamoto, G. Fujii, R. Nakanishi, W. Onuma, Y. Ozaki, K. Fujimoto, T. Yano, M. Mutoh. Suppression of intestinal carcinogenesis in

Apc-mutant mice by limonin. *Journal of Clinical Biochemistry and Nutrition*. 2015, 57, 39.

[13] Y. Shia, Y. Zhang, H. T. Li, C. H. Wu, H. R. El-Seedi, W. K. Ye, Z. W. Wan, C. B. Li, X. F. Zhan, G. Y. Kai. Limonoids from Citrus: Chemistry, anti-tumor potential, and other bioactivities. *Journal of Functional Foods*, 2020, 75, 104213.

[14] J. Vanamala, T. Leonardi, B.S. Patil, S. S. Taddeo, M. E. Murphy, L. M. Pike, R. S. Chapkin, J. R. Lupton, N.D. Turner. Suppression of colon carcinogenesis by bioactive compounds in grapefruit. *Carcinogenesis* 2006, 27, 1257.

[15] M. H. Liu, X.D. Zhou. Limonin inhibits the PM2.5 inhalation-induced airway inflammation and mucus hypersecretion in rats. *Basic Medical Sciences and Clinical Medicine*. 2018, 38, 433.

[16] S. A. M. Abdelgaleil, F. Hashinaga, M. Nakatani. Antifungal activity of limonoids from *Khaya ivorensis*. *Pest Management Science*, 2005, 1, 186.

[17] D. Hamdan, M. Z. El-Readi, A. Tahrani, F. Herrmann, D. Kaufmann, N. Farrag, A. El-Shazly, M. Wink. Secondary metabolites of ponderosa lemon (*Citrus pyriformis*) and their antioxidant, anti-inflammatory, and cytotoxic activities. *Zeitschrift für Naturforschung*, 2011, 66, 385.

[18] J. Bickii, N. Njifutie, J. Ayafor, Foyere, L. K. Basco, P. Ringwald. In vitro antimalarial activity of limonoids from *Khaya grandifoliola* C.D.C. (Meliaceae).

[19] W. Maneerat, S. Laphookhieo, S. Koysomboon, K. Chantrapromma. Antimalarial, antimycobacterial and cytotoxic limonoids from *Chisocheton siamensis*. *Phytomedicine*, 2008, 15, 1130.

[20] Z. Herman, C. H. Fong, S. Hasegawa. Analysis of limonoids in citrus seeds. In *Modern methods of plant analysis: Seed analysis*. Springer-Verlag 1992.

[21] G. D. Manners, S. A. Hasegawa. New normal phase liquid chromatographic method for the analysis of limonoids in Citrus. *Phytochemical Analysis*, 1999, 10, 76.

[22] R. L. Rouseff, J. F. Fisher. Determination of limonin and related limonoids in citrus juices by high performance liquid chromatography. *Analytical Chemistry*, 1980, 52, 1228.



[23] G. D. Manners, A. P. Breksa. Identifying citrus limonoid aglycones by HPLC-EI/MS and HPLC-APCI/MS techniques. *Phytochemical Analysis*, 2004, 15, 372.

[24] Q. Tian, S. J. Schwartz. Mass spectrometry and tandem mass spectrometry of citrus limonoids. *Analytical Chemistry*, 2003, 75, 5451.

# 5 Carotenoids and apocarotenoids

---

## 5.1 Characteristics of carotenoids and apocarotenoids

Carotenoids are isoprenoid compounds consisting of long chains of 40 carbon atoms with 10-12 conjugated double bonds and often ending in a saturated or unsaturated ring.

The ability of carotenoids to absorb ultraviolet and visible light is determined by the number and configuration of the double bonds, this determines their color.

Carotenoids are mainly produced by plants and by some photosynthetic and heterotrophic microorganisms [1]. They are essential for these organisms, as they improve the absorption of photons, necessary for photosynthetic processes, and protect chlorophylls and other molecules from photodegradation and photooxidation [2].

These pigments color flowers and fruits from yellow to red making them clearly visible and "palatable" for pollinating insects that facilitate the pollination of Gymnosperm and Angiosperm plants and for animals that eat the fruit by spreading the seeds in the neighboring territories.

Furthermore, carotenoids are present in pollen as they have a protective and antioxidant effect on the male gametophytes necessary for the fertilization of the pistil [3].

Carotenoids, in humans, have an antioxidant effect and are the precursors of vitamin A (retinol), moreover, recent studies have shown their importance as co-activators and co-inhibitors of numerous metabolic processes.

Carotenoids, based on their molecular structure, are divided into two categories; carotenes (hydrocarbon chains without heteroatoms) such as  $\beta$ -carotene and lycopene and xanthophylls (hydrocarbon chains with hydroxyl and/or carbonyl groups) such as lutein and zeaxanthin (Figure 5.1).

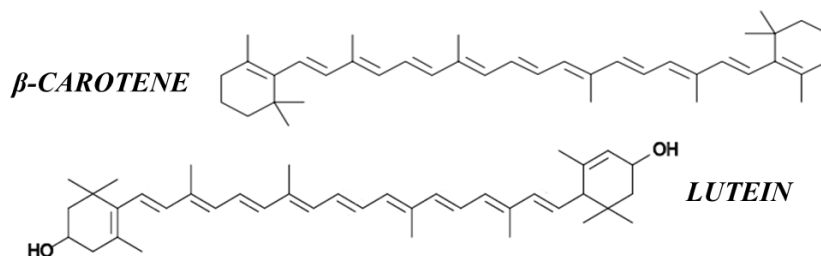


**Figure 5.1** Molecular structure of  $\beta$ -carotene (carotene) and lutein (xanthophyll).

Carotenoids can be classified also according to their terminal groups (acyclic, monocyclic and bicyclic) or by the isomeric configuration of their double bonds (E-Z) [1,2]

Carotenoids are the precursors of a series of compounds called apocarotenoids (Figure 5.2), which make up a large family of multifunctional metabolites, including antioxidant activities.

Apocarotenoids are biologically produced through the specific oxidative cleavage of the double bonds of carotenoids by iron-dependent enzymes (CCDs). In mammals, the cytoplasmic enzyme  $\beta$ -carotene-15-15'-oxygenase 1 (BCO1) and the mitochondrial enzyme  $\beta$ -carotene-9'-10'-oxygenase 2 (BCO2), responsible, respectively, for the cleavage of the double bond central and successive double bonds of a large class of carotenoids [4,5].

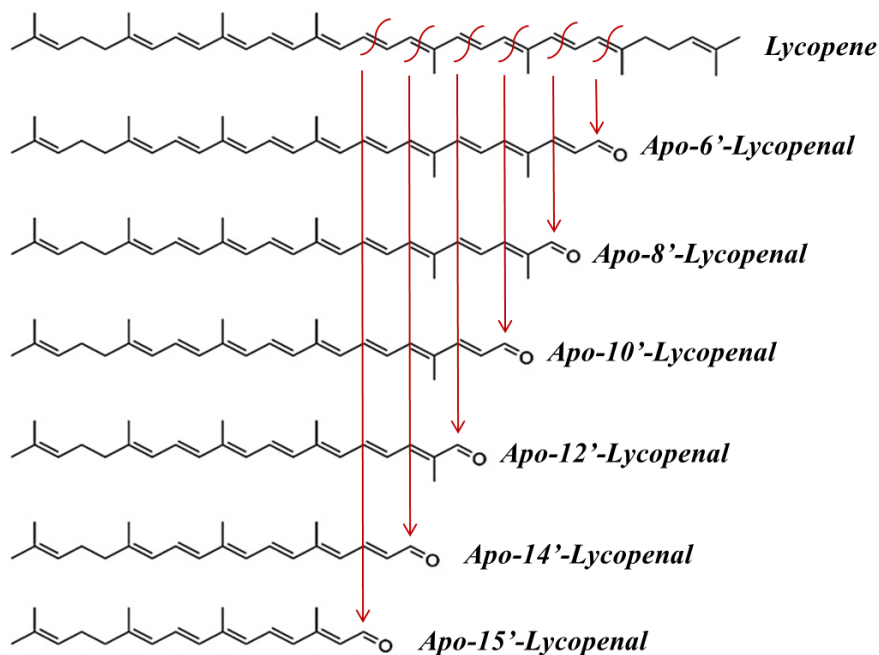


**Figure 5.2** Oxidative cleavage of lycopene and formation of apo-lycopenals.

This biological differentiation in the oxidative cleavage of carotenoids is fundamental for the regulation of the production of symmetrical and asymmetric apocarotenoids. For example, vitamin A (essential for numerous biological processes such as vision and cell differentiation) is produced by the symmetrical oxidative cleavage of  $\beta$ -carotene and in minimal quantities by that of  $\alpha$ -carotene and  $\gamma$ -carotene [6].

Apocarotenoids can also be produced from their precursors through non-specific oxidative reactions, using oxidizing compounds.

Apocarotenoids are usually named based on the number of the carbon atom where the oxidative cleavage occurs and with the name of their precursor but using the prefix "apo".

In some cases, different carotenoids are the precursors of identical apocarotenoid, this happens for the asymmetric carotenoids from which

different apocarotenoid families are formed according to the point of cleavage.

Often, in nature hydroxycarotenoids and apohydroxycarotenoids are mono or di esterified with fatty acids, the most common esters are formed with lauric (C12:0), myristic (C14:0) and palmitic (C16:0) acids. These molecules have no proven biological effects, but esterification provides greater stability to the initial molecule, their formation is thought to be due to a form of conservation and storage within the organism of the precursor molecules [7].

## **5.2 Protective and preventive bioactivities**

Carotenoids are associated with numerous metabolic processes within the human organism, the most important, and the best known, is the formation of vitamin A or retinol (Figure 5.3 A), which is essential for the development of visual processes.

Retinol is a metabolite of retinal or apo-15-carotenal (Figure 5.3 B) an apocarotenoid which is mainly obtained from the oxidative cleavage of  $\beta$ -carotene (Figure 5.3 C) [6].

The  $\beta$ -carotene is absorbed by the intestine and being a symmetrical molecule, it is split into two retinaldehyde molecules, which are transformed into retinol through an enzymatic reduction of the carbonyl group. All carotenoids that have at least one unsubstituted  $\beta$ -ionone ring such as  $\alpha$ -carotene and  $\gamma$ -carotene follow the same metabolic path but from their oxidative cleavage only one retinaldehyde molecule is formed, being asymmetric molecules [8].

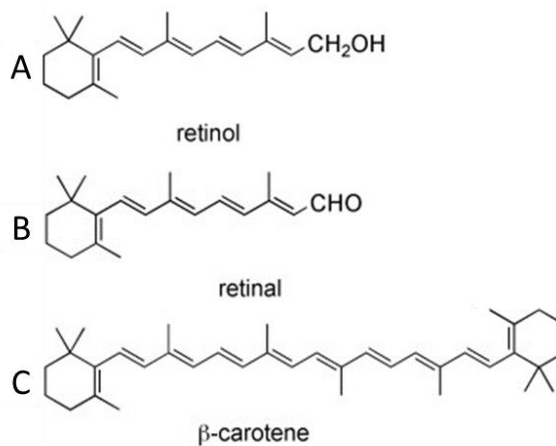


**Figure 5.3** Structures of retinol (A), retinal (B) and β-carotene (C).

Retinoic acid, one of the metabolites of retinol, plays a role in the process of embryonic maturation and in the differentiation of some cell lines, as it determines the regulation of the expression of some genes [9].

Another biologically active retinol derivative is retinol-phosphate which acts as a sugar donor in the process of glycoprotein formation.

Finally, vitamin A is necessary for the production of collagen, an essential protein for giving elasticity to the skin, preventing and delaying the appearance of wrinkles and other skin imperfections [6].

Numerous scientific studies have shown that a higher than average level of carotenoids in the body is correlated with a lower incidence of chronic diseases.

β-carotene and lycopene are linked to a lower risk of cardiovascular disease, while lutein and zeaxanthin are associated with a lower development of eye disorders [10].

Several studies also underline the importance of carotenoids in preventing and combating some forms of cancer.

Lycopene has a positive effect on some types of prostate cancer, for example it reduces the expression of the SRD5A1 gene which produces the protein responsible for converting testosterone into 5 $\alpha$ -dihydrotestosterone which induces the formation of transgenic adenocarcinoma [11].

Carotenoids are thought to have gene hypoexpressive effects in breast cancers as well.  $\beta$ -carotene decreases the expression of the anti-apoptotic proteins, Bcl-2 and PARP which induce the multiplication of diseased cells.

While lycopene caused a decrease in proliferation and an increase in apoptosis in MCF-7 breast cancer cells through the suppression of a mutated gene that produces inactive apoptotic proteins [12].

Other carotenoids such as cryptoxanthin, zeaxanthin and lutein and the corresponding families of apocarotenoids show strong antioxidant actions. Numerous in vitro, animal and human experiments have been done to study the antioxidant activity of carotenoids and apocarotenoids.

They are able to reduce the oxidative effect of UV rays on human dermal fibroblasts (FEK4), which allows the skin to be protected from the oxidative processes induced by ultra-violet rays [6].

$\beta$ -carotene,  $\alpha$ -carotene, lutein and lycopene, together with other antioxidant molecules, tend to decrease mitochondrial oxidative stress, while in the cytoplasm they block pro-oxidant species [7,13].

On the other hand, interesting is the in vitro effect of  $\beta$ -carotene, lutein and zeaxanthin which tend to increase the amount of reactive oxygen species (ROS) and oxidized cellular glutathione in leukemia and adenocarcinoma cell lines in the colon [14].

### **5.3 Methods of analysis**

The extraction process of carotenoids and apocarotenoids depends on the matrix to be analyzed, therefore there is no single method for the extraction of these molecules.

Generally, one or more organic solvents are used to perform a liquid-liquid or liquid-solid extraction [15].

Non-polar solvents, such as hexane, are a good choice for non-polar carotenoids for their apo derivatives and esterified species, while polar solvents, such as ethanol and acetone, are more used for polar carotenoids and their derivatives apo. The latter group is the most complex due to the considerable structural differences, they can be found in both free and mono or diesterified form.

Due to the complexity of the extract, saponification is often performed before chromatographic analysis to eliminate lipids and chlorophylls which can complicate the interpretation of the results [16].

The identification of carotenoids and apocarotenoids in a matrix extract can be easily done with an HPLC-RP system coupled to a UV-Vis detector, with C18 or C30 bound phase packed columns and mobile phases including solvents with medium polarity high according to the class of carotenoids to be analyzed [17].

Some papers also report the use of HPLC-NP techniques for specific classes of carotenoids and UHPLC systems for fast analyzes [17,18].

Specific identification of carotenoids can be done by liquid chromatography coupled to an MS detector with APCI interface, using standards it is possible to determine and quantify them.

The most used interface is APCI even if the ESI one has given good results of both positive and negative ionization using additives such as:



ammonium acetate, acetic acid, formic acid and eluents containing halogens [19].

In the case of unknown chromatographic peaks, coupling with UV-Vis and MS detectors can provide valuable data for their identification.

The problem with the MS technique is that there are no standards available for all carotenoids and apocarotenoids and often the costs of some compounds are very high. Identifying compounds without standards can be difficult as carotenoids (and consequently also apocarotenoids) have an identical basic structure and many have the same molecular weight. In this case the simple MS system is not powerful enough for their discrimination, so MS/MS systems are needed.

The PIS and MRM modes in MS/MS systems allow to distinguish molecules with similar structures and with the same molecular weight [20,21].

## References

- [1] M. H. Walter, D. Strack. Carotenoids and their cleavage products: Biosynthesis and functions. *Natural Product Reports*, 2011, 28, 663.
- [2] H. Hashimoto, C. Uragami, R. J. Cogdell. Carotenoids and photosynthesis. *Carotenoids in Nature*, 2016, 1, 111.
- [3] R. Mărgăoan, L. A. Mărghitaş, D. S. Dezmiorean, F. V. Dulf, A. Bunea, S. Ancuţa Socaci, O. Bobiş. Predominant and secondary pollen botanical origins influence the carotenoid and fatty acid profile in fresh honeybee-collected pollen. *Journal of Agricultural and Food Chemistry* 2014, 62, 6306.
- [4] E. Giordano, L. Quadro. Lutein, zeaxanthin and mammalian development: metabolism, functions and implications for health, *Archives of Biochemistry and Biophysics*, 2018, 647, 33.
- [5] A. Eroglu, E.H. Harrison, Carotenoid metabolism in mammals, including man: formation, occurrence, and function of apocarotenoids, *Journal of Lipid Research*, 2013, 1, 54.
- [6] J. Bailly, M. Crettaz, M. H. Schiffers, J. P. Marty. In vitro metabolism by human skin and fibroblasts of retinol, retinal and retinoic acid. *Experimental Dermatology*, 2007, 7, 27.
- [7] C. Stange. *Carotenoids in Nature*. Springer, 2016.
- [8] L. Joseph. Biochemical Pathways of Retinoid Transport, Metabolism, and Signal Transduction. *Clinical Immunology and Immunopathology*, 199, 680, 52.
- [9] R. Kin, T. Kam, Y. Deng, Y. Chen, H. Zhao. Retinoic acid synthesis and functions in early embryonic development. *Cell & Bioscience*, 2012, 2, 11.
- [10] J. S. L. Tan, J. J. Wang, V. Flood, E. Rochtchina, W. Smith, P. Mitchell. Dietary Antioxidants and the Long-term Incidence of Age-Related Macular Degeneration: The Blue Mountains Eye Study. *Ophthalmology*, 2008, 115, 334.
- [11] E. Giovannucci, E. B. Rimm, Y. Liu, M. J. Stampfer, W. C. Willett. A Prospective Study of Tomato Products, Lycopene, and Prostate Cancer Risk. *Journal of the National Cancer Institute*, 2002, 94, 391.
- [12] R. M. Tamimi, S. E. Hankinson, H. Campos, D. Spiegelman, S. Zhang, G. A. Colditz, Wa. C. Willett, D. J. Hunter. Plasma Carotenoids, Retinol, and

Tocopherols and Risk of Breast Cancer. *American Journal of Epidemiology*, 2005, 161, 153.

[13] W. Stahl, H. Sies. Antioxidant activity of carotenoids. *Molecular Aspects of Medicine*, 2003, 24, 345.

[14] J. Shin, M. Song, J. Oh, Y. Keum, R. K. Saini. Pro-oxidant Actions of Carotenoids in Triggering Apoptosis of Cancer Cells: A Review of Emerging Evidence. *Antioxidants*, 2020, 9, 532.

[15] B. K. Ishida, M. H. Chapman. Effects of a hydrodynamic process on extraction of carotenoids from tomato. *Food Chemistry*, 2012, 132, 1156.

[16] E. Murillo, D. Giuffrida, D. Menchaca, P. Dugo, G. Torre, A.J. Meléndez-Martínez, Luigi Mondello. Native carotenoids composition of some tropical fruits. *Food Chemistry*, 2013, 140, 825.

[17] K. T. Amorim-Carrilho, A. Cepeda, C. Fente, P. Regal. Review of methods for analysis of carotenoids. *Trends in Analytical Chemistry*, 2014, 56, 49.

[18] H. Li, Z. Deng, R. Liu, S. Loewen, R. Tsao, Carotenoid compositions of coloured tomato cultivars and contribution to antioxidant activities and protection against H<sub>2</sub>O<sub>2</sub>-induced cell death in H9c2. *Food Chemistry*, 2013, 136, 878.

[19] T. Lacker, S. Strohschein, K. Albert. Separation and identification of various carotenoids by C30 reversed-phase high-performance liquid chromatography coupled to UV and atmospheric pressure chemical ionization MS detection. *Journal of Chromatography A*, 1999, 854, 37.

[20] F. Cacciola, P. Donato, M. Beccaria, P. Dugo, L. Mondello. Advances in LC-MS for Food analysis. *LCGC Europe*, 2012, 1, 15.

[21] M. Herrero, V. García-Cañas, C. Simo, A. Cifuentes. Recent advances in the application of CE method for food analysis and foodomics. *Electrophoresis*, 2010, 31, 205.

# 6 Supercritical fluid chromatography mass spectrometry for the characterization of limonoid aglycones in *Citrus* essential oils

---

## 6.1 Introduction

*Citrus* essential oils are obtained by cold pressing from *Citrus* peels fruits like bergamot, lemon, mandarin, sweet orange, grapefruit, lime, and bitter orange using mechanical systems [1]. These oils are added as ingredients in food stuffs for their organoleptic properties, and also for their antimicrobial, anticancer, anti-inflammatory, antiviral, and antioxidant properties [2].

The non-volatile fraction of *Citrus* essential oils is composed of long chain hydrocarbons, fatty acids, sterols, wax, carotenoids, coumarins, psoralens, polymethoxylated flavones but also limonoids [3].

Limonoids are highly oxygenated modified triterpenes derived from a precursor with 4,4,8-trimethyl-17-furanylsteroid skeleton biosynthesized from acetate-mevalonate pathway in *Citrus*.

These molecules have been investigated intensively due to their wide range of biological activities. For example, some limonoids have antimicrobial activity, offer some protection capacity against low-density lipoprotein (LDL) oxidation, and possess a strong antioxidant action [4].

Since 1966, several analytical techniques were employed for the identification and quantification of limonoids but starting from the

1990s, the most employed analytical technique to analyze limonoids in *Citrus* fruits was reversed phase liquid chromatography coupled to a UV–Vis detector or in many cases with a mass spectrometer detector. In the last years, due to significant technological instrumental advancements, supercritical fluid chromatography (SFC) coupled to mass spectrometry system has gained attention as a green, fast, and useful technology [5]. This work provides a qualitative profile of limonoid aglycones and quali/quantitative for limonin in different *Citrus* essential oils, by means of anSFC-QqQ MS system, in a fast, efficient, and environmentally friendly way. Among the samples analyzed, differences in the composition of limonoids were observed, adding further data to the characterization of *Citrus* species.

## **6.2 Experimental section**

### *6.2.1 Samples and sample preparation*

In the present research were analyzed 11 cold-pressed *Citrus* essential oils (bergamot, sweet orange, clementine, bitter orange, blood orange, mandarin green, mandarin yellow, mandarin red, pink grapefruit and two of lemon oils) supplied by a Sicilian company. All samples were analyzed without any pre-treatment and injected into the SFC system for three consecutive times. Moreover, limonoids, contained in lemon seeds, were extracted three times starting from 5 g with 40 mL of methanol (MeOH), 40 mL of acetone, and 40 mL of ethyl acetate. The extracts were washed with 50 mL of n-hexane, gathered, dried with anhydrous sodium sulfate, filtered on filter paper, and brought to dryness in a rotary evaporator; the extract thus obtained was dissolved

in 10 mL of ethyl acetate, filtered on filter 0.45- $\mu\text{m}$  and injected into SFC.

The limonin standard used in the analyzes had previously been isolated in our laboratory from bergamot seeds [6].

Limonin standard was used to confirm the identification and for quantitative analysis, while lemon seeds extract was used as reference material containing the following: nomilin, limonin, ichangin, deacetylномilin, and obacunone.

### *6.2.2 SFC-APCI-QqQ MS Analysis*

The SFC-QqQ MS analyses were performed on a Shimadzu Nexera-UC system, consisting of a CBM-20A controller, two LC-20ADXR dual-plunger parallel-flow pumps, an LC-30ADSF CO<sub>2</sub> pump, two SFC-30A back pressure regulator, a DGU degasser, a CTO-20AC column oven, a SIL-30AC autosampler, an LCMS-8050 triple quad mass spectrometer equipped with an APCI source. The entire system was controlled by the LabSolution ver. 5.8. Separations were performed on an Ascentis™ C18, 250 × 4.6 mm, 5  $\mu\text{m}$  d.p. column; the mobile phase consisted of the following: eluent A, CO<sub>2</sub>; eluent B MeOH; make-up solvent, MeOH. The following gradient was used: 0 min, 0% B; 20 min 12% B, and the flow rate was of 2 mL min<sup>-1</sup> (total flow pump A and B) and 0.5 mL min<sup>-1</sup> make-up pump. The column oven temperature was 35 °C and the back-pressure regulator was 150 bar. The injection volume was 3  $\mu\text{L}$ . The MS was set as follows: acquisition mode (+): SCAN; selective ion monitoring (SIM); multiple reaction monitoring (MRM). Interface temperature: 350 °C; DL temperature: 300 °C; block heater temperature: 300 °C; nebulizing gas flow (N<sub>2</sub>) 4

Lmin<sup>-1</sup>; drying gas flow (N<sub>2</sub>) 5 mLmin<sup>-1</sup>; full scan range: 200–800 m/z; event time 0.03 s for each event; argon was used as collision gas with a pressure of 270 kPa.

The different limonoids were first recognized by using the positive SIM and in the case of limonin also by comparison with the available standard. The transitions used in the multiple reaction monitoring (MRM) experiments were optimized starting from the product ion scan (PIS) of the relative radical ions, using various collision energies (CE) from 5 to 50 V in positive mode.

The ratio of quantifier (Q) and qualifier (q) ions, in MRM mode, for each compound was taken into account in order to provide a further identificative parameter [5]. PIS acquisition mode was also used for the structure elucidation of isobaric compounds.

### 6.2.3 Using the MS/MS system

Non-volatile fraction of *Citrus* essential oils has been mainly investigated by using HPLC-PDA-MS [2] instrumentation.

SFC technique allows, however, for short run time without losing of separation power, by using low amount of organic solvent [5,7]

The use of a photodiode array as detector in the UV range, and an MS system after the chromatographic separation, are not sufficient for a deep characterization of unknown samples. Instead, the use of a MS/MS detector, due to its great selectivity and sensitivity, allows the identification of targeted and non-targeted compounds, thanks to its high resolution and the possibility of carrying out structural tests on the analyzed compounds. The pairs of the molecule here analyzed are isobaric species with the same structural formula and with the same

molecular weight. For such a reason, the use of a high-resolution MS system is not able to discriminate: limonexin and limonexic acid: molecular weight 502.516 ( $C_{26}H_{30}O_{10}$ ); deoxylimonin and obacunone: molecular weight 454.519 ( $C_{26}H_{30}O_7$ ); nomilin and 7- $\alpha$ -limonyl acetate: molecular weight 514.56 ( $C_{28}H_{34}O_9$ )]. A triple quadrupole MS detector represents one of the best choices for the identification of limonoid aglycones in cold-pressed *Citrus* essential oils.

#### 6.2.4 SFC-QqQ MS optimization

The first step was the optimization of the SFC conditions according to injection volume, elution gradient, and back pressure. Two different columns were tested, a C18 fused core Ascentis Express ( $150 \times 4.6$  mm,  $2.7 \mu\text{m}$  d.p.) and a conventional C18 Ascentis ( $250 \times 4.6$  mm,  $5 \mu\text{m}$  d.p.). In both cases, the best gradient was from 0 to 20 min increasing up to 12% of MeOH, with an injection volume of  $3 \mu\text{L}$  and a back pressure of 150 bar. However, despite the higher efficiency of the fused core one, the best results were obtained by using a conventional C18 with  $5 \mu\text{m}$  of d.p.

The SFC method here developed, despite the use of a conventional  $5 \mu\text{m}$  column, provided a fast separation of the target analytes in less than 7 min (without considering the reconditioning time) with a total consumption of  $170 \mu\text{L}$  of organic solvent (MeOH), representing an attractive alternative to the conventional LC methods.

Following, the aim of the work was devoted to a targeted screening, by using both full scan and SIM mode, of the essential oil samples, of 19



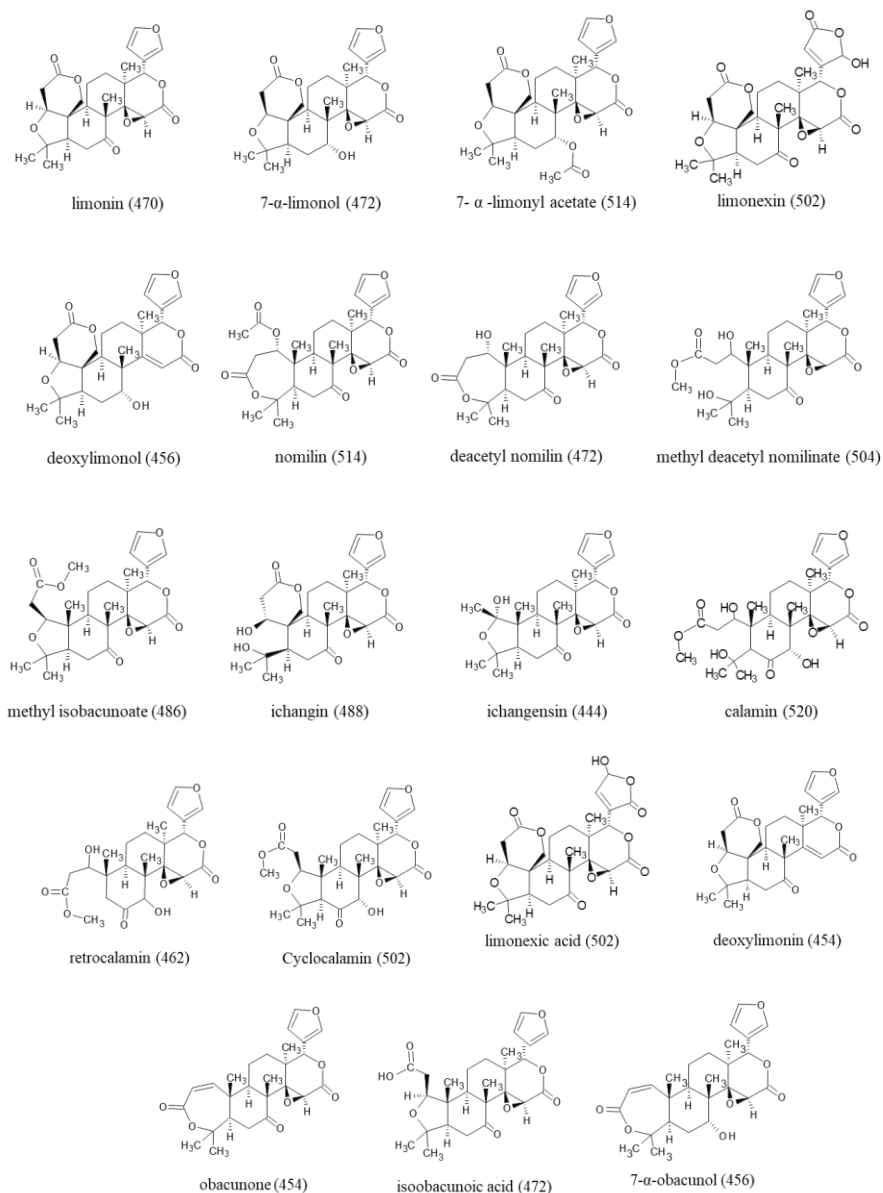


**Figure. 6.1** Molecular structure of principal limonoid with their respective molecular weights (M.W.).

limonoid aglycones most commonly found in seeds, peels, and juices of *Citrus* species (Figure 6 1), as reported in available literature [6,8,9].

The results of the initial screening, showed the presence of 12 limonoid aglycones with respect to the 19 originally selected. Particularly, for all cases of isobaric molecules, mentioned above, only one signal (with the same retention time) was detected in each oil samples. For such a reason, further investigation was needed the correct identification of the isobaric compounds.

#### *6.2.5 Tentative identification of isobaric compounds*

For tentatively identify the limonoid aglycones, the PIS mode was used to obtain a fragmentation pattern correlated to the characteristic structures of the selected  $[M+H]^+$ . PIS and MRM analyses of each compound were carried out injecting samples, which show the most abundant content. Only in one case, namely limonin, the MRM transitions were optimized by injecting a pure standard.

As can be seen in Figure 6.1, nomilin and 7- $\alpha$ -limonyl acetate present a different A ring: a seven-membered oxepine ring for the first one, while 7- $\alpha$ -limonyl acetate belong to the A-secolimonoids.

After a careful interpretation of the PIS, of the ion  $[M+H]^+$  515, two characteristic fragments of the nomilina ( $m/z$  369 and  $m/z$  351) were found as reported in Figure 6.2. Because the most likely fragmentation pathway is the one leading to the formation of ions characterized by the seven membered oxepine A ring structure intact as confirmed by [10].

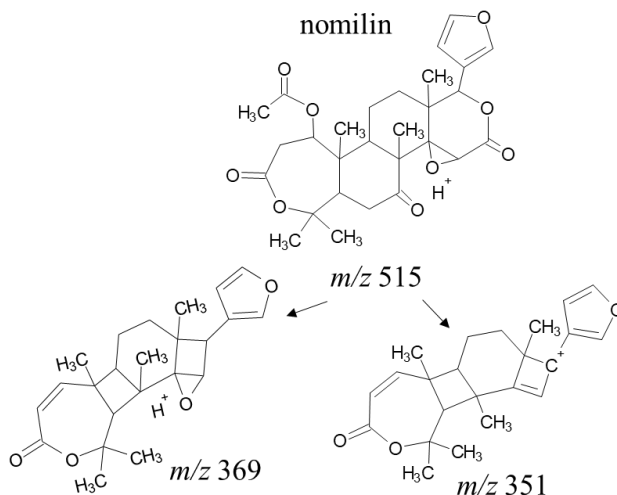


**Figure 6.2** Theoretical fragmentation of the nomilin by means of the fragments obtained from the PIS mode.

As can be observed in Figure 6.1, the molecular structure of obacunone and deoxylimonin differs for the A ring as in the case of nomilin and 7- $\alpha$ -limonyl acetate, and for the D ring. In the D ring, carbons 14 and 15 show a double bond in the case of deoxylimonin, while obacunone presents an epoxy-ring. PIS for the  $[M+H]^+$  455 show two characteristic fragments with  $m/z$  value of 391 and  $m/z$  349 that can be associated to the obacunone molecule tentatively identified, as can be seen in Figure 6.3.

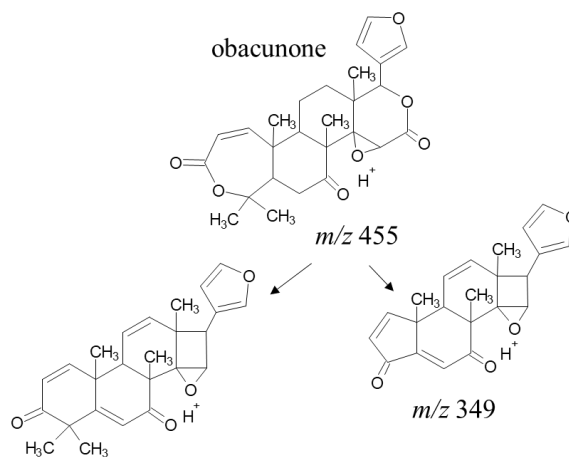


**Figure 6.3** Theoretical fragmentation of the obacunone by means of the fragments obtained from the PIS mode.

The same considerations can be made for 7- $\alpha$ -obacunol and deoxylimonol couple (Figure 6.4). These two molecules show the same molecular structures of obacunone and deoxylimonin, respectively, but with a hydroxyl group in position 7 of the B ring, instead of the carbonyl group. The fragment with  $m/z$  187 allows the tentative identification of the 7- $\alpha$ -obacunol considering the fragmentation pathway as reported in Figure 6.4.

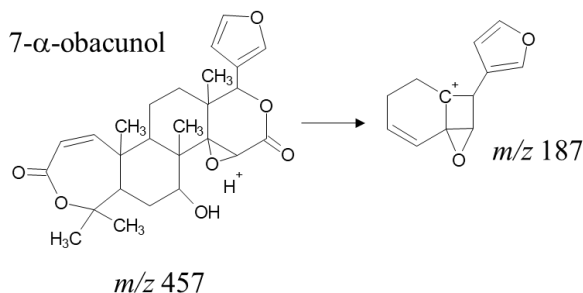


**Figure 6.4** Theoretical fragmentation of the 7- $\alpha$ -obacunol by means of the fragments obtained from the PIS mode.

Also, for the following molecules: deacetyl nomilin, isoobacunoic acid, and 7- $\alpha$ -limonol, the major structural differences come from the A ring (Figure 6.5). But, after a careful investigation of the fragments derived from the PIS, the most characteristic part of the molecule seems to be the presence of the hydroxyl group in the B ring. In fact, only the presence of the hydroxyl group can justify the formation of the ions with value of  $m/z$  352 and  $m/z$  337 from the  $[M+H]^+$  473 (Figure 6.5).

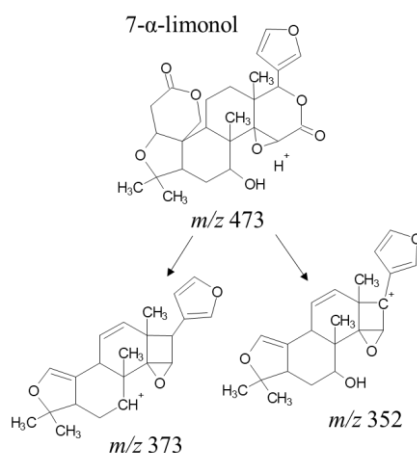


**Figure 6.5** Theoretical fragmentation of the 7- $\alpha$ -limonol by means of the fragments obtained from the PIS mode.

The isobaric compounds limonexic acid, limonexin, and cyclocalamin, reported in Figure 6.6, with a  $[M+H]^+$  503 differ each other for the substituent in position 17 of the D ring.

Characteristic, for the tentative identification, is the furanic ring presents only in the cyclocalamin, thus generating the characteristic ions with  $m/z$  243 and  $m/z$  189 during the PIS experiments. In fact, limonexic and limonexin show in position 17 of the D ring a hydroxy butenolide molecule as reported in Figure 6.6.

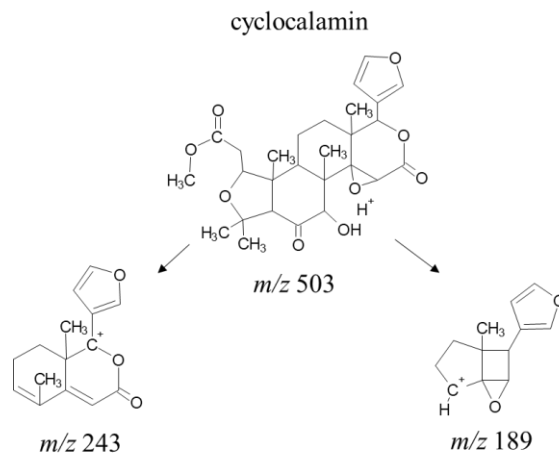


**Figure 6.6** Theoretical fragmentation of the cyclocalamin by means of the fragments obtained from the PIS mode.

#### 6.2.6 Quali/quantitative characterization

The SFC-QqQ MS developed method was used for the characterization of limonoid aglycones in the 11 cold-pressed *Citrus* essential oils. Calibration curve of limonin was constructed under the same chromatographic conditions optimized for the sample analysis to quantify the limonin content.

The linearity and the goodness of the curve used were confirmed using Mandel's fitting tests. The significance of the intercept was established running a t test. All the statistical tests were carried out at the 5% significance level. Limits of detection (LoD) and quantification (LoQ) were calculated by multiplying the standard deviation of the limonin area at the lowest concentration level ( $n = 5$ ), three and ten times, respectively, and then by dividing the result by the slope of the calibration curve. The validation process provided the following LoD and LoQ values: 0.006 and 0.021 mg L<sup>-1</sup>, respectively. Excellent linearity was obtained for limonin as confirmed by the correlation

coefficient  $R^2$  0.9998. Concerning the intraday precision, percentage coefficient of variation (%CV) value of 4% demonstrated very good precision at the concentration level tested. Concerning recovery, value of 98% was obtained thus demonstrating an excellent accuracy.

Accuracy was measured by spiking  $0.05 \text{ mg L}^{-1}$  of limonin a bergamot sample, a value close to the LoQ, bergamot sample was chosen because in this sample, limonin was not detected.

Finally, an inter-day precision value of 6% was obtained.

For the tentative identification, the MRM optimized transitions with quantifier and qualifier ion ratio (Q/q) and retention times were used.

In total, 12 different limonoid aglycones were provisionally identified in 11 *Citrus* essential oils. Table 1 reports the qualitative composition of all the samples analyzed and the amount of limonin expressed as  $\text{mg L}^{-1}$ . The most complex sample, from a qualitative point of view, is pink grapefruit essential oil [11], with 10 tentatively identified limonoid aglycones, whose chromatogram with MRM transitions is shown in figure 6 7.

Green mandarin essential oil differs from yellow and red mandarin for the presence of obacunone and the absence of ichangesin present in the other two mandarin essential oil samples [12].

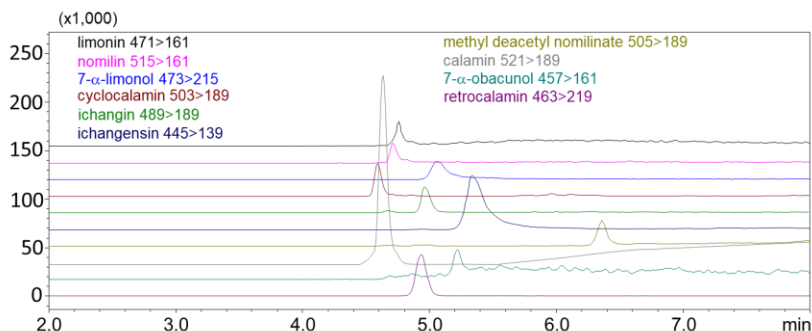


**Figure 6.7** Pink grapefruit essential oil MRM transition chromatograms.

**Table 6.1** Quantitative representation of limonin and qualitative representation of other limonoids in the essential oils analyzed.

Characterization	Limonin	Nomilin	Obacunone	Ichangensin	Ichangin	7- $\alpha$ -Limonol	methyl deacetyl Nomilinate	methyl Isobacunoate	Cyclocalamin	Calamin	Retrocalamin	7- $\alpha$ -Obacunol
Green mandarin	4.5 $\pm$ 0.1	×	×	-	-	-	-	-	-	-	-	-
Yellow mandarin	1.2 $\pm$ 0.2	×	-	×	-	-	-	-	-	-	-	-
Red mandarin	1.1 $\pm$ 0.2	×	-	×	-	-	-	-	-	-	-	-
Bergamot		×	-	×	-	-	-	-	-	-	-	-
Sweet blond orange	1.8 $\pm$ 0.1	×	×	× <sup>a</sup>	-	× <sup>a</sup>	-	× <sup>a</sup>	-	-	-	-
Blood sweet orange	0.9 $\pm$ 0.1	×	× <sup>a</sup>	× <sup>a</sup>	-	-	-	× <sup>a</sup>	-	-	-	-
Bitter orange			-	× <sup>a</sup>	×	-	× <sup>a</sup>	-	× <sup>a</sup>	× <sup>a</sup>	× <sup>a</sup>	-
Lemon 1	4.4 $\pm$ 0.5	×	×	× <sup>a</sup>	-	-	-	-	-	-	-	-
Lemon 2	5.3 $\pm$ 1.0	×	-	× <sup>a</sup>	-	-	-	-	-	-	-	-
Pink grapefruit	3.7 $\pm$ 0.5	×	-	× <sup>a</sup>	× <sup>a</sup>	× <sup>a</sup>	× <sup>a</sup>	-	× <sup>a</sup>	× <sup>a</sup>	× <sup>a</sup>	× <sup>a</sup>
Clementine	0.5 $\pm$ 0.1	×	-	× <sup>a</sup>	× <sup>a</sup>	-	-	-	-	-	-	-

<sup>a</sup>Compound, to the best of the authors' knowledge, identified for the first time



### 6.3 Conclusion

The SFC-APCI-QqQ MS method developed in this work represents a valid tool for the rapid characterization (ca. 7 min) using a very low amount of organic solvent (MeOH, 170  $\mu$ L) per analysis. The use of a triple quadrupole MS detector allowed to reach a very high sensitivity thus identifying 12 limonoid aglicones in 11 cold-pressed *Citrus* essential oil, and to the best of our knowledge, most of them were tentatively identified for the first time. Moreover, the use of MRM acquisition mode allowed the discrimination of isobaric molecules.

The validated method enabled the quantification of limonin with a low LoD and LoQ. The concentration range 0.5-21.2 mg L<sup>-1</sup> of limonin in the various samples analyzed should not represent a problem for the food industries, due to the low amount of essential oils added in the food and beverage products.

## References

- [1] G. Dugo, A. Di Giacomo. *Citrus: the genus Citrus*. Taylor & Francis, 2002.
- [2] B. Adorjan, G. Buchbauer. Biological properties of essential oils: an updated review. *Flavour and Fragrance Journal* 2010, 25, 407.
- [3] G. Dugo, L. Mondello. *Citrus oils: composition, advanced analytical techniques, contaminants, and biological activity*. Taylor & Francis, 2010.
- [4] J. Yu, L. Wang, R. L. Walzem, E. G. Miller, L.M. Pike, B.S. Patil. Antioxidant activity of Citrus Limonoids. *Journal of Agricultural and Food Chemistry*, 2005, 53, 2009.
- [5] D. Giuffrida, M. Zoccali, S.V. Giofrè, P. Dugo, L. Mondello. Apocarotenoids determination in *Capsicum chinense* Jacq. cv. Habanero, by supercritical fluid chromatography-triple-quadrupole/mass spectrometry. *Food Chemistry*, 2017, 231, 316.
- [6] M. Russo, A. Arigò, M. L. Calabrò, S. Farnetti, L. Mondello, P. Dugo. Bergamot (*Citrus bergamia* Risso) as a source of nutraceuticals: limonoids and flavonoids. *Journal of Functional Foods*, 2016, 20, 19.
- [7] M. Zoccali, D. Giuffrida, P. Dugo, L. Mondello. Direct online extraction and determination by supercritical fluid extraction with chromatography and mass spectrometry of targeted carotenoids from red habanero peppers (*Capsicum chinense* Jacq.). *Journal of Separation Science* 2017, 40, 3905.
- [8] A. P. III Breksa, M.B. Hidalgo, Y.M. Lee. Liquid chromatography electrospray ionization mass spectrometry method for the rapid identification of citrus limonoid glucosides in citrus juices and extracts. *Food Chemistry*, 2009, 117, 739.
- [9] A. P III Breksa, T. Kahn, A. A. Zukas, M. B. Hidalgo, M. L. Yuen. Limonoid content of sour orange varieties. *Journal of Agricultural and Food Chemistry*, 2011, 91, 1789.

[10] W. Ren, S. Xin, L. Han, R. Zuo, Y. Li, M. Gong, X. Wei, Y. Zhou, J. He, H. Wang, N. Si, H. Zhao, J. Yang, B. Bian. Comparative metabolism of four limonoids in human liver microsomes using ultra-high performance liquid chromatography coupled with high-resolution LTQ-Orbitrap mass spectrometry. *Rapid Commun Mass Spectrom*, 2015, 29, 2045.

[11] T. Kikuchi, Y. Ueno, Y. Hamada, C. Furukawa, T. Fujimoto, T. Yamada, R. Tanaka. Five new Limonoids from peels of Satsuma Orange (*Citrus reticulata*). *Molecules*, 2017, 22, 907.

[12] J. Kim, G.K. Jayaprakasha, B.S. Patil. Limonoids and their antiproliferative and antiaromatase properties in human breast cancer cells. *Food Funct*, 2013, 4, 258.

# 7 Extraction and characterization of carotenoids and apocarotenoids from microalgae by supercritical fluid system

---

## 7.1 Introduction

The carotenoids composition of microalgae has been widely investigated [1-4] and, recently, the occurrence of carotenoids esters in microalgae has also been reported [5]. The carotenoid profiles are known to vary greatly between species, as are the algae's ability to accumulate different carotenoids during stress exposure [6]. The production of carotenoids from microalgae is continuously growing since natural and controlled production sources of carotenoids are highly desirable because of their economic and environmental positive aspects [7]. Different analytical methods for extraction and analysis of carotenoids in microalgae samples were reported mainly based on liquid extraction and liquid chromatography approaches [8], but they were also based on supercritical fluids approaches [9,10]. Both enzymatic or oxidative carotenoids cleavages often occur in plants that produce a wide range of bioactive apocarotenoids [11,12]. No detailed data is available in the literature on the apocarotenoids occurrence in microalgae. Therefore, the aim of this investigation was to determine the occurrence of apocarotenoids in four selected different microalgae strains: *Chlamydomonas sp.* (CCMP 2294), *Tetraselmis chuii* (SAG 8-6), *Nannochloropsis gaditana* (CCMP 526), and *Chlorella sorokiniana* (NIVA-CHL 176).

## 7.2 Experimental section

### 7.2.1 Standards and samples

The standard carotenoids  $\beta$ -carotene, zeaxanthin and lutein were acquired while the apo-carotenals, apo-zeaxanthines and apo-lutein were obtained by non-specific oxidative cleavage as reported in references [13-15].

The four strains of algae were grown in the best climate conditions at different sites.

*Chlamydomonas sp.* (CCMP 2294): light intensity 70–80  $\mu\text{mol}/\text{m}^2/\text{s}$ , temperature 4 °C, 6 L cultures in 10 L flasks bubbled with air added 1%  $\text{CO}_2$ , growth medium L1 [16].

*Tetraselmis chuii* (SAG 8-6): light intensity 130  $\mu\text{mol}/\text{m}^2/\text{s}$ , temperature 25 °C, 1 L cultures in 2 L Erlenmeyer flasks on shaking table, air with 3%  $\text{CO}_2$  was added to headspace; Light intensity: 50  $\mu\text{mol}/\text{m}^2/\text{s}$ , temperatures 22 °C, 5–6 L cultures in 10 L flasks bubbled with air added 3%  $\text{CO}_2$ , both with growth medium L1.

*Nannochloropsis gaditana* (CCMP 526): light intensity 130  $\mu\text{mol}/\text{m}^2/\text{s}$ , temperature 25 °C, 1 L cultures in 2 L Erlenmeyer flasks on shaking table, air with 3%  $\text{CO}_2$  was added to headspace; Light intensity: 50  $\mu\text{mol}/\text{m}^2/\text{s}$ , temperatures 22 °C, 5–6 L cultures in 10 L flasks bubbled with air added 3%  $\text{CO}_2$ , both with growth medium L1.

*Chlorella sorokiniana* (NIVA-CHL 176): light intensity 150  $\mu\text{mol}/\text{m}^2/\text{s}$ , temperatures 25 °C, 1 L cultures in 1,2 L flat flasks bubbled with air added 2-3%  $\text{CO}_2$ . Growth medium Tris-Acetate-Phosphate (TAP) [17], modified by replacing acetate with HCl. All the above described microalgae biomasses were lyophilized before apocarotenoids analyzes.

### *7.2.2 SFE-SFC-MS Instrumentation*

The SFE-SFC-MS analyses were carried out on a Shimadzu Nexera-UC system, composed of a CBM-20A controller, an SFE-30A module for supercritical fluid extraction, two LC-20ADXR dual-plunger parallel-flow pumps, an LC-30ADSF CO<sub>2</sub> pump, two SFC-30A back pressure regulator, a DGU degasser, a CTO-20AC column oven, a SIL-30AC autosampler, an LCMS-8050 mass spectrometer equipped with an atmospheric pressure chemical ionization (APCI) source. The entire system was controlled by the LabSolution ver. 5.8.

### *7.2.3 Configuration of the SFE-SFC system*

A scheme of the SFE-SFC-MS system is reported in Figure 7.1. The system operates in three different steps: (A) SFE static extraction mode, (B) SFE dynamic extraction mode, and (C) SFC chromatographic separation. During the static extraction mode, the vessel was pressurized for 3 min (Figure 7.1 A), then the extraction was carried out in the dynamic mode for one min (Figure 7.1 B). During this step, the mobile phase flows through the vessel continuously and the extracts are transferred into the analytical column. After the SFEs steps 1 and 2, the analytes undergo the SFC analysis (Figure 7.1 C).

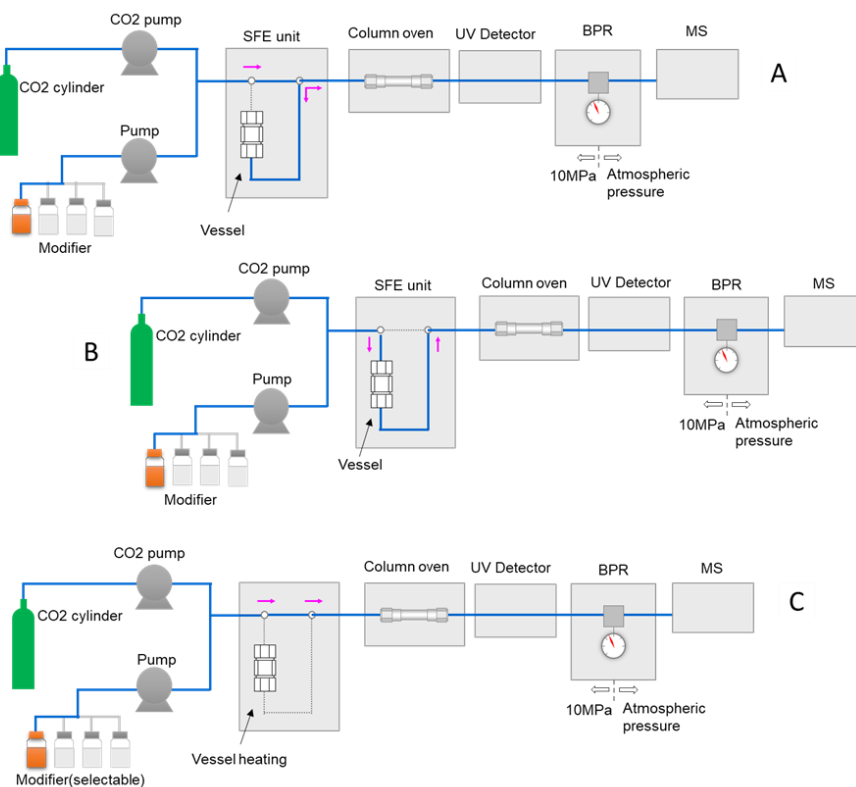


**Figure 7.1** Scheme of the SFE-SFC-MS system: (A) Static extraction mode, (B) Dynamic extraction mode, (C) Analysis mode.

#### 7.2.4 Optimization of the analytical method

The SFE conditions were as follows: 0-3 min static extraction mode, and 3-4 min dynamic extraction mode; Extraction vessel temperature: 80 °C. Back pressure regulator: 150 bar.

Solvent (A) CO<sub>2</sub> and solvent (B) CH<sub>3</sub>OH; Gradient: From 0 to 3 min, 5% of B; then from 3 to 4 min, 10% of B. Flow rate: 2 mL/min.

The SFC conditions were as follows: Solvent (A) CO<sub>2</sub> and solvent (B) CH<sub>3</sub>OH. Gradient: from 4 to 6.0 min 0% B, from 6 to 14 min increasing from 0 to 40% in 8 min, then 40% for 5 min. Flow rate: 2 mL/min.

Separation were carried out on an Ascentis Express C30, 150 mm × 4.6 mm × 2.7 μm<sub>d.p.</sub>.

The used eluents were: A, CO<sub>2</sub>; B CH<sub>3</sub>OH; make-up solvent, CH<sub>3</sub>OH; 35 °C was the column oven temperature and 150 bar was the regulator back pressure. The injection volume for standards was 3 μL. The MS was set as follows: Acquisition mode: SCAN in negative mode (-) and selected ion monitoring (SIM) (-). Interface temperature 350 °C, DL temperature 200 °C, block heater temperature 200 °C, nebulizing gas flow (N<sub>2</sub>) 3 L/min, drying gas flow (N<sub>2</sub>) 5 L/min, full scan range 200-1200 m/z, event time 0.05 sec for each event. The available standards, full scan, SIM, and multiple reaction monitoring (MRM) experiments were used for the apocarotenoid identifications.

β-Carotene and β-apo-8'-carotenal were quantitatively determined by multiple extractions as reported by Giuffrida et al. [15]. Six-point calibration curves were constructed in the 0.1-20 mg L<sup>-1</sup> range.

The derived calibration curves had a coefficient of determination (R<sup>2</sup>) of 0.9996 and 0.9991, respectively, for β-carotene and β-apo-8'-carotenal. Linearity was further confirmed using Mandel's fitting test. Limits of detection (LoD) were 0.03 and 0.04 mg L<sup>-1</sup>, while limits of quantification (LoQ) were 0.091, 0.134 mg L<sup>-1</sup>, respectively, for β-carotene and β-apo-8'-carotenal. Further, they were calculated by multiplying the standard deviation of the standard area at the lowest concentration level, three and ten times, respectively, and then were divided by the slope of the calibration curve.



### 7.2.5 Results of microalgae analyses

The carotenoids composition of the selected four different microalgae species (*Chlamydomonas sp.*, *Tetraselmis chuii*, *Nannochloropsis gaditana*, *Chlorella sorokiniana*) were reported in [18-23]. However, what determined the study of these species was the possible presence of apocarotenoids that had never been studied before.

Some *Chlamydomonas sp.* and *C. sorokiniana* have been reported to produce lutein as the main carotenoid [20,22].

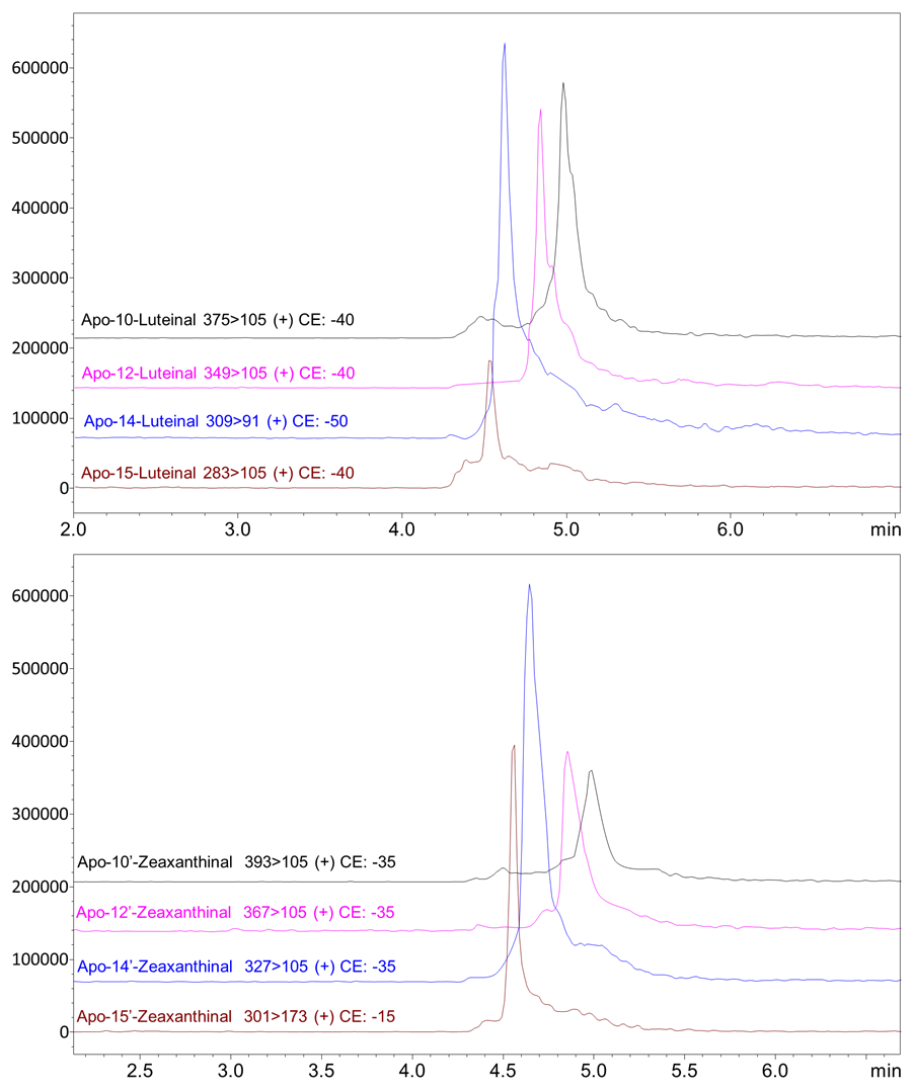
*T. chuii* is a food approved species and has been reported to accumulate  $\alpha$  and  $\beta$ -carotenes, whereas *N. gaditana*, which is frequently used in aquaculture feed due to its high eicosapentaenoic fatty acid (EPA) content, has been reported to accumulate violaxanthin and zeaxanthin [19,23]. SIM detections and MRM transitions were applied to all the detected apocarotenoids except for the apo-violaxanthinals and apo-fucoanthinals that were identified only using SIM detections, due to the lack of the respective standards.

Table 7.1 shows the overall apocarotenoids occurrence in the four microalgae strains. In general, it can be observed that the apocarotenoids were occurring in the microalgae strains in a scattered order although apo-12'-zeaxanthinal,  $\beta$ -apo-12'-carotenal, apo-12'-luteinal, and apo-12'-violaxanthal were detected in all the investigated strains together with the two apocarotenoid esters, apo-10'-zeaxanthinal-C4:0, and apo-8'-zeaxanthinal-C8:0. The *Chlamydomonas sp.* strain showed the highest apocarotenoids occurrence among the investigated strains. In fact, 25 apocarotenoids were detected in this microalga.

**Table 7.1** Overall apocarotenoids occurrence in four microalgae strains.

Compound	<i>Chlorella sorokiana</i>	<i>Nanochloropsis gaditana</i>	<i>Tetraselmis chui</i>	<i>Chlamydomonas sp.</i>
Apo-8'-Zeaxanthinal	-	×	-	×
Apo-10'-Zeaxanthinal	×	-	-	×
Apo-12'-Zeaxanthinal	×	×	×	×
Apo-14'-Zeaxanthinal	×	-	×	×
Apo-15'-Zeaxanthinal	-	×	×	×
β-Apo-8'-Carotenal	×	-	×	-
β-Apo-10'-Carotenal	×	×	-	×
β-Apo-12'-Carotenal	×	×	×	×
β-Apo-14'-Carotenal	×	-	×	×
Apo-10'-Zeaxanthinal -C4:0	×	×	×	×
Apo-10'-Zeaxanthinal -C10:0	×	×	-	×
Apo-10'-Zeaxanthinal -C12:0	×	-	-	×
Apo-10'-Zeaxanthinal -C14:0	×	-	×	×
Apo-8'-Zeaxanthinal-C8:0	×	×	×	×
Apo-8'-Zeaxanthinal-C10:0	×	×	-	×
Apo-8'-Zeaxanthinal-C12:0	×	×	-	×
Apo-8-Luteinal	-	×	×	-
Apo-10-Luteinal	×	×	×	×
Apo-12-Luteinal	×	×	×	×
Apo-14-Luteinal	×	-	×	×
Apo-15-Luteinal	×	-	-	×
Apo-8'-Violaxanthin	×	-	×	×
Apo-12'-Violaxanthin	×	×	×	×
Apo-14'-Violaxanthin	×	-	×	×
Apo-15'-Violaxanthin	-	×	×	×
Apo-8'-Fucoxanthinal	-	×	×	×
Apo-10'-Fucoxanthinal	-	×	-	-
Apo-14'-Fucoxanthinal	×	-	-	-
Apo-15'-Fucoxanthinal	×	-	×	×

In Figure 7.2 are shown as example, the MRM analysis enlargements (transitions in APCI positive) relative to the detected apo-Zeaxanthinals, and apo-Luteinals in the different microalgae strains, while figure 7.3 shows the oxidative cleavages of lutein and zeaxanthin and the formation of apo-lutein and apo-zeaxanthin. Further, it can be appreciated that all the different apocarotenoids were identified in less than 6 min of SFE-SFC-MS analysis. Although the purpose of this investigation was a qualitative apocarotenoids that profiled the four different microalgae strains, the available standards allowed us to also carry out a quantitative evaluation of the  $\beta$ -carotene and  $\beta$ -apo-8'-carotenal contents in the investigated samples. The amount of  $\beta$ -carotene was 89.7, 46.9, 20.6, and 4.2 ng mL<sup>-1</sup> respectively in the *C. sorokiniana*, *N. gaditana*, *T. chuii*, and *Chlamydomonas sp.* samples, while  $\beta$ -apo-8'-carotenal was detected only in *C. sorokiniana* and *T. chuii* samples, with an amount of 0.7 and 0.5 ng mL<sup>-1</sup>, respectively. Therefore, interestingly, considering the reported preliminary quantitative data the  $\beta$ -apo-8'-carotenal content was around the 0.8% and the 2.4% of the parent carotenoid in *C. sorokiniana* and *T. chuii*, respectively.



**Figure 7.2** The corresponding chromatograms obtained in MRM analysis relative to the detected  $\epsilon$ -apo-luteinals and apo-zeaxanthinals.

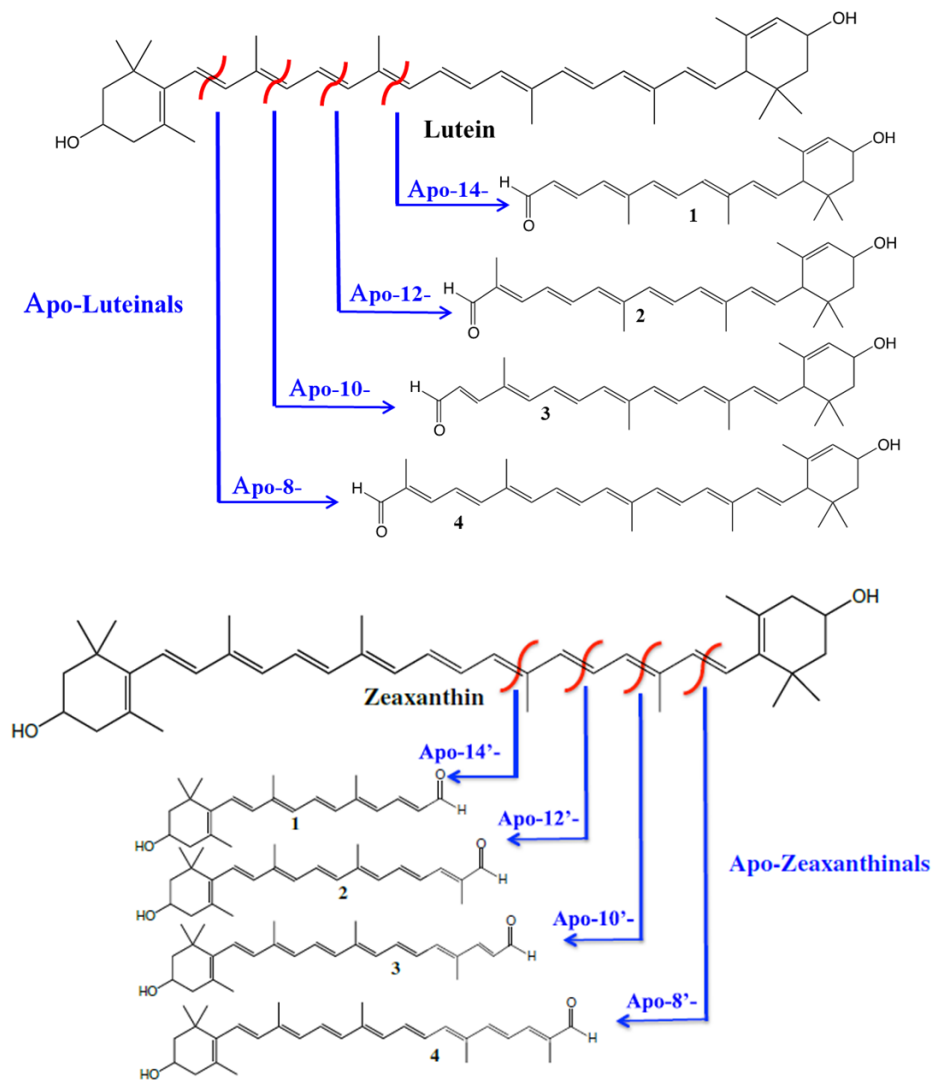


Figure 7.3 Oxidative cleavage of Lutein and Zeaxanthin with formation of the relative apocarotenoids (apo-Zeaxanthinals and apo-Luteinals).

### **7.3 Conclusions**

Microalgae represents one of the most promising sources of bioactive molecules, including carotenoids [24,25]. In fact, they have the ability to adapt and grow in many different environmental conditions, going from tropic to temperate and arctic waters [26]. In addition, many algae strains representing most habitats have stress handling mechanisms that frequently involve increased carotenoid production when exposed to unfavorable environmental conditions [27,28]. Studies on the identification of carotenoids in microalgae are not many and there is currently no qualitative/quantitative information for apocarotenoids.

The here reported methodology allowed for the determination of the native apocarotenoids profile in four different microalgae species for the first time; a total of 29 different apocarotenoids, including various apocarotenoid fatty acid esters, were detected. The overall extraction and detection time for all the apocarotenoids was less than 10 min, including apocarotenoids esters, with an overall analysis time less than 20 min.

## References

- [1] M. Gong, A. Bassi, Carotenoids from microalgae: A review of recent developments. *Biotechnology Advances* 2016, 34, 1396.
- [2] J. Matos, C. Cardoso, N. M. Bandarra, C. Afonso. Microalgae as healthy ingredients for functional food: A review. *Food & Function*, 2017, 8, 2672.
- [3] R. Sathasivam, J.-S. Ki. A review of the biological activities of microalgal carotenoids and their potential use in healthcare and cosmetic industries. *Marine Drugs* 2018, 16, 26.
- [4] D. Mc Gee, L. Archer, A. Paskuliakova, G. R. Mc Coy, G. T. A. Fleming, E. Gillespie, N. Touzet. Rapid chemotaxonomic profiling for the identification of high-value carotenoids in microalgae. *Journal of Applied Phycology* ,2018, 30, 385.
- [5] M. M. Maroneze, E. Jacob-Lopez, L. Queiroz Zepka, M. Roca, A. Perez-Galvez. Esterified carotenoids as new food components in cyanobacteria. *Food Chemistry*, 2019, 287, 295.
- [6] A. K. Minhas, P. Hodgson, C. Barrow, A. Adholeya. A review on the assessment of stress conditions for simultaneous production of microalgal lipids and carotenoids. *Frontiers in Microbiology*. 2016, 7, 546.
- [7] J. Liu, Z. Sun, H. Gerken. *Recent Advances in Microalgae Biotechnology*; OMICS Group eBooks, 2014.
- [8] M. C. Ceron-Garcia, C. V. Gonzalez-Lopez, J. Camacho-Rodriguez, L. Lopez-Rosales, F. Garcia-Camacho, E. Molina-Grima. Maximizing carotenoid extraction from microalgae used as food additives and determined by liquid chromatography (HPLC). *Food Chemistry* 2018, 257, 316.
- [9] V. Abrahamsson, I. Rodriguez-Meizoso, C. Turner. Determination of carotenoids in microalgae using supercritical fluid extraction and chromatography. *Journal of Chromatography A* 2012, 1250, 63.
- [10] S. R. Pour Hosseini, O. Tavakoli, M. H. Sarrafzadeh. Experimental optimization of SC-CO<sub>2</sub> extraction of carotenoids from *Dunaliella salina*. *The Journal of Supercritical Fluids* 2017, 121, 89.

- [11] X. Hou, J. Rivers, P. Leon, R. P. McQuinn, B. J. Pogson, Synthesis and function of apocarotenoid signals in plants. *Trends Plant Science*. 2016, 21, 792.
- [12] D. Giuffrida, P. Donato, P. Dugo, L. Mondello. Recent analytical techniques advances in the carotenoids and their derivatives determination in various matrixes. *Journal of Agricultural and Food Chemistry*, 2018, 66, 3302.
- [13] E. H. Harrison, L. Quadro. Apocarotenoids: Emerging roles in mammals. *Annual Review of Nutrition* 2018, 38, 153.
- [14] E. B. Rodriguez, D. B. Rodriguez-Amaya. Formation of apocarotenals and epoxy-carotenoids from  $\beta$ -carotene by chemical reactions and by autoxidation in model system and processed foods. *Food Chemistry*, 2007, 101, 563.
- [15] D. Giuffrida, M. Zoccali, S. V. Giofrè, P. Dugo, L. Mondello. Apocarotenoids determination in *Capsicum chinense Jacq. cv Habanero*, by supercritical fluid chromatography-mass spectrometry. *Food Chemistry* 2017, 231, 316.
- [16] M. Zoccali, D. Giuffrida, F. Salafia, S. V. Giofrè, L. Mondello. Carotenoids and apocarotenoids determination in intact human blood samples by online supercritical fluid extraction-supercritical fluid chromatography-tandem mass spectrometry. *Analytica Chimica Acta* 2018, 1032, 40.
- [17] R. R. L. Guillard, P. E. Hargraves. *Stichochrysis immobilis* is a diatom, not a chrysophyte. *Phycologia* 1993, 32, 234.
- [18] E. H. Harris. *The Chlamydomonas Sourcebook. A comprehensive Guide to Biology and Laboratory*. Academic Press, 1989.
- [19] E. Forján, I. Garbayo, C. Casal, C. Vílchez. Enhancement of carotenoid production in *Nannochloropsis* by phosphate and sulphur limitation. *Communicating Current Research and Educational Topics and Trends in Applied Microbiology*. 2007, 1, 356.
- [20] H. Safafar, J. van Wageningen, P. Møller, C. Jacobsen. Carotenoids, Phenolic Compounds and Tocopherols Contribute to the Antioxidative Properties of Some Microalgae Species Grown on Industrial Wastewater. *Marine Drugs*, 2015, 13, 7339.



- [21] G. Di Lena, I. Casini, M. Lucarini, G. Lombardi-Boccia. Carotenoid profiling of five microalgae species from large-scale production. *Food Research International*, 2019, 120, 810.
- [22] L. Montero,; M. Sedghi,; Y. Garcia,; C. Almeida,; C. Safi,; N. Engelen-Smit,; A. Cifuentes. Pressurized liquid extraction of pigments from *Chlamydomonas* sp. and chemical characterization by HPLC-MS/MS. *Journal of Analytical Toxicology* 2018, 2, 149.
- [23] B. F. Cordero, L. Obraztsova, I. Couso, R. Leon, M. A.Vargas, H. Rodriguez, Enhancement of lutein production in *Chlorella sorokiniana* (Chlorophyta) by improvement of culture conditions and random mutagenesis. *Marine Drugs* 2011, 9, 1607.
- [24] L. M. Lubian. *Nannochloropsis* (Eustigmatophyceae) as source of commercially valuable pigments. *Journal of Applied Phycology* 2000, 12, 249.
- [25] S. Singh,; B. N. Kate, U. C. Banerjee. Bioactive compounds from cyanobacteria and microalgae: An overview. *Critical Reviews in Biotechnology*. 2005, 25, 73.
- [26] C. Galasso, C. Corinaldesi, C. Sansone, Carotenoids from marine organisms: Biological functions and industrial applications. *Antioxidants* 2017, 6, 96.
- [27] M. I. Khan, J. H. Shin, J. D. Kim. The promising future of microalgae: Current status, challenges, and optimization of a sustainable and renewable industry for biofuels, feed, and other products. *Microbial Cell Factories*, 2018, 17, 36.
- [28] F. Ahmed, K. Fanning, Netzel, M.; Turner, W.; Li, Y.; Schenk, P.M. Profiling of carotenoids and antioxidant capacity of microalgae from subtropical coastal and brackish waters. *Food Chemistry* 2014, 165, 300.
- [29] K. Skjånes, C. Rebours, P. Lindblad. Potential for green microalgae to produce hydrogen, pharmaceuticals and other high value products in a combined process. *Critical Reviews in Biotechnology*, 2013, 33, 172.

# 8 Characterization of native composition of Orange *cv* *Pera* peel with carbon dioxide extraction and separation

---

## 8.1 Introduction

Citrus fruits are among the most produced and consumed fruits worldwide, either fresh or as juice, and especially oranges (*Citrus sinensis* L. Osbeck), which are known for their large consumption and economic importance. Brazil is one of the largest exporters of orange juice around the world; among the most important cultivars in Brazil, the sweet orange *cv. Pera* has good juice quality and accounts for approximately 30% of the orange crop expected for 2019-2020 [1]. However, this high volume of juice production generates a large amount of waste. The orange peel in turn, can represent an interesting source of carotenoids, which are natural pigments responsible for adding the color to fruits and vegetables, and for providing health-related benefits when ingested by humans [2]. Carotenoid intake is related to improvements in the immune system and reduced risk of developing degenerative diseases, such as cardiovascular diseases, cancer, macular degeneration, and Alzheimer's disease [3–5].

The main class of carotenoids found in oranges is the hydroxylated carotenoids, which include violaxanthin, luteoxanthin, lutein, cryptoxanthin, antheraxanthin, mutatoxanthin, and zeaxanthin [6-8]. These can be presented in their free form or acylated with fatty acids

(FAs) in the case of mono- and polyhydroxylated xanthophylls, commonly forming monoesters or diesters [9,10]. In the plant tissues, the esterification helps carotenoid storage and protects sensitive molecules from photo-oxidation [11,12], in addition to increasing the possible structures found in nature, and consequently, the analytical complexity [9,13].

Specifically, for matrices rich in carotenoids esters, like oranges, it is crucial to obtain the carotenoids extracts using alternative solvents and to characterize them in their native composition form, to establish associations between all the compounds present in the natural matrix and their benefits to human health. Thus, the aim of the study was to evaluate the native carotenoids composition of orange peel (*cv. Pera*) using alternative approaches with a supercritical fluid extraction (SFE), followed by supercritical fluid chromatography with atmospheric pressure chemical ionization and triple quadrupole mass spectrometry detection (SFC-APCI/QqQ/MS) in an online system.

## **8.2 Experimental section**

### *8.2.1 Standard and sample*

The carotenoid standards used were acquired, while the apocarotenoid standards were produced by oxidative cleavage as described in the previous chapter. The solvents used are of MS purity.

Oranges (*Citrus sinensis L. Osbeck*) *cv. Pera* were obtained at a local market in Santos city (São Paulo, Brazil), totalizing a single sample batch of about 10 kg of fruits, further reduced to laboratory samples. The oranges were squeezed in an industrial processor and the peels were processed in a grinder, before being subsequently freeze-dried.

### 8.2.2 Optimization of the analytical method

The instrument setup and conditions for MS and MS/MS analysis were as those described in the previous chapter.

The supercritical fluid extraction and supercritical fluid chromatography was performed in an on-line combined instrument the Shimadzu Nexera-UC. The sample preparation and the SFE conditions were as follow: briefly, the freeze-dried sample of orange peel (10.0 mg) was mixed with 1 g of an adsorbent powder and placed in the extraction vessel of 0.2 mL in the SFE unit (the ID of the extraction chamber was 6 mm and the length was 12 mm), loaded with 100 mg of sample/adsorbent. So, a final amount of 1.0 mg of sample was used, considering the dilution factor [28].

Then, supercritical CO<sub>2</sub> and methanol were introduced into the vessel, and pressure and temperature conditions of extraction were optimized, as follows: CO<sub>2</sub> (A) and methanol (B) solvents were used in a gradient as follows: 5% B for 3 min, increasing from 5% to 10% B for 1 min, and changing to 0% B into the SFC analysis mode: flow rate, 2 mL/min; extraction mode, 0-3 min static mode, 3-4 min dynamic mode; extraction vessel temperature, 80 °C; and backpressure regulator, 150 bar [14].

The SFC conditions were solvent A (CO<sub>2</sub>) and solvent B (MeOH) in a gradient as follows: 0% B from 4 to 6 min, increasing from 0% to 40% from 6 to 14 min, and maintaining 40% for 2 min [14] at a flow rate of 2.0 mL/min and make-up solvent MeOH at flow 1.0 mL/min [14]. Separations were performed on a partially porous Ascentis Express C30, 150 mm, 4.6 mm, 2.7 μm<sub>d.p.</sub>. The column oven temperature was

set to 35 °C and the back-pressure regulator to 150 bar. The injection volume for standards was 2  $\mu$ L.

The different carotenoids and apocarotenoids were characterized by SIM and MRM and PIS experiments, as in the chapter described above and as reported by Giuffrida et al. [15].

### 8.2.3 Results of *cv. Pera peel analyze*

According to the results from the SFE-SFC-MS/MS analysis, were detected nine free carotenoids, six carotenoids esters, 19 apocarotenoids, and eight apo-esters, that were identified using the available standard, the compounds' elution order, along with a full scan, selected ion monitoring (SIM), and multiple reaction monitoring (MRM) experiments. The most abundant compounds found were  $\beta$ -citraurinol and apo-14'-violaxanthinal. Table 8.1 lists the overall free and esterified carotenoid, Table 8.2 reports free and esterified apocarotenoids, detected in orange peel by SFE-SFC APCI/QqQ/MS analysis.

Through the use of this methodology, many apocarotenoids were detected compared to the HPLC, analysis in fact Chedea et al. [16] reports only a fraction of the carotenoids we identified in the orange peel of the Valencia variety.

This was the first attempt to analyze an orange peel sample using the SFE-SFC-APCI/QqQ/MS system, resulting in the most detailed apocarotenoids and apocarotenoid esters characterization in oranges, and in particular in the *cv Pera* variety, which could be also used as a fruit authenticity parameter.

**Table 8.1** free and esterified carotenoids present in the peel of Orange *cv Pera*.

<b>Apo-Carotenoids</b>	<b>SIM (-) m/z</b>	<b>MRM (+) Q (CE)</b>	<b>MRM (+) q (CE)</b>	<b>Ion Ratio %</b>
β-Citraurinol	434			
β-Apo-8'-Carotenal	416	+ 417 > 119 (-25)	+ 417 > 105 (-35)	73
β-Apo-10'-Carotenal	376	+ 377 > 105 (-35)	+ 377 > 119 (-30)	79
β-Apo-12'-Carotenal	350	+ 351 > 105 (-35)	+ 351 > 119 (-25)	74
β-Apo-14'-Carotenal	310	+ 311 > 105 (-25)	+ 311 > 119 (-25)	77
Apo-8'-Zeaxanthinal	432	+ 433 > 119 (-30)	+ 433 > 105 (-35)	95
Apo-10'-Zeaxanthinal	392	+ 393 > 105 (35)	+ 393 > 119 (-25)	92
Apo-12'-Zeaxanthinal	366	+ 367 > 105 (-35)	+ 367 > 119 (-30)	80
Apo-14'-Zeaxanthinal	326	+ 327 > 105 (-35)	+ 327 > 119 (-30)	61
Apo-15'-Zeaxanthinal	300	+ 301 > 173 (-15)	+ 301 > 105 (-30)	57
Apo-8'-Luteinal	432	+ 415 > 119 (-40)	+ 415 > 91 (-50)	95
Apo-10'-Luteinal	392	+ 375 > 105 (-40)	+ 375 > 91 (-50)	91
Apo-12'-Luteinal	366	+ 349 > 105 (-40)	+ 349 > 91 (-50)	90
Apo-14'-Luteinal	326	+ 309 > 91 (-50)	+ 309 > 105 (-40)	55
Apo-8'-Violaxanthinal	448			
Apo-10'-Violaxanthinal	408			
Apo-12'-Violaxanthinal	382			
Apo-14'-Violaxanthinal	342			
Apo-15'-Violaxanthinal	316			
<b>Apo-Esters</b>				
Apo-10'-Zeaxanthinal-C4:0	462	+ 463 > 105 (-40)	+ 463 > 119 (-35)	71
Apo-10'-Zeaxanthinal-C10:0	546	+ 547 > 105 (-35)	+ 547 > 119 (-30)	87
Apo-10'-Zeaxanthinal-C12:0	574	+ 575 > 105 (-35)	+ 575 > 119 (-30)	75
Apo-10'-Zeaxanthinal-C14:0	602	+ 603 > 105 (-40)	+ 603 > 119 (-30)	77
Apo-8'-Zeaxanthinal-C6:0	530	+ 531 > 119 (-40)	+ 531 > 105 (-40)	78
Apo-8'-Zeaxanthinal-C8:0	558	+ 559 > 105 (-40)	+ 559 > 119 (-40)	70
Apo-8'-Zeaxanthinal-C10:0	586	+ 587 > 119 (-40)	+ 587 > 105 (-40)	81
Apo-8'-Zeaxanthinal-C12:0	614	+ 615 > 105 (-40)	+ 615 > 119 (-40)	79

**Table 8.2** free and esterified apocarotenoids present in the peel of Orange *cv Pera*.

Free Carotenoids	SIM (-) m/z	MRM (+) Q (CE)	MRM (+) q (CE)	Ion Ratio %
Luteoxanthin	600			
Antheraxanthin	478			
Lutein	568			
Zeaxanthin	568	+ 569 > 119 (-39)	+ 569 > 135 (-22)	95
$\beta$ -cryptoxanthin	552	+ 553 > 119 (-32)	+ 553 > 145 (-38)	61
Phytoene	544			
$\beta$ -Carotene	536	+ 537 > 119 (-39)	+ 537 > 121 (-32)	84
$\beta$ -Cryptoxanthin-5,6-epoxide	568			
$\beta$ -Carotene-5,6-epoxide/ $\beta$ -carotene-5,8-epoxide	552			
<b>Carotenoids Esters</b>				
Antheraxanthin-C12:0	766			
Zeaxanthin-C12:0	750			
Lutein-C14:0/zeaxanthin-C14:0	778			
$\beta$ -Cryptoxanthin-C12:0	734			
$\beta$ -Cryptoxanthin-C14:0	762			
$\beta$ -Cryptoxanthin-C16:0	790			

### 8.3 Conclusions

The literature reports carbon dioxide (CO<sub>2</sub>) as one of the most widely used supercritical fluids, which is especially convenient for carotenoid extraction; it is the most preferred in the pharmaceuticals and food industries due to its relatively low critical properties, making it ideal for thermally labile components, such as the carotenoids [17,18].

In the present work, freeze-dried samples of orange peel (*cv. Pera*) were used in the SFE, which lasted a total of four minutes, followed by the SFC analysis that was performed in 12 min; so, the final result generated from the whole process was achieved in 16 min. This methodology can be considered innovative compared with traditional solid-liquid extraction and conventional liquid chromatography, which require a much longer analytical time and use more solvent, and this method is fully automated, reducing operator error and analyte loss.



## References

- [1] FUNDECRITRUS Inventário da safra de laranja 2019/2020 do cinturão citrícola de São Paulo e Triângulo/Sudoeste Mineiro.
- [2] F. C. Petry, F. B. de Nadai, M. Cristofani-Yaly, R. R. Latado, A. Z. Mercadante. Carotenoid biosynthesis and quality characteristics of new hybrids between tangor (*Citrus reticulata* x *C. sinensis*) cv. 'Murcott' and sweet orange (*C. sinensis*) cv. 'Pêra'. Food Research International, 2019, 122, 461.
- [3] I. D. Nwachukwu, C. C. Udenigwe, R. E. Aluko. Lutein and zeaxanthin: Production technology, bioavailability, mechanisms of action, visual function, and health claim status. Trends Food Science. Technology, 2016, 49, 74.
- [4] M. Rodriguez-Concepcion, J. Avalos, M. L. Bonet, A. Boronat, L. Gomez-Gomez, D. Hornero-Mendez, M. C. Limon, A. J. Melendez-Martinez, B. Olmedilla-Alonso, A. Palou. A global perspective on carotenoids: Metabolism, biotechnology, and benefits for nutrition and health. Progress in Lipid Research, 2018, 70, 62.
- [5] A. F. G. Cicero, A. Colletti. Effects of carotenoids on health: Are all the same Results from clinical trials. Current Pharmaceutical Design 2017, 6, 290.
- [6] L. R. B. Mariutti, A. Z. Mercadante. Carotenoid esters analysis and occurrence: What do we know so far. Archives of Biochemistry and Biophysics. 2018, 648, 36.
- [7] P. J. Harrison, T. D. H. Bugg. Enzymology of the carotenoid cleavage dioxygenases: Reaction mechanisms, inhibition and biochemical roles. Archives of Biochemistry and Biophysics. 2014, 544, 105.
- [8] R. K. Saini, S. H. Nile, S. W. Park. Carotenoids from fruits and vegetables: Chemistry, analysis, occurrence, bioavailability and biological activities. Food Research International. 2015, 76.
- [9] F. C. Petry, A. Z. Mercadante. Composition by LC-MS/MS of New Carotenoid Esters in Mango and Citrus. Journal of Agricultural and Food Chemistry 2016, 64, 8207.
- [10] D. Giuffrida, P. Dugo, A. Salvo, M. Saitta, G. Dugo. Free carotenoid and carotenoid ester composition in native orange juices of different varieties. Fruits 2010, 65, 277.
- [11] C. I. Cazzonelli, B. J. Pogson. Source to sink: Regulation of carotenoid biosynthesis in plants. Trends Plant Science, 2010, 15, 266.

- [12] C. A. Howitt, B. J. Pogson. Carotenoid accumulation and function in seeds and non-green tissues. *Plant, Cell and Environ.* 2006, 29, 435.
- [13] A. Z. Mercadante, D. B. Rodrigues, F. C. Petry, L. R. B. Mariutti. Carotenoid esters in foods-A review and practical directions on analysis and occurrence. *Food Research International* 2017, 99, 830.
- [14] D. Giuffrida, M. Zoccali, A. Arigo, F. Cacciola, C. O. Roa, P. Dugo, L. Mondello. Comparison of different analytical techniques for the analysis of carotenoids in tamarillo (*Solanum betaceum Cav.*). *Archives of Biochemistry and Biophysics*, 2018, 646, 161.
- [15] D. Giuffrida, M. Zoccali S. V. Giofrè, P. Dugo, L. Mondello, Apocarotenoids determination in *Capsicum chinense Jacq. cv. Habanero*, by supercritical fluid chromatography-triple-quadrupole/mass spectrometry. *Food Chemistry* 2017, 231, 316.
- [16] V. S. Chedea, P. Kefalas, C. Socaciu. Patterns of Carotenoid Pigments Extracted from Two Orange Peel Wastes (Valencia and Navel var.). *Journal of Food Biochemistry* 2010, 34, 101.
- [17] P. Adadi, N. V. Barakova, E. F. Krivoshapkina. Selected Methods of Extracting Carotenoids, Characterization, and Health Concerns: A Review. *Journal of Agricultural and Food Chemistry*, 2018, 66, 5925.
- [18] E. Uquiche, J. M. del Valle, J. Ortiz, Supercritical carbon dioxide extraction of red pepper (*Capsicum annuum L.*) oleoresin. *Journal of Food Engineering*, 2004, 65, 55.

# 9 Apocarotenoids profiling in different *Capsicum* species by supercritical fluid extraction and supercritical fluid chromatography

---

## 9.1 Introduction

Free carotenoids and carotenoid esters composition in chilli peppers cultivars has been widely investigated [1,2], but only a very limited number of reports on the presence of apocarotenoids in chilli peppers are available in the literature [3,4], the aim of this study was the investigation of both the free apocarotenoids and apocarotenoids esters presence in seventeen chilli peppers cultivars belonging to the *Capsicum baccatum*, *C. annuum* and *C. chinense* species, in order to further demonstrate the widespread occurrence and role of those phytochemicals in fruits. Moreover, their possible use as an authenticity parameter and fingerprint should also be considered.

## 9.2 Experimental section

### 9.2.1 Standard and sample

Chemicals, carotenoids (zeaxanthin, lutein, capsanthin,  $\beta$ -carotene and  $\beta$ -cryptoxanthin) and apocarotenoids ( $\beta$ -Apo-8'-carotenal and Apo-8'-zeaxanthinal, commonly named  $\beta$ -citraurin) were used.

Seventeen fresh chilli peppers samples belonging to the genus *Capsicum* were kindly provided by Italian company, namely: Aji limòn

Capsicum baccatum (Sample 1, Color yellow), Erotic Capsicum baccatum (Sample 2, Color orange), Jimmy Capsicum baccatum (Sample 3, Color orange), Banana Pepper Capsicum annuum (Sample 4, Color yellow), Cayenna Impala Capsicum annuum (Sample 5, Color red), Jalapeño Capsicum annuum (Sample 6, Color red), Terenzio Capsicum annuum (Sample 7, Color red), Calabrian pepper Capsicum annuum (Sample 8, Color red), Scotch Bonnet Capsicum chinense (Sample 9, Color orange), Habanero Red Savina Capsicum chinense (Sample 10, Color red), Habanero Fatalii Capsicum chinense (Sample 11, Color yellow), Habanero Chocolate Capsicum chinense (Sample 12, Color brown), Naga Morich Capsicum chinense (Sample 13, Color red), Naga Yellow Capsicum chinense (Sample 14, Color yellow), Naga Chocolate Capsicum chinense (Sample 15, Color brown), Trinidad Scorpion Capsicum chinense (Sample 16, Color red), Trinidad Scorpion Moruga Capsicum chinense (Sample 17, Color orange). In Figure 9.1 are shown the respective pictures of the investigated chilli peppers samples.



**Figure 9.1** The investigated seventeen chilli peppers samples.

### 9.2.2 Optimization of the analytical method

The SFE-SFC-QqQ/MS analyses were carried out as follow: CO<sub>2</sub> (A) and CH<sub>3</sub>OH (B) were utilized for the SFE in the following way: 0-3 min, 10% MeOH (Static extraction mode); 3-4 min, 0% B (Dynamic extraction mode). Flow rate: 2 mL min<sup>-1</sup>; Backpressure regulator: 150 bars; vessel temperature: 80 °C. CO<sub>2</sub> (A) and CH<sub>3</sub>OH (B) were utilized for the SFC in the following way: 4-6 min 0% B, then 6-21 min to 80% B, then 21-22 min to 100% B and then 100% B for 2 min. Flow rate: 2 mL min<sup>-1</sup>. Make-up solvent CH<sub>3</sub>OH at flow 1.2 mL min<sup>-1</sup>. Chromatography was carried out on an Ascentis Express C30, 150 mm × 4.6 mm × 2.7 μm<sub>d.p.</sub>. The oven was at 35 °C and the back-pressure regulator was 150 bars.

The MS and MS/MS conditions are similar to those described in the previous chapters.

Compounds were identified by using the available standard, scan, SIM and MRM transitions for the different compounds: β-apocarotenals, apozeaxanthinals, apocapsorubinals, ε-apoluteinals, apo-β-carotenals and 4-oxo-apo-β-carotenals. Multiple extractions, until depletion, were performed in order to quantify the selected carotenoids (zeaxanthin, lutein capsanthin, β-carotene and β-cryptoxanthin) and apocarotenoids (β-Apo-8'-carotenal and β-citraurin) using six points calibration curves of the available standards, carrying out the analyses in triplicate.

Recovery of the analytes of interest was measured performing multiple extraction on the same sample. Specifically, all the samples were extracted three consecutive time. The sum of the areas was used for quantitative data. Six-points calibration curves were constructed for targeted analytes, the least-squares method was used to estimate the

regression line for the construction of the calibration curves. The linearity and goodness of-fit measurements of the curves were confirmed using Mandel's fitting tests. Limits of detection (LoD) and limits of quantification (LoQ) were calculated by multiplying the SD of the area at the lowest calibration curve level three and ten times, respectively, and then dividing the result by the slope of the calibration curve.

### 9.2.3 *Capsicum species chillies profile*

A total of 19 free apocarotenoids and 8 apocarotenoids fatty acid esters were identified, by the application of an online supercritical fluid extraction-supercritical fluid chromatography-triple quadrupole/mass spectrometry methodology, in the first apocarotenoids profiling of seventeen different chilli peppers cultivars belonging to *C. annuum*, *C. baccatum* and *C. chinense* species, as shown in Table 9.1. All the MRM transition used for the different apocarotenoids identification were previously optimized and reported in previous chapters.

**Table 9.1** Qualitative profile of the free apocarotenoids and apocarotenoid esters.

Compounds	Baccatum			Annum					Chinense								
	1	2	3	4	5	6	7	8	9	10	11	12	13	14	15	16	17
β-Citraurin	-	-	-	-	-	×	-	-	×	×	-	-	×	-	×	-	×
Apo-10'-Zeaxanthinal	-	×	-	-	-	-	-	-	-	×	-	-	-	-	-	×	-
Apo-14'-Zeaxanthinal	-	×	-	-	-	-	-	-	×	×	-	-	-	-	-	-	-
Apo-15'-Zeaxanthinal	-	×	-	-	-	-	-	-	-	-	-	-	-	-	-	-	-
Apo-8'-Carotenal	×	×	×	-	×	-	×	-	×	×	×	×	×	-	×	-	×
Apo-10'-Carotenal	-	×	-	-	-	-	-	-	×	×	-	-	×	×	×	×	×
Apo-12'-Carotenal	×	×	-	-	-	-	-	-	-	×	×	-	×	-	×	×	×
Apo-14'-Carotenal	×	×	-	-	-	×	-	×	-	-	-	-	-	-	×	-	×
Apo-8'-Luteinal	-	-	-	-	-	-	-	-	-	×	-	-	-	-	-	-	-
Apo-10'-Luteinal	-	-	×	-	×	×	-	×	-	-	-	-	-	-	-	-	-
Apo-12'-Luteinal	-	-	×	-	-	-	-	-	-	-	-	×	-	-	-	-	-
Apo-14'-Luteinal	×	-	×	-	-	×	-	-	-	×	-	-	-	-	-	-	-
Apo-15'-Luteinal	-	-	×	-	×	-	-	-	-	-	-	-	-	-	-	-	-
Apo-10'-Capsorubinal	-	-	-	-	×	-	-	-	-	×	-	-	-	×	-	-	-
Apo-12'-Capsorubinal	-	×	-	×	×	-	-	×	×	×	-	-	-	×	-	-	-
Apo-14'-Capsorubinal	-	-	-	-	-	×	-	-	-	-	-	-	-	-	-	-	-
Apo-15'-Capsorubinal	-	-	-	-	-	×	-	-	-	-	-	-	-	-	-	-	-
Apo-12'-Canthaxantinal	-	-	-	-	-	-	-	-	-	-	-	-	-	-	-	-	×
Apo-14'-Canthaxantinal	-	-	-	-	-	-	×	-	-	-	-	-	-	-	-	-	×
Apo-10'-Zeaxanthinal-C4:0	×	-	×	×	×	-	-	-	-	-	-	×	-	-	-	-	-
Apo-10'-Zeaxanthinal-C10:0	-	-	-	×	-	-	-	-	-	-	-	-	-	-	-	-	-
Apo-10'-Zeaxanthinal-C12:0	×	×	×	×	×	×	-	-	×	-	-	×	×	×	×	×	×
Apo-10'-Zeaxanthinal-C14:0	-	-	-	-	-	-	-	-	×	-	-	×	×	-	×	-	×
Apo-8'-Zeaxanthinal-C6:0	-	-	-	-	-	-	×	-	×	×	-	×	-	-	-	-	-
Apo-8'-Zeaxanthinal-C10:0	-	-	-	-	-	-	-	-	-	-	-	-	×	-	-	-	-
Apo-8'-Zeaxanthinal-C12:0	×	×	-	×	×	×	-	-	-	-	-	×	×	×	×	×	×
Apo-8'-Capsorubinal-C12:0	-	-	-	-	-	-	-	-	-	-	-	-	-	-	-	-	×

Different  $\epsilon$ - apoluteinals and 4-oxo-apo- $\beta$ -carotenals were detected in *Capsicum* species also for the first time and in any food matrix, while apo-8'-capsorubinal and Apo-12'-zeaxanthinal that were previously reported in chilli pepper species [3, 5, 6], were not detected in any of the investigated cultivars in this study. Interestingly,  $\beta$ -citraurin was not detected in any of the *C. baccatum* cultivars and was mainly present in the *C. chinense* cultivars.  $\beta$ -Apo-8'-carotenal was detected in all the *C. baccatum* cultivars and was also the most represented apocarotenoid among the investigated cultivars, being present in twelve out of seventeen cultivars, followed by  $\beta$ -apo-10'-carotenal and  $\beta$ -apo-12'-carotenal; on the contrary apo-14'-capsorubinal and apo-15'-capsorubinal were detected only in the Jalapeno cultivar. The Habanero Red Savina cultivar showed the highest presence of different apocarotenoids, in fact ten out of the overall nineteen detected free apocarotenoids were present in this cultivar. The detected apocarotenoid fatty acid esters were mainly esters of apo-10'-zeaxanthinal and apo-8'-zeaxanthinal; in particular lauric acid esters with both apo-10'-zeaxanthinal and apo-8'-zeaxanthinal were the most represented apocarotenoid esters among all the investigated cultivars, whereas caproic fatty acid esters of apo-10'-zeaxanthinal and apo-8'-zeaxanthinal were only detected, respectively in Banana peppers and Naga Morich cultivars; apo-8'-capsorubinal lauric acid ester was only detected in Trinidad Scorpion Moruga. The above described different remarks on the apocarotenoids and apocarotenoid esters occurrence in the various investigated cultivars should also be considered for a possible use as an authenticity parameter and fingerprint.



$\beta$ -apo-8'-carotenal and apo-8'-zeaxanthinal ( $\beta$ -citraurin) were also quantified, together with the selected carotenoids (zeaxanthin, lutein capsanthin,  $\beta$ -carotene and  $\beta$ -cryptoxanthin), as shown in Table 9.2, and the  $\beta$ -apo-8'-carotenal occurrence was in the percentage range relative to  $\beta$ -carotene of 0.03-3.87%. The  $\beta$ -carotene amounts reported in Table 9.2, were consistent with the literature reports, whereas the other reported carotenoids contents were lower than the usual average values reported in the literature because in this study the saponification step was not carried out and only free carotenoids amounts were determined [2,7,8].

It is also interesting to note that Capsorubinal is not present among the carotenoids but there are numerous apo-capsorubinals. This is caused by the oxidative cleavage of Capsanthin which forms apo-Capsorubinals and apo-Zeaxanthines (figure 9.2).

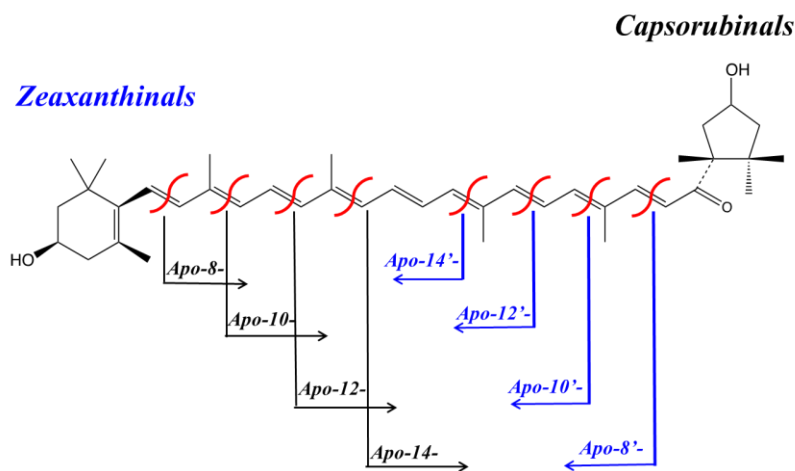


Figure 9.2 Possible oxidative cleavage of Capsanthin in apo-Zeaxanthinals and apo-Capsorubinals.

**Table 9.2** Carotenoids and apocarotenoids contents in the investigated chilli peppers samples, expressed as  $\mu\text{g g}^{-1}$ .

	<b>Zeaxanthin</b>	<b>Lutein</b>	<b>Capsanthin</b>	<b><math>\beta</math>-Cryptoxanthin</b>	<b><math>\beta</math>-Carotene</b>	<b><math>\beta</math>-Citaurin</b>	<b>Apo-8'-Carotenal</b>
<b>Sample 1</b>	1.327	1.050	0.469	0.754	1.291	0.092	0.052
<b>Sample 2</b>	2.093	2.499	0.765	27.813	37.112	$\leq$ LoD	0.068
<b>Sample 3</b>	1.249	0.550	0.494	2.817	36.438	$\leq$ LoD	0.049
<b>Sample 4</b>	1.067	9.390	$\leq$ LoD	1.142	$\leq$ LoD	$\leq$ LoD	$\leq$ LoD
<b>Sample 5</b>	31.132	3.152	66.993	13.298	261.579	$\leq$ LoD	0.143
<b>Sample 6</b>	8.692	9.225	20.297	5.512	$\leq$ LoD	0.090	0.123
<b>Sample 7</b>	5.285	5.837	8.592	3.506	63.453	$\leq$ LoD	0.063
<b>Sample 8</b>	3.096	1.052	2.766	3.131	196.979	$\leq$ LoD	$\leq$ LoD
<b>Sample 9</b>	6.582	2.276	1.447	4.668	2.247	0.126	0.061
<b>Sample 10</b>	6.620	4.330	9.224	7.324	151.078	0.610	0.336
<b>Sample 11</b>	1.954	3.318	0.577	1.426	11.094	$\leq$ LoD	0.051
<b>Sample 12</b>	3.111	6.928	2.907	2.762	172.514	$\leq$ LoD	0.054
<b>Sample 13</b>	3.690	0.950	11.039	4.590	175.864	0.082	0.050
<b>Sample 14</b>	1.681	8.691	0.471	0.901	0.664	$\leq$ LoD	$\leq$ LoD
<b>Sample 15</b>	3.883	0.745	7.626	1.729	148.372	0.142	0.050
<b>Sample 16</b>	2.254	8.735	3.506	1.908	57.640	$\leq$ LoD	$\leq$ LoD
<b>Sample 17</b>	3.923	6.741	0.863	4.408	48.378	0.087	0.057
<b>Min</b>	1.067	0.550	$\leq$ LoD	0.754	$\leq$ LoD	$\leq$ LoD	$\leq$ LoD
<b>Max</b>	31.132	9.390	66.993	27.813	261.579	0.610	0.336
<b>Mean values</b>	5.2	4.4	8.6	5.2	91.0	0.2	0.1
<b><math>\pm</math>SD</b>	7.0	3.3	16.5	6.6	85.0	0.2	0.1

### **9.3 Conclusions**

There are many free apocarotenoids and esters identified in the various pepper samples. Their distribution in the different species can be used as a fingerprint system for the recognition and cataloging of the various peppers, while, together with other data, it is a useful tool for determining the authenticity of a product and therefore against fraud. food.

Further studies will have to be carried out to investigate the possible occurrence of apocarotenoids in different cultivars of other fruits and their uptake in the human body considering their important biological activities and their key role in carotenoids homeostasis, both in plant and human tissues. The role of apocarotenoids fatty acid esterification, probably as a metabolites accumulation process, also deserves further investigations both in plants and human tissues. Apocarotenoids are transported from plastids, where they are biosynthesized, to other subcellular locations by a not yet clear mechanisms Compartmental effects of carotenoid metabolites resulting from different subcellular localization of the different carotenoids cleavage enzymes should also be further investigated.

## References

- [1] D. Giuffrida, P. Dugo, G. Torre, C. Bignardi, A. Cavazza, C. Corradini, G. Dugo. Characterization of 12 *Capsicum* varieties by evaluation of their carotenoid profile and pungency determination. *Food Chemistry*, 2013, 140, 794–802.
- [2] D. Hornero-Mendez. *Carotenoid Esters in Foods: Physical. Chemical and Biological Properties*, 2019.
- [3] D. Giuffrida, M. Zoccali, A. Arigo, F. Cacciola, C. O. Roa, P. Dugo, L. Mondello. Comparison of different analytical techniques for the analysis of carotenoids in tamarillo (*Solanum betaceum Cav.*). *Archives of Biochemistry and Biophysics*, 2018, 646, 161.
- [4] Zoccali, M., Giuffrida, D., Dugo, P., & Mondello, L. Direct online extraction and determination by supercritical fluid extraction with chromatography and mass spectrometry of targeted carotenoids from red Habanero peppers (*Capsicum chinense Jacq.*). *Journal of Separation Science*, 2017, 40, 3905
- [5] J. Deli, Molnar, P. Paprika. Carotenoids: Analysis, isolation, structure elucidation. *Current Organic Chemistry*, 2002, 6, 1197.
- [6] T. Maoka, Y. Fujiwara, K. Hashimoto, A. Akimoto (2001). Isolation of a series of apocarotenoids from the fruits of the red paprika *Capsicum annum L.* *Journal of Agricultural and Food Chemistry*. 2001 49, 1601–1606.
- [7] M. M. Wall, C. A. Waddell, P. W. Bosland. Variation in  $\beta$ -carotene and total carotenoid content in fruits of *Capsicum*. *Hortscience*, 2001, 36, 746.
- [8] E. Murillo, D. Giuffrida, D. Menchaca, P. Dugo, , G. Torre, A. J. Meléndez-Martinez, L. Mondello. Native carotenoids composition of some tropical fruits. *Food Chemistry*, 2013, 140, 825.

# 10 Online supercritical fluid extraction supercritical fluid chromatography method for determination of carotenoids and apocarotenoids in human blood samples

---

## 10.1 Introduction

Around 40 different carotenoids are commonly present in the human diet, only about 20 have been reported in human blood and tissues;  $\beta$ -carotene,  $\alpha$ -carotene, lycopene, lutein, zeaxanthin and  $\beta$ -cryptoxanthin are the most common carotenoids found in human blood and tissues [1-5].

Although carotenoid esters have been detected in human skin [6] and in human colostrum [8], only two reports are available in the literature on the detection of carotenoid esters in human serum or plasma [8,9].

Carotenoids oxidative and enzymatic cleavage products called apocarotenoids are very important bioactive molecules in plants [10,11] and, some of them, have also been reported in humans where they may exert unique biological activities as, for example, transcriptional regulation [12,13].

Relatively few studies are available in the literature on the apocarotenoids detection in human blood samples, and those available studies were focused on the apo-lycopenals and apo- $\beta$ -carotenals occurrence in either serum, plasma or red blood cell [14-17].

Available analytical reports for detecting carotenoids and apocarotenoids in blood samples are based on liquid extraction and liquid chromatography approaches, with relatively long analytical times and substantial organic solvent waste [1-5,8,9,13-19].

Therefore, the aim of this research was focused on the development of an on-line method based on the coupling of supercritical fluid extraction and supercritical fluid chromatography with triple quadrupole mass spectrometry detection (SFE-SFCAPCI/QqQ/MS) for the carotenoids and apocarotenoids detection in intact human blood samples, for the first time; moreover, a further aim was the direct quantification of selected carotenoids, belonging to different carotenoids chemical classes, by the developed methodology also for the first time. The detection of compounds presents in very low amounts like the carotenoids and apocarotenoids in human blood samples, that could be used as biomarkers in large clinical or epidemiological studies, needs the development of very sensitive methodologies like MS/MS systems [20,21].

## **10.2 Experimental section**

### *10.2.1 Standards and blood samples*

All the reagents and solvents used were of analytical or HPLC grade the carotenoids standards used are  $\beta$ -apo-8'-carotenal,  $\beta$ -carotene,  $\beta$ -cryptoxanthin, capsanthin, zeaxanthin and lutein. Human blood was used for the method validation. Stock solutions of the carotenoids compounds were prepared by using a solution of MeOH 90% and  $\text{CHCl}_3$  10% at a concentration level of 10,000 mg L<sup>-1</sup> and stored in dark vials at -20 °C. Calibration standard solutions were prepared in human

blood (matrix matched calibration); these solution were used to determine the recoveries by considering only the carotenoids standard amounts used in the different spiking.

Standard mixtures of carotenoids at the 5000 and 100 mg L<sup>-1</sup> levels, in MeOH, were used for 5000 mg L<sup>-1</sup> and 100 mg L<sup>-1</sup> spiking levels. The two solutions were used to measure recovery.

Apocarotenals were generated by oxidative cleavage of the parent carotenoid by potassium permanganate according to the conditions reported by Rodriguez & Rodriguez-Amaya for  $\beta$ -carotene [22], and also described by Giuffrida et al., for zeaxanthin and capsorubin [23] and here applied to lutein standard as well; therefore, a series of  $\beta$ -apocarotenals, apo-zeaxanthinals, and  $\epsilon$ -apo-luteinals were generated by oxidation of  $\beta$ -carotene, zeaxanthin, and lutein respectively. In the conditions used the potassium permanganate generated oxidative cleavage of the double bonds of the studied carotenoids and gave apocarotenoids without further oxidation to carboxylic acid functions. Aliquots (10  $\mu$ L) of intact blood samples were collected by using a lancing device from a total of eleven healthy human volunteers in our laboratory (7 men and 4 women), between the ages of 25 and 50, which were not following any particular diet or taking any carotenoids supplementation. For privacy reasons, to the volunteers a number of identifications was given and the lancet device used was completely sterile and safe.

#### *10.2.2 SFE-SFC-APCI-MS instrumentation*

The SFE-SFC-MS analyses were performed on a Shimadzu Nexera-UC system, consisting of a CBM-20 A controller, an SFE-30 A module for

SFE, two LC-20ADXR dual plunger parallel-flow pumps, an LC-30ADSF CO<sub>2</sub> pump, two SFC-30 A backpressure regulator, a DGU degasser, a CTO-20 A C column oven, a SIL-30 AC autosampler, and an LCMS-8050 triple quadrupole mass spectrometer equipped with an atmospheric pressure chemical ionization (APCI) source (the entire SFC flow was directed into the MS). The entire system was controlled by the LabSolution ver. 5.8.

### *10.2.3 Optimization of the analytical method*

The intact blood sample (10 µL) aliquots, were directly loaded into the available vessel having a volume of 200 µL without the use of any kind of support material for the SFE extraction and subsequent SFC analysis. The SFE conditions were as follows: Solvent (A) CO<sub>2</sub> and solvent (B) CH<sub>3</sub>OH; from 0 to 3 min 20% MeOH; from 3 to 5 min 0% B. Flow rate: 2mL min<sup>-1</sup>, extraction mode: 0-3 min static mode, 3-5 dynamic mode, extraction vessel temperature: 40 °C. Backpressure regulator: 150 bar. The SFC conditions were as follows: Solvent (A) CO<sub>2</sub> and solvent (B) CH<sub>3</sub>OH. Gradient: from 5 to 19 min increasing from 0 to 100%, then 100% for 2 min. Flow rate: 2mL min<sup>-1</sup>. Makeup solvent CH<sub>3</sub>OH at flow 1mL min<sup>-1</sup>. Separations were performed on an Ascentis Express C30, 150mm, 4.6mm, 2.7 µm<sub>d.p.</sub>. The column oven temperature was 35 °C and the back-pressure regulator was 150 bar. The injection volume for standards was 2 mL.

The MS was set as follows:

- Acquisition mode: SCAN (±), SIM (+) and MRM.



- Interface temperature: 350 °C; DL temperature: 200 °C; Block heater temperature: 200 °C; Nebulizing gas flow (N<sub>2</sub>) 3 L min<sup>-1</sup>; Drying gas flow (N<sub>2</sub>) 5 L min<sup>-1</sup>.
- Scan range: m/z 200-1200; Event time 0.05 s for each event. Carotenoids and apocarotenoids were identified by using the available standard, scan and selected ion monitoring (SIM); moreover, multiple reaction monitoring (MRM) experiments were also carried out for both the apocarotenoids identifications and the selected carotenoids quantifications. Recovery experiments were carried out at two different spiking levels (5000 and 100 mg L<sup>-1</sup>). Repeatability was evaluated at the 100 mg L<sup>-1</sup> level, by performing eight replicates, and expressed as CV. Limits of detection (LoD) and quantification (LoQ) were calculated by multiplying the standard deviation of the analyte area, relative to the blood sample fortified at the lowest concentration level, three and ten times, respectively, and then by dividing the result by the slope of the calibration curve. Matrix-matched linearity was tested at five levels in the 100-5000 mg L<sup>-1</sup> range (at the 100, 250, 500, 1000, and 5000 mg L<sup>-1</sup> levels), performing four replicates at each level. Calibration curves were then constructed using the least squares method to estimate the regression line; the linearity and the goodness of the curve used were confirmed using Mandel's fitting tests. The significance of the intercept was established running a t-test. All the statistical tests were carried out at the 5% significance level. For absolute quantification purposes, matrix-matched calibration was used.

#### 10.2.4 SFE-SFC-MS intact blood analyses

The extraction process was carried out by using 8.8 mL of CO<sub>2</sub> and 1.2 mL of MeOH and by using 10 µL of intact blood sample, thus saving a considerable amount of solvents and sample, compared to, for example, the 6 mL or the 0.1 mL human serum amounts used respectively by Khachik et al. [3], and Matsubara et al. [20]. The developed method has been optimized considering: extraction time (both static and dynamic), amount of co-solvent (MeOH), flow rate and chromatographic gradient. Initially, a Whatman paper was used as support for the collected blood samples, however, despite the high selectivity of the MRM, several interferences coming from the support were detected running a blank sample. For such a reason, it was decided to use directly the available vessel having a volume of 200 mL without the use of any kind of support material (Figure 10.1).

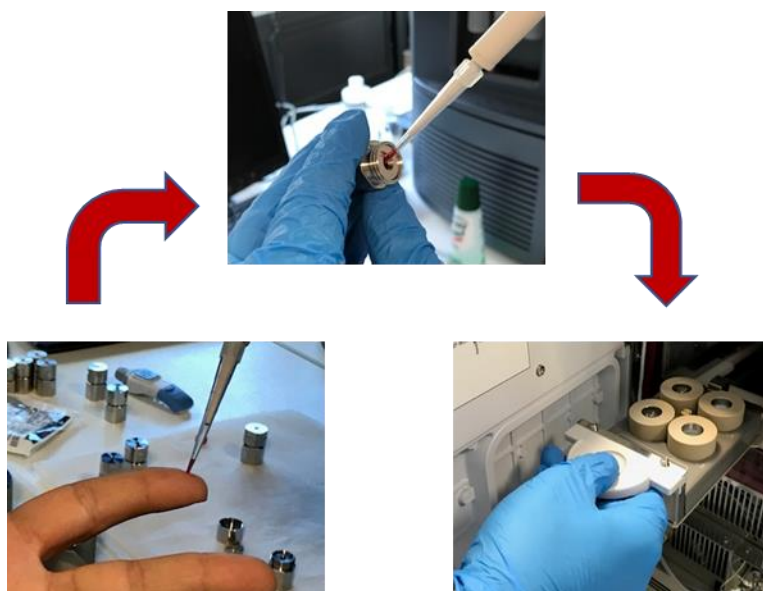


**Figure 10.1** Method of taking and analyzing blood samples.

The method has been developed using standards belonging to different carotenoid classes, in order to cover a different range of polarity, namely:  $\beta$ -carotene (hydrocarbon),  $\beta$ -cryptoxanthin (monohydroxy-), zeaxanthin (dihydroxy-), capsanthin (b,  $\kappa$ -rings, hydroxyl- and carbonyl functions) and  $\beta$ -apo-8'-carotenal (apo- $\beta$ -carotenoid).

Table 1 shows the determined concentrations of the selected carotenoids in the eleven different blood samples analyzed by the developed SFE-SFC-MS methodology. The determined average content of  $\beta$ -carotene was  $123.8 \text{ nmol L}^{-1}$  (range  $18.7\text{-}485.1 \text{ nmol L}^{-1}$ ), of  $\beta$ -cryptoxanthin was  $385.3 \text{ nmol L}^{-1}$  (range  $72.5\text{-}1920.3 \text{ nmol L}^{-1}$ ), of zeaxanthin was  $396.9 \text{ nmol L}^{-1}$  (range  $< \text{LoD e } 1795.8 \text{ nmol L}^{-1}$ ) and of capsanthin was  $38.9 \text{ nmol L}^{-1}$  (range  $< \text{LoD e } 188.4 \text{ nmol L}^{-1}$ ).

A liquid extraction protocol followed by supercritical fluid chromatography with mass spectrometry detection of carotenoids in human plasma was reported by Matsubara et al. [20], which quotes  $\beta$ -carotene,  $\beta$ -cryptoxanthin and zeaxanthin concentrations in the ranges of respectively  $68\text{-}320 \text{ nmol L}^{-1}$ ,  $42\text{-}250 \text{ nmol L}^{-1}$ , and  $70\text{-}270 \text{ nmol L}^{-1}$ . Comparing carotenoids concentration in blood samples show wide differences among population which are also depending on different dietary intake and also differences may arise from different analytical procedures employed for their evaluation.

Interestingly, the obtained quantitative results can be considered consistent with the quantitative ranges for the investigated carotenoids reported in similar studies carried out with different analytical approaches.

The MRM mode is particularly effective in the identification of low abundance compounds and the specificity of MRM transitions

optimized on the available standards, was advantageous because allowed to determine a series of Apo-lycopenals (apo-6'-, apo-8'-, apo-10'-, apo-12'- e apo-14'- lycopenals) (Figure 10.2) whose presence was reported by Kopec et al. [14].

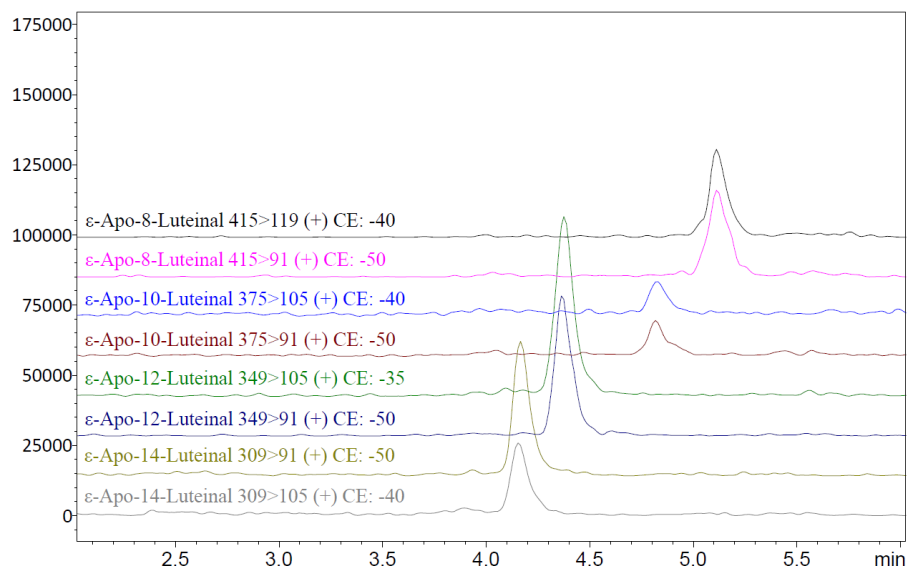


**Figure 10.2** Chromatograms of the MRM transitions of the various  $\epsilon$ -apo-lycopenals identified.

Interestingly,  $\beta$ -apo-12'-carotenal, apo-100-zeaxanthinal, apo-12'-zeaxanthinal, apo-14'-zeaxanthinal,  $\epsilon$ -apo-8-luteinal,  $\epsilon$ -apo-12-luteinal and  $\epsilon$ -apo-14-luteinal were detected in human blood for the first time, in this study. Figure 10.3 shows the corresponding enlargements of the ion chromatograms obtained in MRM analysis relative to the detected  $\beta$ -apo-carotenals (1.  $\beta$ -apo-8'-carotenal, 2.  $\beta$ -apo-12'-carotenal, and 3.  $\beta$ -apo-14'-carotenal; A), apo-zeaxanthinals (4. apo-10'-zeaxanthinal, 5. apo-12'-zeaxanthinal, and 6. apo-14'-zeaxanthinal; B) and  $\epsilon$ -apo-

luteinals (7.  $\epsilon$ -apo-8-luteinal, 8.  $\epsilon$ -apo-12-luteinal and 9.  $\epsilon$ -apo-14-luteinal; C), in intact human blood.

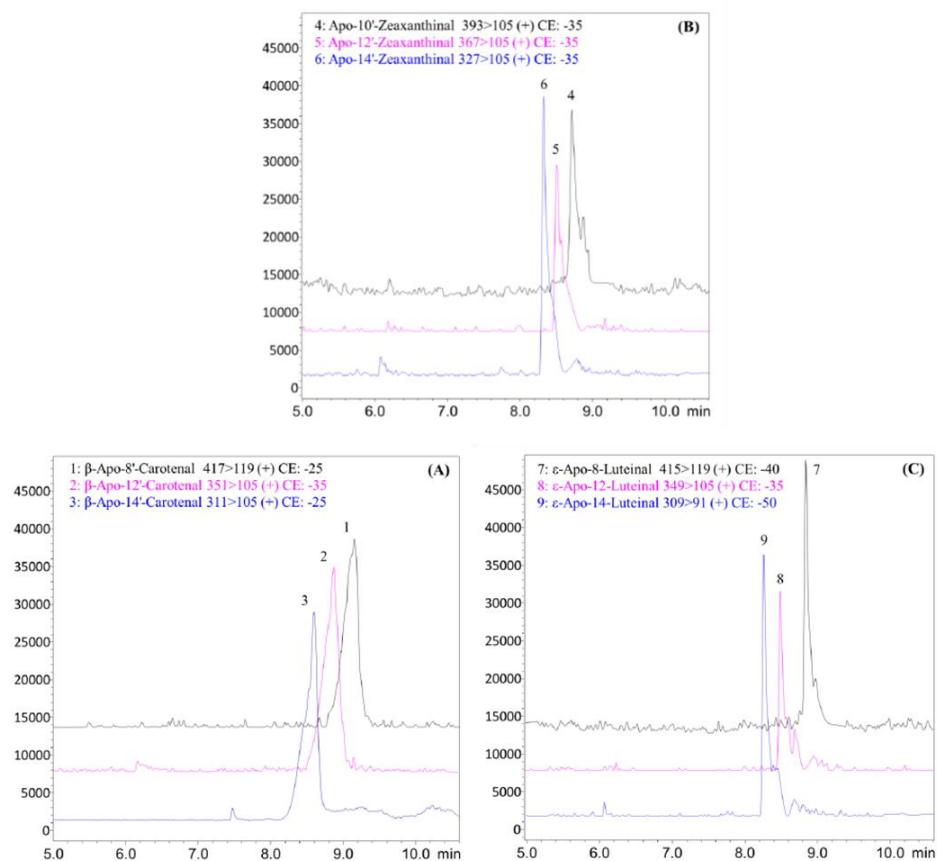


**Figure 10.3** The corresponding chromatograms obtained in MRM analysis relative to the detected  $\beta$ -apo-carotenals, apo-zeaxanthins and  $\epsilon$ -apo-luteinals in intact human blood.

### 10.3 Conclusions

In most studies the carotenoids analysis of human blood samples consisted of a series of different steps: i) deprotonation, ii) solvent (often hexane) extraction and vortex, iii) centrifugation and concentration and iv) re-dissolution for the v) following liquid

chromatographic analysis [19]. In this study, the intact collected blood samples were directly analyzed by the developed SFE-SFC-MS methodology. The intrinsic properties of supercritical carbon dioxide (CO<sub>2</sub>) like its low viscosity, high density and high diffusion coefficient makes it a very efficient fluid for the carotenoids extraction and also for chromatographic separation characterized by high resolution and speed [25]. In addition, the high sensitivity and selectivity of the SFE-SFC-MS system allowed the detection of the various analytes investigated present in very small quantities in the blood samples with a total analysis time of just over 20 min and minimal operator error, losses of analytes or formation of artifacts that occur during the entire procedure.

## References

- [1] B. P. Arathi, P. R. Sowmya, K. Vijay, V. Baskaran, R. Lakshminarayana. Metabolomics of carotenoids: the challenges and prospects- A review. *Trends in Food Science and Technology*, 2015, 45, 105.
- [2] F. Khachik. Distribution and metabolism of dietary carotenoids in humans as a criterion for development of nutritional supplements. *Pure and Applied Chemistry*, 2006, 78, 1551.
- [3] F. Khachik, C.J. Spangler, J. Cecil Smith. Identification, quantification, and relative concentrations of carotenoids and their metabolites in human milk and serum. *Analytical Chemistry*, 1997, 69, 1873.
- [4] B. Olmedilla, F. Granado, S. Southon, A. J. A. Wright, I. Blanco, E. Gil-Martinez, H. Van Den Berg, B. Corridan, A. M. Roussel, M. Chopra, D. Thurnham. Serum concentrations of carotenoids and vitamins A, E, and C in control subjects from five European countries. *British Journal of Nutrition*, 2001, 85, 227.
- [5] A. Nishino, T. Ichihara, T. Takaha, T. Kuriki, H. Nihei, K. Kawamoto, H. Yasui, T. Maoka. Accumulation of paprika carotenoids in human plasma and erythrocytes. *Journal of Oleo Science*, 2015, 64, 1135.
- [6] T. Wingerath, H. Sies, W. Stahl. Xanthophyll esters in human skin. *Archives of Biochemistry and Biophysics*, 1998, 355, 271.
- [7] J. J. Rios, A. A. O. Xavier, E. Diaz-Salido, I. Arenilla-Velez, M. Jaren-Galan, J. Garrido-Fernandez, J. Aguaya-Moldonado, A. Perez-Galvez. Xanthophyll esters are found in human colostrum. *Molecular Nutrition and Food Research*, 2017, 61, 1.
- [8] F. Granado, B. Olmedilla, E. Gil-Martinez, I. Blanco. Lutein ester in serum after lutein supplementation in human subjects. *British Journal of Nutrition*, 1998, 80, 445.
- [19] J. Hempel, A. Fischer, M. Fischer, J. Hogel, A. Bosy-Westphal, R. Carle, R. M. Schweiggert. Effect of aggregation form on bioavailability of zeaxanthin in humans: a randomised cross-over study. *British Journal of Nutrition* 2017, 118, 698.
- [10] M. Havaux, Carotenoid oxidation products as stress signals in plants, *Plant Journal*, 2014, 79, 597.

- [11] X. Hou, J. Rivers, P. Leon, R.P. McQuinn, B. J. Pogson, Synthesis and function of apocarotenoid signals in plants. *Trends Plant Science*, 2016, 21, 792.
- [12] E. Giordano, L. Quadro. Lutein, zeaxanthin and mammalian development: metabolism, functions and implications for health. *Archives of Biochemistry and Biophysics*, 2018, 647, 33.
- [13] A. Eroglu, E. H. Harrison. Carotenoid metabolism in mammals, including man: formation, occurrence, and function of apocarotenoids. *Journal of Lipid Research*, 2013, 54, 1719.
- [14] R. E. Kopec, K.M. Riedl, E. H. Harrison, R. W. Curley, D. P. Hruszkewycz, S. K. Clinton, S. S. J. Schwartz. Identification and quantification of apolycopenals in fruits, vegetables, and human plasma, *Journal of Agricultural and Food Chemistry*, 2010, 58, 3290.
- [15] E. H. Harrison, C. Dela Sena, A. Eroglu, M. K. Fleshman. The formation, occurrence, and function of  $\beta$ -apocarotenoids:  $\beta$ -barotene metabolites that may modulate nuclear receptor signaling. *The American Journal of Clinical Nutrition*, 2012, 96, 1189S.
- [16] C. C. Ho, F. F. de Moura, S. H. Kim, A. J. Clifford. Excentral cleavage of  $\beta$ -carotene in vivo in a healthy man. *American Journal of Clinical Nutrition*, 2007, 85, 770.
- [17] A. Eroglu, D. P. Hruszkewycz, C. dela Sena, S. Narayanasamy, K. M. Riedl, R. E. Kopec, S. J. Schwartz, R. W. Curley, E. H. Harrison. Naturally occurring eccentric cleavage products of provitamin A b-carotene function as antagonists of retinoic acid receptors, *The American Journal of Clinical Nutrition*, 2012, 287, 15886.
- [18] K. T. Amorim-Carvalho, A. Cepeda, C. Fente, P. Regal. Review of methods for analysis of carotenoids. *Trends in Analytical Chemistry*, 2014, 56, 49.
- [19] F. Petruzzello, A. Grand-Guillaume Perrenoud, A. Thorimbert, M. Fogwill, S. Rezzi. Quantitative profiling of endogenous fat-soluble vitamins and carotenoids in human plasma using an improved UHPSFC-ESI-MS interface. *Analytical Chemistry*, 2017, 89, 7615.
- [20] A. Matsubara, T. Uchikata, M. Shinohara, S. Nishiumi, M. Yoshida, E. Fukusaki, T. Bamba. Highly sensitive and rapid profiling method for carotenoids and their epoxidized products using supercritical fluid



chromatography coupled with electrospray ionization-triple quadrupole mass spectrometry, *Journal of Bioscience and Bioengineering*, 2012, 113, 782.

[21] L. R. B. Mariutti, A. Z. Mercadante. Carotenoid esters analysis and occurrence: what do we know so far ? *Archives of Biochemistry and Biophysics*, 2018, 648, 36.

[22] E.B. Rodriguez, D.B. Rodriguez-Amaya. Formation of apocarotenals and epoxy-carotenoids from  $\beta$ -carotene by chemical reactions and by autoxidation in model system and processed foods. *Food Chemistry*, 2007, 101, 563.

[23] D. Giuffrida, M. Zoccali, S.V. Giofr e, P. Dugo, L. Mondello. Apocarotenoid determination in *Capsicum chinense* Jacq. cv Habanero, by supercritical fluid chromatography-mass spectrometry. *Food Chemistry*, 2017, 231, 316.

[24] D. Giuffrida, P. Donato, P. Dugo, L. Mondello. Recent analytical techniques advances in the carotenoids and their derivative determination in various matrices. *Journal of Agricultural and Food Chemistry*, 2018, 66, 3302.

# 11 Analysis of human colostrum for the determination of carotenoids and apocarotenoids

---

## 11.1 Introduction

The role of apocarotenoids, which are metabolites derived from carotenoid enzymatic or nonenzymatic oxidative cleavage, is emerging in mammals [1,2]. The physiological and biological activity of apocarotenoids has been reviewed and their role in gene expression and modulation of ligand activated nuclear receptors has been outlined [3, 4], suggesting that they are involved in different biological activity such as the possible prevention of some types of cancer, in fact, probably due to their transcriptional activity, apocarotenoids may have beneficial health properties superior to those of their parent carotenoids [5].

Apocarotenoids may be absorbed from the diet or may be produced by the parent carotenoid cleavage enzymes.

Figure 11.1 shows an example of possible eccentric oxidative cleavage sites of  $\beta$ -carotene leading to the production of various b-apocarotenals,  $\beta$ -apo-15-carotenals (Retinal) for example being widely distributed in different Citrus species [6].

Apocarotenoids in plants are known to be produced by nonenzymatic oxidation or by different carotenoid cleavage dioxygenase enzymes (CCDs) [7]. Researchers have recently reported the detection of apocarotenoids in intact human blood [8]. While the presence of carotenoids in human colostrum has been reported in various studies [9-

11] no reports are available on the presence of apocarotenoids in human colostrum. Therefore, the purpose of the present study was to search for the possible occurrence of apocarotenoids, including apocarotenoid esters, in human colostrum for the first time by applying an online SFE-SFC-MS methodology.

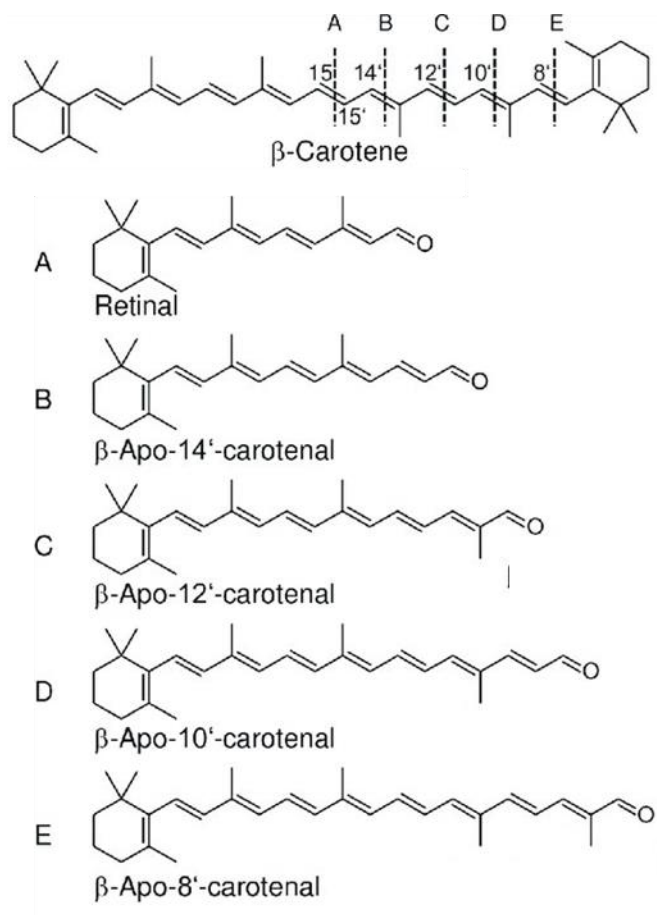


**Figure 11.1** Possible eccentric oxidative cleavage sites of  $\beta$ -carotene

## 11.2 Experimental section

### 11.2.1 Standards and samples

The standards used were: capsanthin,  $\beta$ -carotene,  $\beta$ -cryptoxanthin, and zeaxanthin, apo-8'- $\beta$ -carotenal, apo-8'-lycopenal, and  $\beta$ -citraurin (apo-8'-zeaxanthinal). For method validation, colostrum samples were used. Carotenoid and apocarotenoid stock solutions were prepared using a 1:1 (v/v) mixture of hexane and  $\text{CH}_2\text{Cl}_2$  at a concentration of  $1000 \text{ mg L}^{-1}$ , and the solutions were stored in vials in the dark at  $-20 \text{ }^\circ\text{C}$ .

Calibration standard solutions were prepared in colostrum (matrix-matched calibration).

In addition, apocarotenoids were prepared  $\beta$ -apocarotenals, apolycopenals, apocanthaxanthinals, apozeaxanthinals, apocapsorubinals, and  $\epsilon$ -apoluteinals were generated by oxidative cleavage of  $\beta$ -carotene, lycopene, canthaxanthin, zeaxanthin, capsorubin, and lutein, respectively, following the procedure described by Rodriguez and Rodriguez-Amaya for  $\beta$ -carotene [12], and also reported by Giuffrida et al. for zeaxanthin and capsorubin [13], and Zoccali et al. for lutein [8].

Aliquots of a few milliliters of colostrum were collected from six women volunteers, who had a normal diet without any type of carotenoid supplementation; the samples were collected from the volunteers at the third or fifth postpartum day.

### 11.2.2 Instrument and analytical conditions

A Shimadzu Nexera-UC system was used for the analyses; the instrumental parts used are identical to those described in the previous chapter.

The analytical conditions are similar to those described in the previous chapter in order to optimize the chromatographic separation for the analytes investigated.

Twenty-microliter aliquots of intact colostrum samples were utilized for each analysis, with no sample preparation step. Solvent (A) CO<sub>2</sub> and solvent (B) CH<sub>3</sub>OH were used for the SFE as follows: from 0 to 3 min, 20% CH<sub>3</sub>OH, from 3 to 5 min, 0% B. Flow rate: 2 mL min<sup>-1</sup>; extraction mode: 0–3 min static mode, 3–5 dynamic mode; back-pressure regulator: 150 bar; extraction vessel temperature: 40 °C. Solvent (A) CO<sub>2</sub> and solvent (B) CH<sub>3</sub>OH were used for the SFC as follows: from 5 to 22 min increasing from 0 to 80% B, then from 22 to 23 min increasing to 100% B, and then 100% B for 2 min. Flow rate: 2 mL min<sup>-1</sup>. Make-up solvent CH<sub>3</sub>OH at flow 1.2 mL min<sup>-1</sup>. Chromatography was carried out on an Ascentis Express C30, 150 mm × 4.6 mm × 2.7 μm<sub>d.p.</sub>. The column oven temperature was 40 °C and the-back pressure regulator was 150 bar. Standard injection volume was 2 μL.

The conditions of the mass spectrometer are identical to those discussed in the previous chapter

Carotenoids and apocarotenoids were identified using the available standard, full scan, and selected ion monitoring (SIM). Multiple reaction monitoring (MRM) experiments were also carried out for the identification of carotenoids and apocarotenoids according to previously optimized transitions reported for carotenoids, β-apocarotenals, apozeaxanthinals, apocapsorubinals, and ε-apoluteinals [8,13].

### *11.2.3 Method validation*

Mixtures of carotenoid and apocarotenoid standards at concentrations of 5000, 10,000, and 50,000  $\mu\text{g L}^{-1}$  in hexane were used with spiking concentrations of 500, 1000, and 5000  $\mu\text{g L}^{-1}$  for recovery calculations. Recovery and repeatability (expressed as %CV) experiments, performed on the colostrum sample of a volunteer, were carried out at three concentrations of 500, 1000, and 5000  $\mu\text{g L}^{-1}$ . The colostrum sample was analyzed previously in order to subtract the detected area of the targeted carotenoids and apocarotenoids.

Matrix-matched linearity was tested by performing four replicates at each concentration level. A total of five levels were selected, ranging from 50 to 5000  $\mu\text{g L}^{-1}$  (50, 100, 500, 1000, and 5000  $\mu\text{g L}^{-1}$ ).

The least-squares method was used to estimate the regression line for the construction of the calibration curves.

For the calculation of both the limit of quantification (LoQ) and limit of detection (LoD), the standard deviation of the analyte area relative to the colostrum sample fortified at the lowest concentration level was multiplied three and ten times, respectively, and the result was divided by the slope of the calibration curve.

### *11.2.4 SFE-SFC-MS intact human colostrum analyses*

Previously reported carotenoid determination in human colostrum was carried out by means of separate liquid extraction and liquid chromatography approaches [9,11].

An online SFE-SFC-MS methodology was applied here for the first time for both the identification and quantification of selected carotenoids and apocarotenoids in human colostrum. The online nature

of this technique provides high sensitivity, minimizing sample losses. The colostrum samples were analyzed without any sample preparation or carotenoid ester saponification steps.

Four selected carotenoids and three selected apocarotenoids were identified and quantified in samples of human colostrum as shown in Table 11.1. The quantitative data reported for the carotenoids are within the range reported by Patton et al. [10], and Rios et al. [11].

**Table 11.1** Carotenoids and apocarotenoids quantification in six different colostrum samples by SFE-SFC-QqQ/MS.

Volunteer	Zeaxanthin		Capsanthin		$\beta$ -Carotene		$\beta$ -Cryptoxanthin		Apo-8'-lycopenal		$\beta$ -Citraurin		$\beta$ -Apo-8'-Carotenal	
	$\mu\text{g dL}^{-1}$	$\text{nmol L}^{-1}$	$\mu\text{g dL}^{-1}$	$\text{nmol L}^{-1}$	$\mu\text{g dL}^{-1}$	$\text{nmol L}^{-1}$	$\mu\text{g dL}^{-1}$	$\text{nmol L}^{-1}$	$\mu\text{g dL}^{-1}$	$\text{nmol L}^{-1}$	$\mu\text{g dL}^{-1}$	$\text{nmol L}^{-1}$	$\mu\text{g dL}^{-1}$	$\text{nmol L}^{-1}$
1	60.6	2132	29.5	1010	27	1008	48.2	1746	2.9	141	4.5	209	3.3	158
2	< LoD	< LoD	24.8	850	19.5	728	47.2	1710	2.3	111	3.9	180	3.3	156
3	59.8	2106	24.1	825	72.4	2700	56.1	2034	2.1	99	3.1	146	4.9	238
4	59.5	2095	23.9	817	21.2	792	51.9	1882	2.5	121	2.7	127	3	145
5	58.9	2075	23.5	806	< LoD	< LoD	49.8	1804	1.9	93	2.5	117	4.7	226
6	58.4	2058	23.5	806	< LoD	< LoD	47.5	1722	1.9	89	3.2	146	2	96
Min	< LoD	< LoD	23.5	806	< LoD	< LoD	47.2	1710	1.9	89	2.5	117	2	96
Max	60.6	2132	29.5	1010	72.4	2700	56.1	2034	2.9	141	4.5	209	4.9	238
Average	49.5	1744	24.9	852	23.4	872	50.1	1816	2.3	109	3.3	154	3.5	170
SD $\pm$	22.2	780	2.1	72	24.2	904	3.1	113	0.4	18	0.7	32	1	49

LoD = Limit of Detection

SD= ( $\pm$ ) Standard deviation



Figure 11.2 shows the different MRM analysis enlargements of the carotenoids and apocarotenoids quantified in the human colostrum samples.

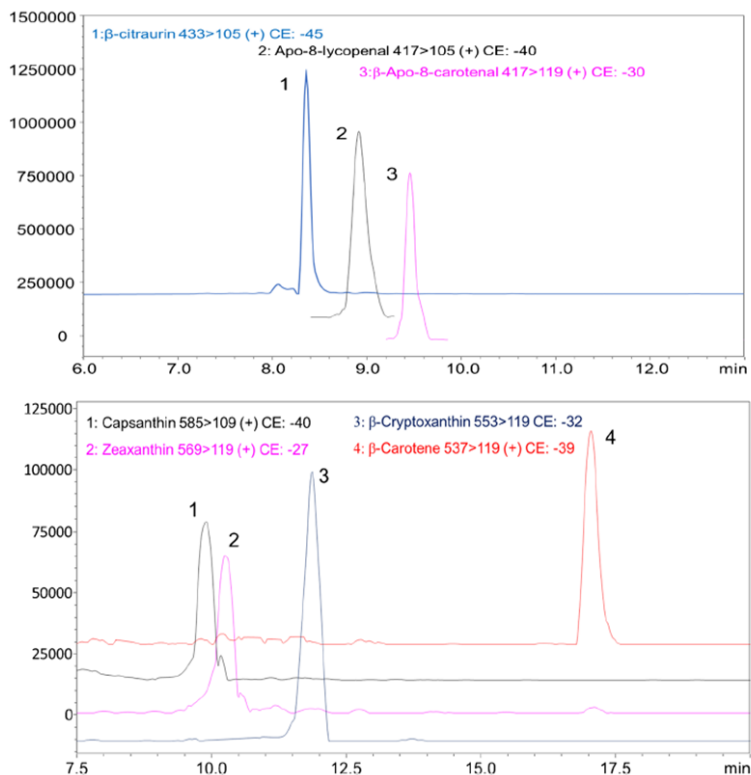


**Figure 11.2.** MRM analysis enlargements of the different carotenoids and apocarotenoids quantified by SFE-SFC-APCI/QqQ/MS analysis in human colostrum samples.

The applied methodology allowed for the detection of 16 different free apocarotenoids and 10 different apocarotenoid fatty acid esters in human colostrum for the first time, as shown in Table 11.2 together with the relative MRM experimental data. Table 11.2 also reports the optimized transitions for the detected apolycoplenals and apocanthaxanthinals.

Interestingly, only  $\epsilon$ -apo-8-luteinal and only apo-12'-zeaxanthinal were detected among the different  $\epsilon$ -apo-luteinals and apozeaxanthinals sought. While free capsanthin was also detected in human colostrum here for the first time; these reported qualitative findings may be related to the diet of the lactating mothers.

All the analytes were analyzed in less than 18 min including the extraction step.

**Table 11.2** Overall apocarotenoids detected by SFE-SFC-APCI(±)/QQ MS analysis in colostrum samples.

<b>Compounds</b>	<b>Volunteer 1</b>	<b>Volunteer 2</b>	<b>Volunteer 3</b>	<b>Volunteer 4</b>	<b>Volunteer 5</b>	<b>Volunteer 6</b>
β-Citraurin	×	×	×	×	×	×
Apo-12'-Zeaxanthinal	×	×	×	×	×	×
β-Apo-8'-Carotenal	×	×	×	×	×	×
β-Apo-10'-Carotenal	×	-	×	×	×	-
β-Apo-12'-Carotenal	×	×	-	-	×	-
β-Apo-14'-Carotenal	-	×	-	×	-	-
Apo-8'-Lycopenal	×	×	×	×	×	×
Apo-10'-Lycopenal	×	×	×	×	×	×
Apo-12'-Lycopenal	-	×	-	×	×	×
Apo-14'-Lycopenal	×	×	×	×	×	×
ε-Apo-8'-Luteinal	×	×	×	×	×	×
Apo-10'-Capsorubinal	×	×	×	×	×	×
Apo-12'-Capsorubinal	×	×	×	×	×	×
Apo-14'-Capsorubinal	-	-	×	×	×	×
Apo-10'-Canthaxantinal	×	×	×	×	×	×
Apo-12'-Canthaxantinal	×	×	×	×	×	-
Apo-8'-Capsorubinal-C12:0	×	×	-	×	-	-
Apo-8'-Capsorubinal-C16:0	-	-	-	×	-	-
Apo-10'-Zeaxanthinal-C4:0	-	×	×	×	-	×
Apo-10'-Zeaxanthinal-C10:0	×	×	×	×	×	×
Apo-10'-Zeaxanthinal-C12:0	×	×	×	×	×	×
Apo-10'-Zeaxanthinal-C14:0	×	×	×	×	×	×
Apo-8'-Zeaxanthinal-C6:0	-	×	-	-	-	×
Apo-8'-Zeaxanthinal-C8:0	×	×	-	-	-	-
Apo-8'-Zeaxanthinal-C10:0	×	×	×	×	×	×
Apo-8'-Zeaxanthinal-C12:0	-	×	×	×	×	×

### **11.3 Conclusions**

Although the maternal diet certainly influences the carotenoid and apocarotenoid content in mammalian tissue, and the quantified amounts of apocarotenoids reported here are average values calculated from only six volunteers, they do provide a first indication of the order of magnitude at which apocarotenoids might be present in human colostrum. Moreover, the detection of 16 different free apocarotenoids and 10 different apocarotenoid fatty acid esters in human colostrum for the first time represents interesting evidence for the possible role of these metabolites in mammalian colostrum, and consequently probably for the newborn; their occurrence in human colostrum certainly has implications for newborn health status, since colostrum is the only form of food for the newborn during the very first days of life.

Further studies will be needed to achieve a broader understanding of the occurrence of apocarotenoids in lactating mothers in different geographical areas. These findings thus further confirm the importance of these metabolites in mammals and encourage additional investigation of the possible presence and roles of the apocarotenoids in human biological fluids and tissues.

## References

- [1] E. H. Harrison, L. Quadro. Apocarotenoids: emerging roles in mammals. *Annual Review of Nutrition*, 2018, 38, 153.
- [2] V. Shete, L. Quadro. Mammalian metabolism of  $\beta$ -carotene: gaps in knowledge. *Nutrients*, 2013, 5, 4849.
- [3] A. Eroglu, E. H. Harrison. Carotenoid metabolism in mammals, including man: formation, occurrence, and function of apocarotenoids. *Journal of Lipid Research*, 2013, 54, 1719.
- [4] A. J. Meléndez-Martínez. An overview of carotenoids, apocarotenoids, and vitamin a in agro-food, nutrition, health, and disease. *Molecular Nutrition and Food Research*, 2019, 63,1801.
- [5] D. Giuffrida, P. Donato, P. Dugo, L. Mondello. Recent analytical techniques advances in the carotenoids and their derivatives determination in various matrixes. *Journal of Agricultural and Food Chemistry*, 2018, 66, 3302.
- [6] G. Ma, L. Zhang, A. Matsuta, K. Matsutani, K. Yamawaki, M. Yahata. Enzymatic formation of  $\beta$ -citraurin from  $\beta$ -cryptoxanthin and zeaxanthin by carotenoid cleavage dioxygenase4 in the flavedo of *Citrus* fruit. *Plant Physiology*, 2013, 163, 682.
- [7] X. Hou, J. Rivers, P. Leòn, R. P. McQuinn, B. J. Pogson. Synthesis and function of apocarotenoid signals in plant. *Trends Plant Science*, 2016, 21, 792.
- [8] M. Zoccali, D. Giuffrida, F. Salafia, S. V. Giofrè, L. Mondello. Carotenoids and apocarotenoids determination in intact human blood samples by online supercritical fluid extraction-supercritical fluid chromatography-tandem mass spectrometry. *Analytica Chimica Acta*. 2018, 1032, 40.
- [9] A. A. O. Xavier, E. Díaz-Salido, Arenilla-Vélez I, J. Aguayo-Maldonado, J. Garrido-Fernández, J. Fonteca, A. Sàñches-García, A. Pérez-Gálvez. Carotenoid content in human colostrum is associated to preterm/full-term birth condition. *Nutrients* 2018, 10, 1654.
- [10] S. Patton, L. M. Canfield, G. E. Huston, A. M. Ferris, R. G. Jensen. Carotenoids in human colostrum. *Lipids* 1990, 25, 159.
- [11] J. J. Rios, A. A. O. Xavier, E. Díaz-Salido, I. Arenilla-Vélez, M. Jarén-Galàn, J. Garrido-Fernández, J. Aguayo-Maldonado, A. Pérez-Gálvez.

Xanthophyll esters are found in human colostrum. *Molecular Nutrition and Food Research*, 2017, 61, 10.

[12] E. B. Rodriguez, D. B. Rodriguez-Amaya. Formation of apocarotenals and epoxy-carotenoids from  $\beta$ -carotene by chemical reactions and by autoxidation in model system and processed foods. *Food Chem*, 2007,101, 563.

[13] D. Giuffrida, M. Zoccali, S. V. Giofrè, P. Dugo, L. Mondello. Apocarotenoids determination in *Capsicum chinense* Jacq. cv habanero, by supercritical fluid chromatography-mass spectrometry. *Food Chem*, 2017, 231, 316.